copy #9

VICKERS Nasa CR 65301

RESEARCH AND DEVELOPMENT DEPARTMENT

DESIGN AND DEVELOPMENT OF AN INTEGRATED PULSE MODULATED 60-LB THRUST CHAMBER

FINAL REPORT

Contract No. NAS 9-554

Final Report No.: TR-2-8

Project No.: 9-0765-102-118

April 24, 1963

Prepared by: J. A. Berst
M. Mudryk

Approved by: L. D. Taylor
L. D. Taylor
Chief Engineer
Advanced Systems

Approved by: W. W. Chao
Dr. W. W. Chao
Director of
Research and Development

TABLE OF CONTENTS

SECTION I - INTRODUCTION

Program Objectives
Design Concept

SECTION II - PROGRAM SUMMARY

A. Statement of Work
B. Summary of Results
C. Recommendations

SECTION III - A. Evaluation of Materials and Components

Material Testing - Environmental
Component Environmental Testing
Thrust Chamber
Test Description (Thrust Chamber)
Test Results and Discussion (Thrust Chamber)
Combustion Shell Erosion
Fabrication of Tungsten Sheet Liner
Heat Soak-Back
Ablative Nozzle Extension
Nozzle Erosion
Nozzle Efficiency (Thrust Level)
Nozzle Reliability
Valve Poppet and Seat
Valve Test Requirements
Poppet and Seat Design Check
Bellows Sub-Assembly
Static Seals

B. Solenoid (or Torque Motor) Development

Summary of Development
Description of Characteristics and Factors Affecting Response
Solenoid - Discussion of Modifications

SECTION IV - ENDURANCE AND RELIABILITY

Bench Pulsing Endurance
Test I
Inspection
Solenoid
Valve and Poppet Seat

Bellows Sub-Assembly
Test II
Inspection
Solenoid
Valve Poppet and Seat
Bellows Sub-Assembly
Hot Firing Endurance and Reliability
Response and Minimum Impulse Bit

SECTION V - CALIBRATION CURVES, INSTRUMENTATION, AND SCHEMATICS

APPENDIX A - GAS TO LIQUID LEAKAGE CONVERSION

Liquid Flow Measurements
N_2 Gas Flow Measurements

APPENDIX B - VACUUM EQUIPMENT

Vacuum Coater Model 3166
Ultra High Vacuum Chamber

APPENDIX C - SOLENOID AND LINKAGE TRAIN PARAMETERS

Linkage Train Parameters
Electrical and Magnetic Parameters
Electrical Load Circuit
Magnetic Circuit
Basic Magnetic Equations

LIST OF FIGURES

Figure 1	Initial 60-lb. Pulse Rocket Engine Before Developmental Modifications
Figure 2	Disassembled View - Initial 60-lb. Pulse Rocket Engine Before Developmental Modifications
Figure 3	Delivered 60-lb. Integrated, Thrust Chamber Assembled with Sea Level Nozzle
Figure 4	Electrical Test Circuit Schematic
Figure 5	Valve Poppet and Seat Configuration
Figure 6	Ultra-High Vacuum Chamber Test Circuit
Figure 7	Combustion Efficiency vs O/F Ratio for Various L* Chambers, Single Triplet Injector
Figure 8	Firing Summary - Efficiency vs O/F Ratio
Figure 8A	Single Triplet Injection Fan Spray Pattern
Figure 9	Tungsten Liner Forming Fixture
Figure 10	Tungsten Liner Forming Sequence
Figure 11	Heat Soak-Back
Figure 12	Cutoff Nozzle Extension
Figure 13	Nozzle Weight Loss
Figure 14	Nozzle Comparisons
Figure 15	60-lb. Thrust Chamber Firing Using Optimum Sea Level Nozzle
Figure 16	Over-expanded Nozzle Firing
Figure 17	Poppet Seat
Figure 18	Poppet Seat, Teflon - Ceramic
Figure 19	Poppet Seat, Steel - Ceramic
Figure 20	Seat Before Preforming
Figure 21	Seat After Preforming
Figure 22	Seat Contact Area
Figure 23	Poppet Seating Force

Figure 24 Bench Test Setup

Figure 25 Poppet Seat Area Modifications

Figure 26 Poppet Seat - Teflon Nose Cone

Figure 27 Inverted Teflon Poppet

Figure 28 Threaded Teflon Insert

Figure 29 Solid Teflon Poppet Nose

Figure 30 60-lb. Thrust Chamber and Valve Assembly

Figure 31 Test Valve Fixture

Figure 32 Bellows Sub-Assembly

Figure 33 Valve Poppet Sub-Assemblies

Figure 34 Endurance Test Solenoid

Figure 35 Crown

Figure 36 Test II Fixture - Armature Stop Setup

Figure 37 Final Firing Response Traces

Figure 38 Response Bench Testing

Figure 39 Response - Command to Full Open

Figure 40 Temporary Switching Circuit for Minimum Impulse Bit

Figure 41 Schematic - Test Stand Circuit, Cell 2

Figure 42 Schematic - Test Stand Circuit, Pad 1

Figure 43 Schematic - Instrumentation Circuit

Figure 44 High Response Strain Bridge Load Cell

Figure 45 Flow Pickup Assembly

Figure 46 Load Cell Calibration

Figure 47 OX and Fuel Venturis' Calibration

Figure 48 Water Calibration STV-2 Valve and Injector

Figure 49 Water Calibration STV-2 Injector

Figure 50 Water-to-Gas Flow Test Circuit

Figure 51 Leakage Flow Conversion Curves

Figure 52 N_2 Gas Leakage Conversion Curves

Figure 53 Vacuum Coater - Model 3166

Figure 54 Ultra-High Vacuum Chamber

LIST OF TABLES

Tables 1 & 1A Vacuum Testing

Table 2 Results - Vacuum Testing, Poppet and Seats

Table 3 Vacuum Chamber Test Circuit Operating Cycles

Table 4 Evaluation of Thrust Chamber

Table 5 Log of All Firings

Table 6 Combustion Shell Erosion

Table 7 Test Results with Valve Seat Configuration

Table 8 Valve Seat Area Increase

Tables 9 to 13 Poppet Seat Leakage Tests

SECTION I

INTRODUCTION

SECTION I

INTRODUCTION

Program Objectives

The program documented by this report was initiated by the Energy System Branch, Manned Spacecraft Center, NASA. Mr. Richard Ferguson is the chief of this branch; Mr. Witalij Karakulko is the project officer.

The program objective of NASA Contract No. NAS 9-554 was to establish sufficient characteristic parameters and test experience on an integrated 60 pound thrust pulse-modulated thrust chamber to enable the design and development of prototype flight type units with assurance. The program was to culminate in the delivery of an integrated 60 pound thrust unit to NASA for their further evaluation.

The program objectives as stated above have been attained. An integrated unit has been delivered to NASA. This final report is presented as per contract requirements to summarize the investigations and development work accomplished.

Design Concept

The design concept developed and tested by Vickers to achieve optimum performance of the pulse modulated 60 lb. thrust chamber was to integrate the system components into a compact package. These components consist of a single solenoid, a bipropellant valve, an injector, and a combustion chamber. The advantages derived are a

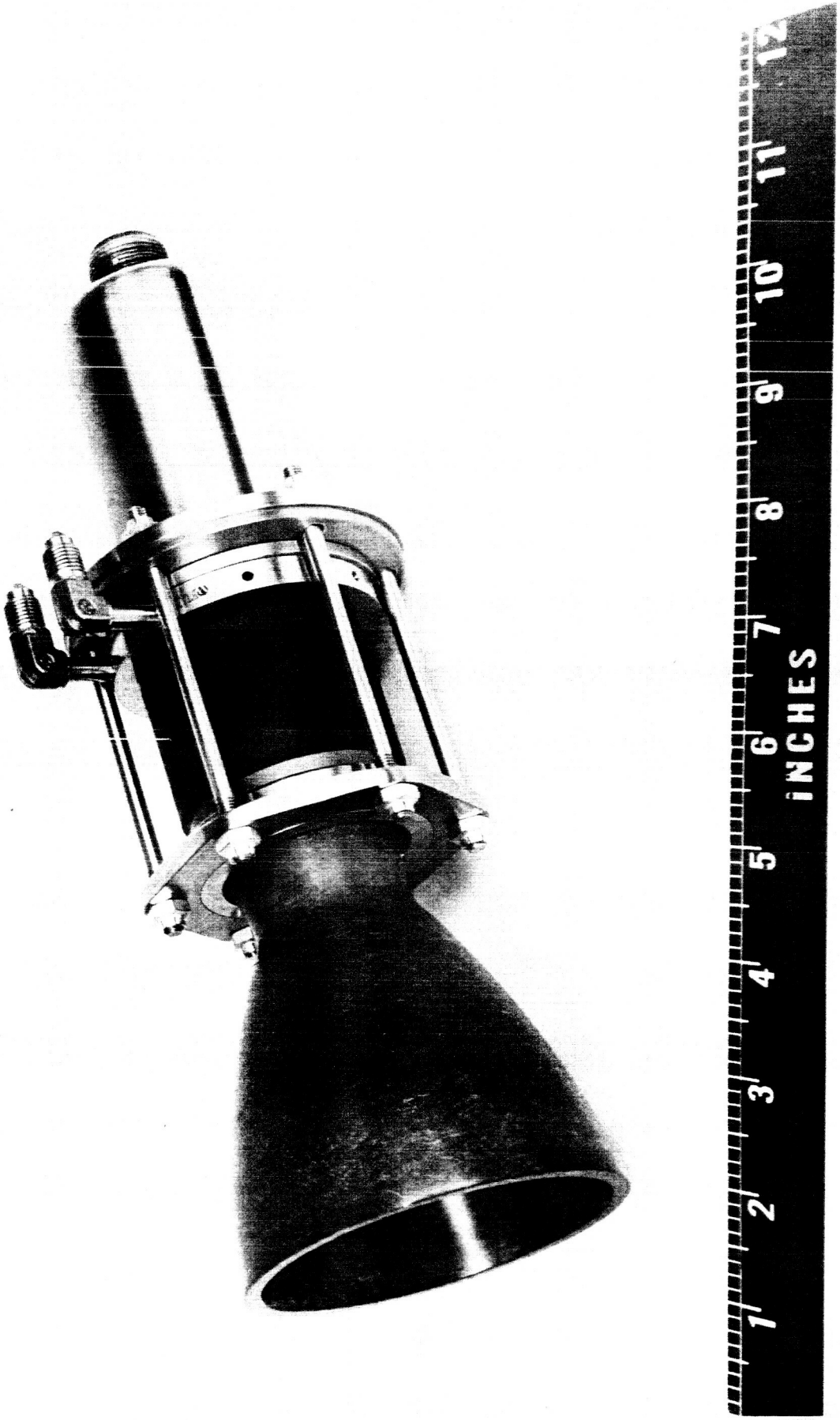

Figure 1

Initial 60# Pulse Rocket Engine Before Developmental Modifications

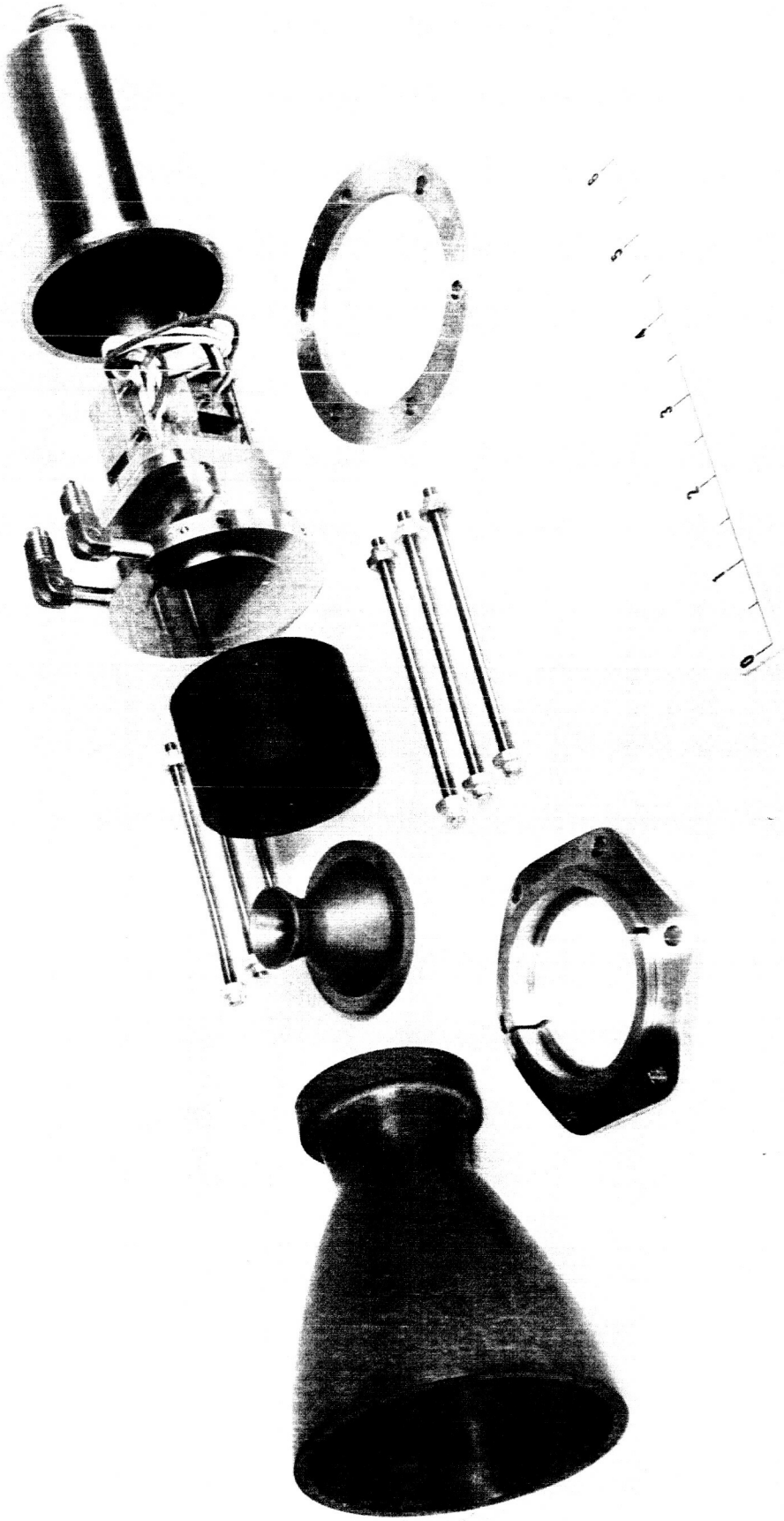

Figure 2
Disassembled View
Initial 60# Pulse Rocket Engine Before Developmental Modifications

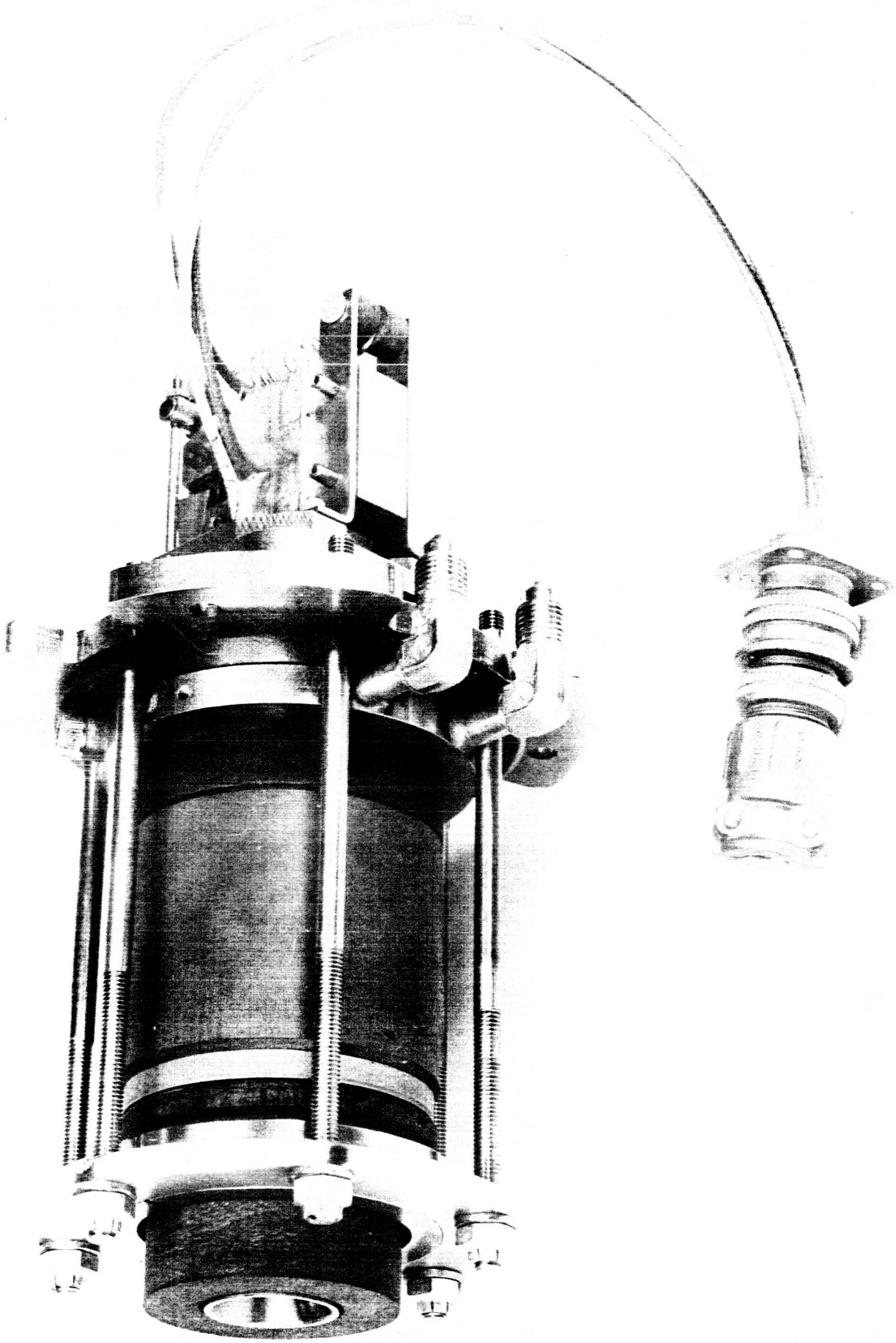

Figure 3
Delivered 60 lb., Integrated, Thrust Chamber
Assembled with Sea Level Nozzle

high response, light-weight system with proven reliability.

Figure 1 and 2 show the initial hardware for the integrated unit. Figure 3 is an assembly of the sea-level portion of the delivered unit.

1. Solenoid Description

   A single solenoid mounted directly on the valve is used to ensure reliable synchronization of the fuel and oxidizer. Redundancy of electrical operation is achieved by the two independent coils operating in parallel. The flapper type, high response solenoid is composed of a laminated magnetic structure with a two step working gap.

2. Bipropellant Valve & Injector Description

   The bipropellant valve incorporates low friction linkages, stainless steel bellows, and zero leakage poppet valves. Similar configurations were previously tested and proven in a Vickers' funded pulse-modulated thrust chamber development. Advantages derived are the high torque amplification from two levers with their pivot points outside the valve, and the small cantilever force to operate the flexible stainless steel bellows used for sealing. The single triplet injector is part of the valve body providing minimum filling time and minimum "dribble".

3. Combustion Chamber and Nozzle

The combustion chamber consists of a cylindrical section made of high density graphite and lined with a wrapped tungsten sheet for greater erosion resistance. A pyrolytic graphite spacer provides a heat shield for the injector face. The nozzle and combustion chamber are joined to the injector-valve body by tension bolts at a preset pressure. The nozzle throat is made of refractory material consisting of tantalum carbide and tungsten carbide. The 40:1 vacuum nozzle extension is an ablative type asbestos-phenolic.

A design feature is the use of belleville spring located behind the injector valve flange, which limits the stress on the bolts during expansion of the chamber and maintains required compression on flange seals.

SECTION II

PROGRAM SUMMARY

SECTION II

PROGRAM SUMMARY

A. Statement of Work

This program was initiated to accomplish development of a prototype 60 lb. thrust pulse rocket based on the concept of an integrated single solenoid-bipropellant valves-injector-thrust chamber. This program resulted in the establishment of sufficient characteristic parameters and test experimence that a prototype valve was designed and test proven.

The initial program was divided into two major parts: (1) the design, fabrication, and test evaluation using the specified bipropellants in an integrated thrust chamber; and (2) the design and test evaluation under hard vacuum conditions of valve seat configurations and materials. The results of these two major sub-programs were combined in one integrated pulse rocket toward the end of the six-month schedule, and this unit was successfully test evaluated for response, endurance, and impulse-bit.

The essential tasks performed by Vickers in the development program for an integrated pulse modulated thrust chamber consisted of:

1. Designing an integrated bipropellant pulse modulated solenoid, valve, and combustion chamber.

2. Fabrication of sufficient hardware to this design to conduct a performance evaluation program and to deliver one complete assembly to NASA.
3. Test evaluation of this design.
4. Design of test fixtures for the evaluation of various valve seat designs and materials to determine that combination most suitable for operation and sealing in a hard vacuum environment.
5. Fabricating this test fixture and valve seat and material combinations for evaluation.
6. Conduct a materials and valve seat evaluation program under hard vacuum conditions.
7. Write and submit progress reports each month during the program.
8. Write and submit a final technical report summarizing the program.
9. Delivering to NASA one integrated pulse modulated thrust chamber for NASA evaluation. This unit was of the same design and materials as that evaluated during the program and was performance checked by Vickers for pulse firing endurance, response, and impulse bit.
10. Vickers delivered one integrated pulse modulated thrust chamber to NASA, MSC, Energy Systems Branch, Houston, Texas.

B. Summary of Results

The following sections of this document contain detailed reports on the various phases of the program. This summarization will be limited to a discussion of the accomplishments under the program with respect to the preliminary target performance specifications established as a guide for the investigation and development efforts.

One objective of the program was to determine design parameters. Therefore, the performance specifications were established as targets and, as was expected, trade-offs were made to achieve specific objectives in line with a typical application.

Stated below are the preliminary performance specifications as they appear in the contract. Below each item is a summary of the actual accomplishments and a discussion of trade-offs where applicable.

1. The pulse modulated thrust chamber shall produce a thrust of 60 lbs. $\pm$ 3% when operated continuously.

   This target was achieved.

2. The response of the thrust chamber should be less than .010 sec. measured from the time rated current is applied to the solenoid to the instant the output thrust equals 80% of rated thrust.

This target was achieved. See items 10 and 12 for further discussion on this subject.

3. The oxidizer to be used shall be nitrogen tetroxide.

Nitrogen tetroxide was used as the oxidizer.

4. The fuel to be used shall be a 50/50 mixture of hydrazine and UDMH.

The fuel used was as specified.

5. The O/F ratio will be specified upon award of contract.

This item was left open and determined by evaluation of various parameters. Data was taken over a wide range of O/F ratios. The general conclusion is that the selection of O/F ratio must be made on the basis of a specific application rather than on combustion efficiency. For example, the variation in efficiency from O/F's of 1.2 to 2 is only in the order of 3%.

6. The combustion chamber pressure shall be 150 psia.

This target was achieved. Tests have indicated that lower chamber pressures are possible and are probably

desirable.

7. The inlet pressure to the injector valve shall be 240 psia. See item 8.

8. The pressure differential across the propellant injector shall be 75 psi.

   This target was achieved as was item 7. The inlet pressure (item 7) is dependent upon chamber pressure and injector pressure drop.

9. The efficiency of the combustion chamber shall be 95% $^{+0}_{-2}$%.

   This target was achieved. There is a trade-off between efficiency and material life. In the latter part of this program the design was targeted at the lower efficiency level (93%) to obtain maximum material life.

10. The minimum pulse bit attainable shall be 0.60 lbs-sec.

    This target specification was bettered by more than a factor of 3. The actual minimum impulse bit attained was .177 pounds-seconds compared with the target specification of 0.6 pound-seconds. Note that this was a trade-off with item 12.

11. The pulse rocket shall be designed for minimum weight and size compatible with a high degree of reliability.

    This has been accomplished. The valve has undergone 466,000 cycles plus, with no significant change in sealing characteristics.

12. The electrical power to operate the solenoid shall be 17 watts maximum.

    The recommended electrical power for the delivered unit is 47 watts, although the unit will operate at the 17 watt level. The higher power level is recommended to achieve good "on" response.

13. The thrust chamber shall be designed to operate under deep space environment conditions.

    This target has been achieved.

14. The injector valve shall be capable of operation for a total of 10 minutes of which 5 minutes shall be continuous and 5 minutes at a pulse rate of 10 cps.

The following duty cycle shall be used:

Frequency	-10 cps
Signal On	-50 msec.
Signal Off	-50 msec.
Number of cycles	-5000

The unit was hot fired for more than 10 minutes using the duty cycle stated. The limitation for longer operational time on the particular unit tested was combustion chamber erosion. Tests conducted by Vickers since the conclusion of the test work under the NASA sponsored program have indicated that solutions are available for extending the operational life.

15. Following step 14 the valve shall demonstrate a total leakage under full feed pressure not to exceed 0.1 cc per hour.

This target specification was achieved. After the conclusion of the 10 minute run described above, no deterioration in sealing capability could be detected.

C. Recommendations

As can be observed from the previous section, the program objective as related to basic design parameters has been accomplished and feasibility has been demonstrated by the construction and evaluation testing of the integrated 60 pound thrust pulse-modulated thrust chamber. The program has demonstrated that very small minimum impulse bits can be obtained through the use of close-coupled, highly integrated, and coordinated valve components. It has also demonstrated the potential reliability of the concept of minimizing the number of unit components.

The next logical step in this advanced development program is to apply the knowledge attained to a unit targeted towards a specific application. This unit should be flight-weight and a flight type and should be suitable for pre-flight qualification testing and eventually flight testing. Vickers recommends this as a follow-on to the present program.

Noting that the primary objective of the present program was the establishment of parameters, it is obvious that there must be specific areas of design improvement that must be made to the present design to achieve a flight-weight and flight-type design. Some specific design improvements recommended are as follows:

1. A flight-weight body.
2. One piece poppet actuating arm from the armature take-off to the bellows header (a simplification of the previous design). This sturdier linkage will minimize deflection.
3. Incorporation of a captive spring plunger assembly with a screw adjustment as the armature return spring (replaces the modification "fix" on the previous unit).
4. Direct contact arm from armature-to-poppet actuating arm with simple screw adjustment for setting stroke (in place of more complicated cam action armature take-off).
5. Larger bellows to minimize bellows spring rate and deflection free bellows header (problem areas on the previous design).
6. Balanced dual pulling gap solenoid to provide for vibration and acceleration environment.
7. Angular mounting of solenoid and bipropellant valves to:
   A. Simplify actuation linkage
   B. Minimize "dribble" volume
   C. Minimum package size
   D. Improve inlet flow passages

8. Incorporation of armature back-stop to insure maximum solenoid pull at instant of command.

In summary, the incorporation of the above features improvements will result in a design that is of flight-type and flight-weight capable of being subjected to a pre-flight qualification test program.

In addition to the specific design improvements stated above, Vickers recommends that a dynamic analysis be accomplished on the solenoid and valve operating mechanism to optimize response and minimize electrical power. The basis for this recommended analysis is being accomplished on a Vickers funded in-house program.

As evolved during discussions between NASA and Vickers and as suggested by Mr. Richard Ferguson of NASA, the integrated concept permits the installation of a transducer (within the package) to sense armature and, therefore, the poppet positions of both bipropellant valves simultaneously. The information available from such a transducer could be used for a variety of purposes including monitoring of valve operation and signaling of an electrical command circuit. This later could make possible the attainment of repeatable partial stroke operation and, therefore, smaller increments of minimum impulse bits independent of large fluctuations of supply voltage.

This concept appears to be entirely feasible. Vickers recommends

that an investigation study and laboratory demonstration program be instigated using as a basis the designs, and to whatever extent possible, the existing valve components from the present program.

SECTION III

A. EVALUATION OF MATERIALS AND COMPONENTS

B. SOLENOID (OR TORQUE MOTOR) DEVELOPMENT

SECTION III

A. EVALUATION OF MATERIALS AND COMPONENTS

Material Testing - Environmental

During the design study, a careful survey was made in materials applicable for this project. Major considerations were compatibility of the materials with the specified propellants (N_2O_4 and UDMH-Hydrazine) and vacuum environment at elevated temperatures. There is considerable experience available with respect to compatibility of materials with the above propellants and no serious problems were expected. Table 1B is a list of materials of construction chosen for established compatibility and desired physical properties. However, a more critical area is the selection of nonmetallic materials for various parts in the design such as seals, solenoid coils, and extension cone in the combustion chamber and their use in vacuum environment. Therefore, a test program was started shortly after beginning work on this contract to determine the effects of hard vacuum and temperature on selected materials. A description of vacuum equipment is presented in Appendix B.

Tables 1 and 1A, describing vacuum tests of selected nonmetallic materials, require explanation of weight loss and the pressure during the run. What was desired from these tests were gross comparisons of material evaporation rates. Samples were weighed before testing, as is, with no bakeout. It should be noted that some tests showed a weight gain after vacuum exposure. This can be explained by the fact

that a small amount of outgassing occurred during vacuum exposure, but air inrush upon shutdown allowed re-absorbtion of slightly heavier atmospheric material. A dust free room with controlled atmosphere would be required to eliminate this phenomena.

The columns in Tables 1 and 1A listing "Pressure During Run" are the stabilized pressures attained in the 10^{-6} and 10^{-9} vacuum chambers respectively. "Stabilized" being defined as the maximum vacuum attainable where no further measurable outgassing occurred. The time required to stabilize is noted in the "time" column.

Some descriptive notes pertaining to these vacuum tests are noted below.

1. It was found that vacuum of 10^{-6} mm Hg combined with elevated temperatures above 400°F was more harmful to most organic material than vacuum of 10^{-9} mm Hg at ambient temperature (70°F).

2. In vacuum of 5×10^{-6} torr and 400°F temperature pure teflon, high density graphite, and high density Al_2O_3 were very stable.

3. Asbestos phenolic and graphite phenolic materials stabilized at 10^{-6} mm Hg at 500°F. A weight loss of 7.44% and 6.5% was recorded after 109 hours in the vacuum chamber. No visible change in the material was noticeable after this period.

4. No impairment was recorded with coil wires in vacuum after 24 hours in vacuum of 5.5×10^{-6} at 520°F. Insulation between wires, twisted together, was maintained as indicated by the nonconduction before and after vacuum exposures.

VACUUM TESTING - SEE WEIGHT LOSS EXPLANATION, Pg 1, THIS SECTION

MATERIAL	WEIGHT BEFORE TEST	TEMP. (°F)	TIME (HOURS)	WEIGHT (GM) AFTER TEST	WEIGHT LOSS %	PRESSURE mm Hg x 10^{-6} DURING RUN
Rubber (Viton A)	0.251	200	5	0.2511	0.0398	6.0
		290				
		300	17	0.2509	0.0398	5.2
		400	28	0.2509	0.0398	6.1
		530	23	0.2502	0.32	7.2
		650	6	0.2499	0.44	10.0
Pure Teflon (Dupont)	3.1358	200	5	3.1354	0.0128	6.0
		290				
		300	17	3.1355	0.0096	5.2
		400	28	3.1354	0.0128	6.1
		530	23	3.1337	0.067	7.2
		650	6	3.1276	0.26	10.0
Teflon (25% glass)	8.6523	200	5	8.6511	0.0139	6.0
		290				
		300	17	8.6502	0.0244	5.2
		400	28	8.6498	0.029	6.1
		530	23	8.6456	0.078	7.2
		650	6	8.6033	0.57	10.0
Tayloron *PA6	1.9449	200				
		290	4	1.9232	1.12	6.1
		300				
		400				
		530				
		650	109	1.8002	7.44	6.4
Tayloron **PG	0.7645	200				
		290	4	0.7546	1.29	6.1
		300				
		400				
		530				
		650	109	0.7148	6.5	6.4

*PA6 is asbestos with phenolic resin
**PG is graphite cloth with phenolic resin

Table I

VACUUM TESTING - SEE WEIGHT LOSS EXPLANATION, Pg 1, THIS SECTION

Table 1A

MATERIAL	WEIGHT BEFORE TEST	TEMP. (°F)	TIME (HOURS)	WEIGHT (BM) AFTER TEST	WEIGHT LOSS %	PRESSURE mm DURING RUN
Al_2O_3	0.3645	70	91.5	0.3646	0.027	3.8×10^{-6}
		385	6.5	0.3645	0	4.3×10^{-6}
		530	23.0	0.3645	0	4.3×10^{-6}
		650	20.0	0.3645	0	6.2×10^{-6}
High Density Graphite	1.0620	70	91.5	1.0628	0.075	3.8×10^{-6}
		385	6.5	1.0616	0.038	4.3×10^{-6}
		530	23.0	1.0616	0.038	4.3×10^{-6}
		650	20.0	1.0614	0.057	6.2×10^{-6}
Teflon Impregnated with 5% Molybdenum	0.4604	360	68	0.461	0.065	8.6×10^{-6}
		660	165	0.4459	3.15	1.0×10^{-5}
15% Lead	0.3218	360	68	0.3214	0.124	8.6×10^{-6}
		660	165	0.3037	5.620	1.0×10^{-5}
10% Graphite	0.2501	360	68	0.2500	0.04	8.6×10^{-6}
		660	165	0.2455	1.84	1.0×10^{-5}
25% Bronze	1.8211	360	68	1.8196	0.082	8.6×10^{-6}
		660	165	1.7451	4.170	1.0×10^{-5}
Asbestos Phenolic PA6	2.0332	70	176	1.9718	3.01	1×10^{-9}
		482	12			
Graphite Phenolic PG	0.8079	70	176			
		482	12	0.7831	3.07	1×10^{-9}
Pure Teflon	2.2155	70	130	2.2145	0.001	1×10^{-9}
		392	96			1×10^{-8}
Coated Teflon	3.2401	70	130	3.2398	0.003	1×10^{-9}
		392	96			1×10^{-8}

VICKERS INCORPORATED
research and development department

Table 1B

MATERIALS IN CONTACT WITH PROPELLANTS

Part Name	Material
Bellows	Inconel
Valve Body and Injector	347 SS
Valve Seat	440C SS
Poppet	440C SS
Poppet Nose	Teflon
Sleeve, Poppet	440C SS
Cover Plates	347 SS
Bellows Flange	AM 350
"O" Ring Seals	Teflon
Header (Bellows Sub-Assembly)	AM350
Rollpin (Poppet Nose Ret.)	302 SS
AN Fittings (Fluid Inlet)	302 SS

Component Environmental Testing

The valve poppet and seat evaluation program continued with testing under hard vacuum environment. This is in conformance with part of Appendix C, Environmental Testing of Sub-Components, NASA Contract 9-554.

To accomplish this, the following equipment was used (Appendix B)

a) The ultra high vacuum chamber and the related electrical control console.

b) An external remote control valving manifold and circuit filtered to the vacuum chamber. Figure 6.

c) A portable DC power supply with a square wave oscillator and related electrical circuitry. Figure 4.

d) A portable dry nitrogen supply with the necessary regulator and gauges.

The two valve poppet and seat configurations Figures 5 and which looked the most promising were selected based on the preliminary tests covered in another section of this report.

Poppet and seat design, Figure 5, was the first configuration installed into the test fixture. It might be pointed out that the fixture was assembled with rubber "O" rings in all the static sealing areas. Since our main objective at this time was to check out the poppet

ELECTRICAL TEST CIRCUIT SCHEMATIC

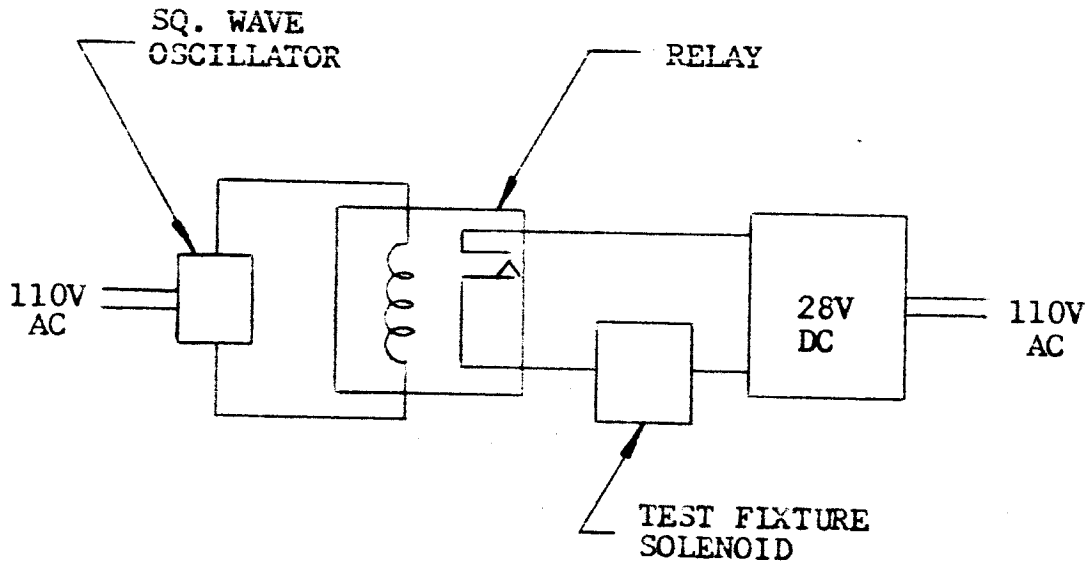

Figure 4

The above electrical circuit was used on both the bench and vacuum tests as a "work horse" circuit during the valve development work.

A more refined circuit was used to obtain the response characteristics of the solenoid and the integrated unit. This work is covered in another section of this report.

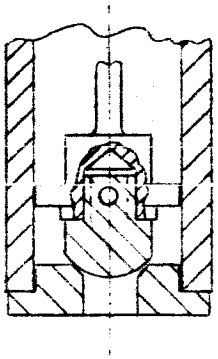

Spherical teflon nose piece, threaded and pinned into poppet with mating conical stainless steel seat.

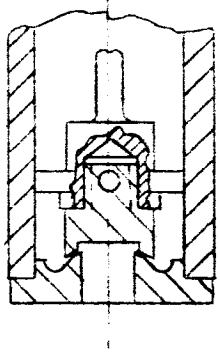

Internal conical teflon nose piece threaded and pinned into poppet with mating convex stainless steel seat.

Valve Poppet and Seat Configurations

Figure 5

and seat design only, it was felt that using rubber seals would offer less difficulty from the sealing stand-point if installed properly. A more detailed treatment of static seals is covered in Section III of this report.

The test fixture was fitted into the vacuum chamber with the remote control circuitry made up using HI-SEAL fittings made by the Emperial Brass Company. These fittings were used in all the tube connections both inside the vacuum chamber and the external circuit except the inlet and outlet ports of the test fixture. Here, standard AN fittings were installed with rubber "O" ring seals.

To ascertain the "vacuum tight" condition of the complete circuit prior to the actual testing at 10^{-8} torr, preliminary pump down cycle was accomplished with a resulting vacuum pressure at the low end of $10 \times {}^{-5}$ torr range. This preliminary test showed that leakage areas existed which must be found and corrected.

A direct approach was taken with the test circuit being disassembled and all possible connections permanently silver brazed. The disconnect joints were fitted with "Swagelock" fittings to facilitate the removal of the fixture from the test circuit. The AN fittings and seals were retained in the inlet and outlet ports of the fixture.

Leakage was also discovered in the static seal areas of the test fixture and corrected by reworking the surface finish of the sealing

grooves.

By taking the corrective action outlined above, a vacuum pressure of 6.0×10^{-8} was attained. This was the highest vacuum obtainable during the overall testing program and was felt adequate to comply with the hard vacuum requirements.

The vacuum chamber was pumped down and leakage tests were performed in two stages for each valve poppet and seat design as shown in Table 2. During the pumping cycle, the test fixture was exposed to $300^{\circ}F$ to $400^{\circ}F$ for 10-15 hours. In the first stage of the vacuum cycle, the poppet and seat were not exposed to vacuum. The purpose here was to make the final overall check on the combined vacuum and electrical circuits. A leakage check of the valve was also performed and recorded as direct comparison data to the leakage data obtained later after the poppet and seat had been exposed to hard vacuum test of the second stage.

Vacuum test results are shown in Table 3. Correlation of nitrogen gas leakage rate with a liquid propellant leakage rate is presented in Appendix A, Gas to Liquid Leakage Conversion.

Poppet and Seat Tested	Cycle Stages	Bake Out Hrs.	Bake Out Temp. °C
Convex Teflon Poppet with Conical Stainless Steel Seat	*1	10	200
	2		
Concave Teflon Poppet with Convex Stainless Steel Seat	*1	10	150
	2		

*Poppets and seats were not exp
the first stages of the vacuum

**With reference to Appendix ,
of N_2O_4 is equivalent to appro
N_2 gas per hour.

Table

Vacuum Exposure Hrs.	N_2 psig	** Leakage (5 minutes)	Vacuum (torr)
0	0 15 100 200 270	-------- 2 bubbles 2 bubbles 0 2 bubbles	$6x10^{-8}$ $6x10^{-8}$ to $1.2x10^{-7}$
75	0 15 100 200 270	-------- 1 bubble 1 bubble 1 bubble 0	$7.8x10^{-8}$ $7.8x10^{-8}$ to $1x10^{-7}$
0	0 15 100 200 270	-------- 0 0 1 bubble 1 bubble	$1x10^{-7}$ $1x10^{-7}$ to $1.3x10^{-7}$
86.5	0 15 100 200 270	-------- 1 bubble 1 bubble 0 0	$1.2x10^{-7}$ $1.2x10^{-7}$ to $2.1x10^{-7}$

osed to vacuum during
cycle.

valve leakage of 0.1 cc/hr.
ximately 100 bubbles of

VACUUM CHAMBER TEST CIRCUIT OPERATING CYCLES
ALL PERTINENT DATA RECORDED

Condition	N_2 in psig	Valve 1	Valve 2	Valve 3	Remarks
1st Stage Vacuum chamber Pumping down	0	Closed	Closed	Closed	Valve not exposed to vacuum. Vacuum chamber pressure prior to start = 1 atmosphere
Hard vacuum established 10^{-8} torr range	0	Open	Closed	Closed	Observed vacuum chamber pressure Valve cycled briefly and valve leakage checked at each pressure level for 5 min. periods each
	15	Open	Open	Closed	
	100	Open	Open	Closed	
	200	Open	Open	Closed	
	270	Open	Open	Closed	
2nd Stage Pumping down	0	Closed	Closed	Open	Valve seat exposed to vacuum
Hard vacuum established 10^{-7} torr range	0	Closed	Closed	Open	Observed chamber vacuum pressure
	15	Open	Open	Closed	Valve cycled briefly and leakage checked at each pressure level for 5 min. periods each
	100	Open	Open	Closed	
	200	Open	Open	Closed	
	270	Open	Open	Closed	
	15	Open	Open	Closed	Rechecked valve leakage at minimum pressure level

NOTE: Reference above table to Figure 6

Table 3

VICKERS INCORPORATED
research and development department

ULTRA HIGH VACUUM CHAMBER TEST CIRCUIT
(EXTERNAL REMOTE CONTROL OPERATION)

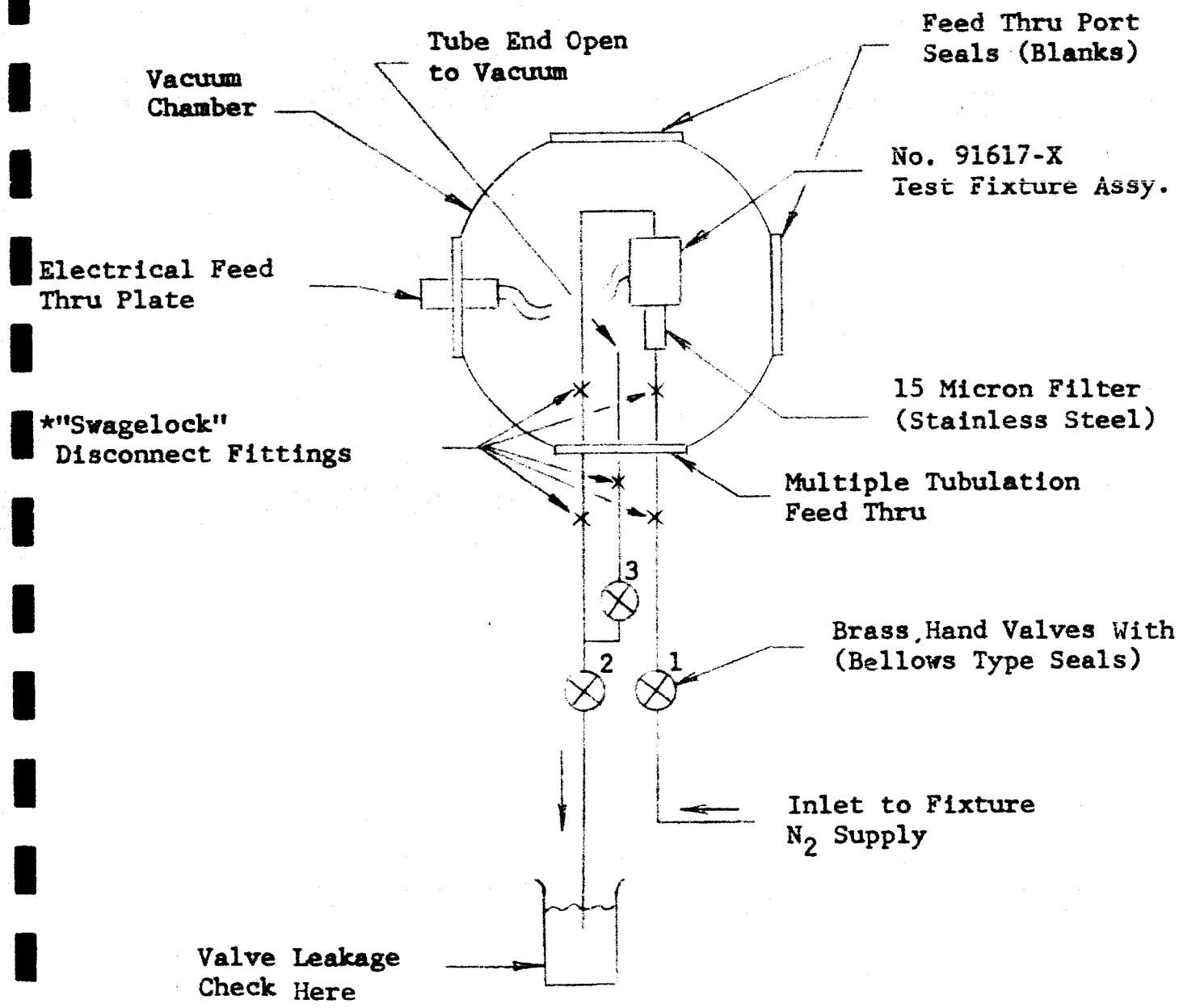

Figure 6

* All other tube connections were permanently silver soldered except the inlet and outlet ports of test fixture. These areas were fitted with AN fittings and Viton A rubber "O" rings.

Thrust Chamber

The basic design combustion chamber assembly was adapted from a proven 25 lb. rocket engine developed with Vickers' funding. The basic components were:

1. A high density graphite (Stackpole 331) combustion chamber shell.
2. A 347 stainless steel injector and mounting plate
3. A sintered 50-50 tantalum-carbide tungsten-carbide nozzle.
4. A Tayloron PA6 ablative nozzle extension.

Major modifications stemming from testing under this contract included addition of a .025 sheet tungsten liner for the combustion shell to reduce shell wall erosion. The liner modification extended engine life to the required 10 minutes firing at 10 cps equal on-off pulse width.

A second major modification reduced heat soak-back from the combustion chamber into the bipropellant valve block. A 0.5 inch thick pyrolytic graphite spacer was used to separate the graphite chamber from the 347 stainless valve block. High conductivity planes were orientated parallel to the injector face to provide accelerated heat rejection

in this area. The inside area of the pyrolytic spacer was contoured to minimize the injector face area exposed to direct flame.

A single triplet injector pattern was used. Two 45° fuel jets impinged on an axial oxidizer jet. This injector did provide the required 93% combustion efficiency (based on frozen equilibrium maximum theoretical C*) with an L* of 20. Further discussion on the injector design may be found in Section III.

The method of sealing combustion gases at flange joints was by compression loading of lapped faces. This method is simple and effective. A belleville type spring washer was part of the compression assembly and served the purpose of compensating for large axial thermal expansion and contraction.

Radiation cooling was the primary means of heat dissipation. Some convection air cooling cannot, of course, be avoided in sea level firings.

Test Descriptions (Thrust Chamber)

Table 4 is a list of tests conducted specifically for evaluation of the thrust chamber itself. Table 5 is a log of all firings.

Theoretical C* used throughout the test calculations was based on the frozen equilibrium value for N_2O_4 - Aerozine 50 of 5640 ft/sec. True theoretical C* lies somewhere between that for frozen equilibrium

To Determine Effect On	Parameter Varied	Type of Test
C*	L*	30 sec steady firing
C*	O/F Ratio	30 sec steady firing
C*	$\dot{\omega}_{total}$	30 sec steady firing
Nozzle Throat erosion	---------	All firings
Combustion chamber Shell Wall Erosion	Physical Design	60 sec steady firing
"	Material	60 sec steady firing
"	Firing Time	Steady & Pulsing @ 10 cps
Heat Soak Back	Physical Design	90 & 60 sec steady firings 10 min. pulse firing
Ablative Nozzle Extension Life	Accumulative firing time	All firings
(Nozzle Efficiency) Thrust Level	Sea level Design Versus Overexpanding Design	60 sec steady firing
Nozzle Reliability (Thermal Shock & hoop strength)	Nozzle Wall thickness	30 & 60 sec steady

Evaluation of Thrust Chamber

Table 4

Firing Number	Date	Firing Time Sec	Injjector	Combust Chamber Shell	Over-All Shell Lgth. Wt. Loss %	Nozz. Ser.#	Nozz. Ext.	L I
60-1	11-9-62	26	ST-1	GR-1 91669-X	1.623	50-50 #1 91687-X	PA6 #1	1
60-2	11-10-62	59	ST-1	GR-1 91669-X	"	50-50 #1	PA6 #1	1
60-3	11-14-62	2.9	ST-1 Lapped	GR-3 91669-X	2.830	50-50 #1	PA6 #1	2
60-4	11-15-62	29.9	ST-1	GR-3 61669-X	"	"	"	2
60-5	11-16-62	29	ST-1	GR-2 61669-X	2.196 0.6%	"	"	2
60-6	11-19-62	28.1	ST-1	GR-4 61669-X	3.427	"	"	3
60-7	11-19-62	33.9	ST-1	GR-4 61669-X	" 1.1%	"	30	3
60-8	11-20-62	30.0	DT-2	GR-5 61669-X	1.623 2.3%	" Failed	"	1
60-9	11-21-62	32.5	ST-1	GR-4 61669-X	3.427 1.1%	50-50 #2	PA6 #2	3
60-10	11-29-62	17	DT-2	GR-6 61669-X	.9375	"	None	1
60-11	Restart of 60-10	15	"	"	" 0.2%	"	"	"

CODE:
S.T. = Single Triplet 91750-X
S.T.V. = Single Triplet with Valve
D.T. = Double Triplet 91767-X

NASA CONTRACT NAS 9-554

FIRING PERFORMANCE EVALUATION

* n	Thrust #	P Chamb. psi-A	OX P tank psi	OX ΔP	OX Flow-meter #ω/sec	FUEL P tank psi	FUEL ΔP	FUEL Flow-meter #ω/sec	ω̇ Tota #/se
5		151	213	77	.138	225	89	.087 Extim.	.225
5		153	208	71	.1385	231	93	.0905	.229
5		152	200	63	.137	212	75	.090	.27
5	36.0	151	214	78	.135	224	88	.0875	.222
0	35.4	147	212	80	.133	224	92	.0865	.219
0	36.0	149	228	94	.136	222	88	.0854	.221
5	.8	149	214	80	.129	226	92	.0865	.215
5	37.2	150	211	76	.131	252	117	.0926	.223
0	37.0	147	205	73	.129	220	88	.0850	.214
0	32.2	141	226	100	.125	240	114	.036	.271
	33.2	137	212	90	.117	240	118	.036	.213
	34.4	138	216	93	.1215	238	115	.0855	.207

2

— Before Firing
— After Firing
— After Sandblast

Throat Area	O/F	(5640 Theo. C*) C*	%	Response Current Start to P_c Max	Throat Diam.	Nozz. Wght.	Max. Soak Temp °F After Firing	Max. Soak Temp °F During Firing
.232	1.59	5000	89.0		.539 .539	gm		
.232	1.53	4995	88.4		.539B .541A	-- -- 189.8		
.2342	1.52	5030	89.1		.541B .542A	189.8 189.4	550	240
.235	1.54	5070	90.0		.542B .542A	189.4	570	240
.235	1.54	5090	90.1		.542B .542A	189.0 189.0 188.7	580	310
.235	1.59	5090	90.1		.542B -- --	188.7 -- --	590	290
.235	1.49	5230	92.8		-- -- .546A	-- 188.2 187.3	680	440
.236	1.42	5190	92.0		.546B -- .559A	187.3 187.0 185.9	740	320
.2315	1.52	5140	91.0		.538B -- .539A	190.8 190.8 190.2	595	320
.232 .232	1.45 1.36	4950 5010	87.8 89.3		.539B -- --	190.2 -- --	505	130
.232	1.42	5090	90.1		-- -- .540A	-- 190.1 189.5	620	330

5

TABLE 5

Firing Number	Date	Firing Time Sec	Inj-jector	Combust Chamber Shell	Ov Al Sh Lg W Lo
60-12	11-30-62	16.5 Fail-ed	ST-1 Lapped	GR=2 61669-X	2.
60-13	12-3-62	31.3	ST-1	GR-2 61669-X	2. 0.
60-14	12-4-62	31.9	ST-1	GR-7 92212-X	1. 2.
60-15	12-5-62	90	ST-1	GR-7 92212-X PG-INSU.	
60-16	12-6	30 10CPS	STV-1	GR-7 92212-X PG-INSU.	1 0
60-17	12-11-62	59	ST-1	GR-7 82212-X SB-2003	1 4.
60-18	12-14	30 10CPS	"	"	"
60-18	12-14	30 RE-START STEADY	"	"	" 0
60-19	12-19-62	15SEC 10CPS 22SEC s.s.	STV-1	GR-7 SK-2003	

NASA CONTRACT NAS 9-554

FIRING PERFORMANCE EVALUATION

er- l ell th. t. ss %	Nozz. Ser.#	Nozz. Ext.	L* In	Thrust #	P Chamb psi-A	OX P tank psi	OX ΔP	OX Flow-meter #ω/sec	FUEL P tank psi	FUEL ΔP	FUEL Flow meter #ω/s
196	50-50 #2	None	20	32.0	140	210	85	.144	187	62	.06
				33.2	144	210	81	.1395	198	69	.07
				33.4	145	212	82	.1395	210	80	.07
				35.4	152	224	87	.145	284	87	.08
196 7%	50-50 #3 91687-X	PA6 #2	20	32.8	142	202		.130	206		.07
				34.0	146	---		.1295	---		.08
				34.8	149	196		.1275	248		.08
				36.0	153	198		.124	262		.09
				36.8	155	198		.1225	280		.09
				37.7	158	---		.122	---		.10
				38.4	160	198		.1205	306		.10
				37.2	158	---		.1215	---		.10
				36.6	156.5	200	.	.1235	278		.09
492 1%	"	"	12	31.6	138.7	196	67	.131	240	111	.07
				33.3	144			.127	240		.08
				33.8	143			.1215			.09
	"	" Failed	"	32.6	143	198	70	Failed	230	102	.08
449 .3%	50-50 #4 91687-X	PA6 #1	"	Not Meas.	141 s.s. 140Ω	274 s.s.	148 s.s.	.1440 s.s.	228 s.s.	102 s.s.	.08 s.
443 .3%	"	"	"	39.8	132	.206		.1325	190		.08
	"	"	"	---	65	226		---	248		Resti Fl
.2%	"	"	"	---	132	230	113	.123	240	123	.0
	50-50 #4 91687-X	PA6 #1	12	--- Erratic Puls	140	240 at 10	115 CPS	.137	260	135	--

V

— Before Firing
— After Firing
— After Sandblast

r ec	ẇ Total #/sec	Throat Area	O/F	(5640 Theo. C*) C*	(5640 Theo. C*) N%	Response Current Start to P_c Max	Throat Diam.	Nozz. Wght.	After Firing Soak Temp °F	During Firing Soak Temp °F
3	.212		2.12	4990	88.5		.540B	189.3	Room	Room
2	.2115	.233	1.935	5150	91.0					
6	.2155		1.835	5090	90.0					
05	.2255		1.80	5100	80.1					
4	.204		1.73	5200	92.1		.539B	191.8	545	240
25	.212		1.54	5150	91.3		---	191.6		
90	.2165		1.405	5150	91.3		.541A	191.0		
30	.217		1.30	5260	93.4					
95	.220	.232	1.266	5220	92.5					
3	.225		1.185	5230	92.9					
7	.2275		1.10	5250	93.0					
3	.2245		1.18	5250	93.0					
9	.2225		1.249	5250	93.0					
5	.206	.2342	1.75	5060	89.7		.541B	191.0	330	Room
7	.214	.2342	1.38	5055	89.7		---	191.0		
50	.2165		1.28	5055	89.7		.542A	190.5		
20	.						.542	190.5	525	305
25 s.	.2265	.2273	1.745	4546	80.6 s.s.	P_c Strt. to P_c Max. 5MSEC	.539B --- .539A	191.5 191.4 191.4	200	100°F
55	.2180	.2307	1.55	4488	79.6		.539B .536 .542A	191.4 191.4 190.8	470	280
icted -- w		.2307	---	---	---	10 MSEC	.542B --- ---	190.8 --- ---	---	---
3	.206	.2307	1.48	4760	84.5		--- --- .542A	--- 190.7 190.3	---	---
.						Erratic	.542B --- .542A	190.3 "		

3

TABLE 5A

Firing Number	Date	Firing Time Sec	Inj-jector	Combust Chamber Shell	Over-All Shell Lgth. Wt. Loss %	Nozz. Ser.#	Nozz. Ext.	L* In	Th
60-20	12-20-62	68	ST-1	GR-8 92644-X 92645-X	1.970 +.500 4.7%	50-50 #5 92472-X	None	20	36
60-21	12-26-62	59 s.s.	STV-1	"	"	50-50 #4 91687-X	PA6 #1	"	--
60-22	12-27-62	74	STV-1	"	"	"	"	"	--
60-23	12-28-62	22.5 s.s. 187.7 100CPS	STV-1	" 92644-X 411SEC Total	" 25%	" 8.8min Total Time Cracked (Therm. Shock)	" 13.2 min. Bndr. Gone	"	--
60-24	1-3-63 Cell 2	3 s.s 120 10CPS	STV-1	GR-9 92644-X 92645-X	" 11.5%	50-50 #3 91687-X	PA6 #3	"	--
60-25	1-7-63 Cell 1	58	ST-1	GR-10 92644-X 92645-X T_aC Plasma	" 7.9%	"	"	"	--
60-26	1-10-63 Cell 1	61	ST-1	GR-11 92644-X 92645-X Pyrol. Infilt.	" 4.9%	50-50 #6 92472-X	PG #1 Pyro Ring	"	--
60-27	1-14-63 Cell 1	407 10CPS	STV-1	GR-12 92644-X 92645-X	" 25%	"	"	"	--

NASA CONTRACT NAS 9-554

FIRING PERFORMANCE EVALUATION

rust	P Chamb psi-A	OX P tank psi	OX ΔP	OX Flow-meter #ω/sec	FUEL P tank psi	FUEL ΔP	FUEL Flow-meter #ω/sec	ω̇ Total #/sec	Thro Area
2	142	226	99	.131	230	103	.0795	.2105	.233
	140	240	117	.138	274	151	.082	.220	.237
	145								
	146	238	107	.138	270	139	.080	.218	.243
	145 10CPS								
	143	220	92	.134	240	112	.091	.225	.246
	145	228 +60 -40	78 avg	---	236 +88 -36	92 avg	---		.246
	128	184	71	.117			.079	.196	
	180			.1215			.083	.2045	
	134			.120			.089	.209	.247
	135			.1195			.0955	.215	
	140			.119			.101	.220	
	135			.123			.083	.206	
	137			.119			.090	.209	
	150			.1325			.090	.2225	.233
	153			.131			.097	.228	
	154			.131			.0985	.2295	
	146 avg Puls.	218			248			.209 avg based on Tank P	.236

2

— Before Firing
— After Firing
— After Sandblast

at	O/F	(5640 Theo. C*) C*	N%	Response Current Start to P_c Max	Throat Diam.	Nozz. Wght.	After Firing Soak Temp °F	During Soak Temp °F
5	1.65	5060	89.7		.540 .540 .543	261.0 260.5 251.9	460	310
5	1.68	4860	84.6	Would Not Cycle	.545B --- .548A	--- --- ---	250M	160
				15 On 9 Off	.548B --- .551A	--- --- ---	330M	
5	1.73	5250	93.1	14MSEC on 9MSEC off	.551B	---	370	305
5	1.47	5040	89.4	15 on 9 off	.555B --- .556A	183.8 182.5 180.2	355	
5								
	1.48 1.66 1.35 1.25 1.18	5200 5065 5115 5010 5075	92.2 89.9 80.6 89.0 90.0		.556B --- .560A	180.2 179.6 178.0	460	310
	1.48 1.32 1.47 1.35 1.33	4920 4920 5060 5040 5055	87.3 87.3 89.7 89.3 89.6		.540B --- .544A	262.8 262.4 259.4	445 (Mass) 690 (Bolt) 1055 (Nozz. Ext at Pyro Ring)	
5	1.40	5310	94.3	14 On 11 Off	.544B --- .558A	259.4 251.8 248.6	430	430

TABLE 5B

3

Firing Number	Date	Firing Time Sec	Inj-jector	Combust Chamber Shell	Over-All Shell Lgth. Wt. Loss %	Nozz. Ser.#	N E
60-28	1-21-63 Cell 2	Pulse Bit	STV-1	GR-11	1.970 +.500	50-50 #5 92472	
60-29	1-21-63	61	ST-1	Low Dens. Pyrolyt. Infilt. GR-13	" 7.3%	50-50 #3	
60-30	1-25-63	66.1 s.s.	ST-1	W-Liner in 92644-X GR-14	" 1.96%	50-50 #5 92472-X	
60-31	1-31-63	15SEC Min. Pulse Bit	STV-2	GR-15 92644-X Flush Seal	"	"	
60-32	2-4-63	58.8 10CPS + 48 Pulse Bit	STV-2	GR-15 + W-Liner	" 25%	"	
60-33	2-13-63	Min. Pulse Bit	STV-2	GR-14	"	"	
60-34	2-18-63	Final Firing 15SEC	STV-2	GR-16 W-Liner	"	50-50 #7 92472-X Flush Seal	PA # P R

NASA CONTRACT NAS 9-554

FIRING PERFORMANCE EVALUATION

ozz. kt.	L* In	Thrust #	P Chamb psi-A	OX P tank psi	OX ΔP	OX Flow-meter #ω/sec	FUEL P tank psi	FUEL ΔP	FUEL Flow-meter #ω/sec	ω Total #/sec	Th Ar
		IMPROPER OPERATION CAUSED BY HIGH FRICTION BIND IN									
	"	---	130	210		.131	212		.0795	.2105	.2
	"	---	134	200		.125	226		.0795	.2060	.2
	"	---	145						XDUCER ERROR		
	"	---	150								
	"	42.0 Surge		235		.1585 Surge	235		.120 Surge		
5 yro ing	"	50.0 Surge		235			235				

— Before Firing
— After Firing
— After Sandblast

at O/F	(5640 Theo. C*) C*	N%	Response Current Start to P_c Max	Throat Diam.	Nozz. Wght.	After Firing Soak Temp °F	During Firing Soak Temp °F
SEMBLY				.543B --- .543A	258.0 --- 258.0		
1.65	4990	88.5		.560B --- .564	178.0 177.2 174.3		
1.544	4930	87.5		.543B --- .548A	258.0 256.3 254.8		
			15 On 10 Off	.548B --- .548A	254.8 --- 254.8		
			25 On 15 Off	.548B --- .557A	254.8 245.0 241.3	460	460
1.32	Minimum Surge Impulse .231 #SEC		16 On 5 Off	.557B --- .557A	241.3 --- 241.3		
	Minimum Impulse .177 #SEC		16 On 3 Off				

TABLE 5C

3

and the higher 5718 ft/sec for shifting equilibrium. It is felt that for these sea level firings, very little equilibrium shift can occur from throat to exit because of the combination of high gas velocity, short expansion length, and relatively small area expansion ratio (2.3). Thus, true theoretical C* can be considered close to the frozen equilibrium value of 5640 ft/sec.

L* was varied by changing the length of graphite combustion chamber shell. The O/F ratio was varied by manipulation of fuel and oxidizer injection pressures.

Nozzle throat erosion was determined by measurement before and after firing. It is important to note, however, that the nozzle material oxidizes when exposed to atmosphere immediately after shutdown from hot firing. Differentiation must be made between actual erosion and oxidation scale. The latter is easily removed by sandblasting and constitutes increase in throat diameter over and above erosion.

Shell wall erosion was determined by % weight loss after firing. Physical design changes to minimize erosion included injector spray pattern modification, vapor deposit of tungsten on graphite, tungsten sheet liner, and shell material changes.

Heat soak-back was measured by chromel-alumel thermocouples placed on the back side of the injector plate and separated from the hot

combustion chamber shell by 3/16 inches of stainless steel. The two prime reasons for controlling heat soak-back are: (1) control of propellant temperature rise in the bipropellant valve with poppets closed; and (2) maintenance of construction material temperatures within the limits for reliable operation.

A maximum of 500°F at the point of temperature measurement was determined to be satisfactory in both respects.

Nozzle reliability was based on absence of failure with repeated steady firings and long pulse firings. Failures are classified as as fracture or excessive erosion. Fractures were experienced during initial phases of testing from thermal shock, undesirable loading, and hoop stress.

Test Results and Discussion (Thrust Chamber)

Figure 7 shows the results how C* or combustion efficiency varied with L* and O/F ratio. Figure 8 shows how C* or combustion efficiency varied with O/F ratio for all firings with L* = 20.

Figure 8 is presented to show that good combustion efficiency could

be attained over a wide range of O/F ratios. The wide spread of efficiencies was a result of multi-parameter variation from test to test where factors other then optimum efficiency were being evaluated. Optimum efficiency can only be achieved, of course, by a particular relationship between total propellant flow, chamber pressure, and nozzle throat area.

An L* of 20 was determined to be the most desirable for this unit.

The designed chamber pressure was 150 psia. Chamber pressure is a function of nozzle throat area, total propellant flow, and C*.

FIGURE 7

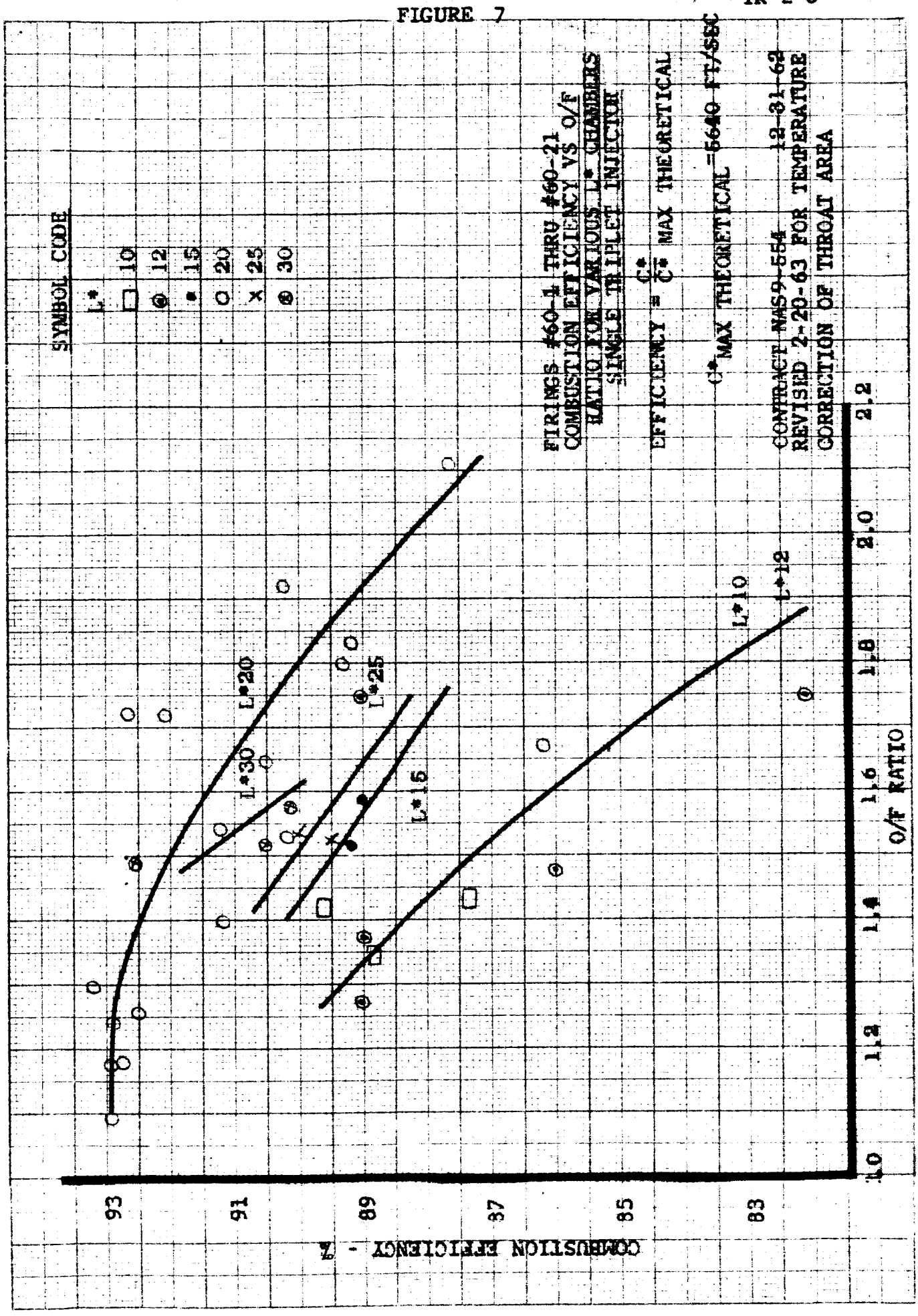
SYMBOL CODE
L* 10
12
15
20
25
30
FIRINGS #60-1 THRU #60-21
COMBUSTION EFFICIENCY VS O/F
RATIO FOR VARIOUS L* CHAMBERS
SINGLE TRIPLET INJECTOR
EFFICIENCY = C*/C* MAX THEORETICAL
C* MAX THEORETICAL = 6640 FT/SEC
CONTRACT NAS9-554 12-31-62
REVISED 2-20-63 FOR TEMPERATURE
CORRECTION OF THROAT AREA
L*10
L*12
L*15
L*20
L*25
L*30
COMBUSTION EFFICIENCY - %
93
91
89
87
85
83
O/F RATIO
1.0
1.2
1.4
1.6
1.8
2.0
2.2

10 X 10 TO THE ½ INCH 359T-11

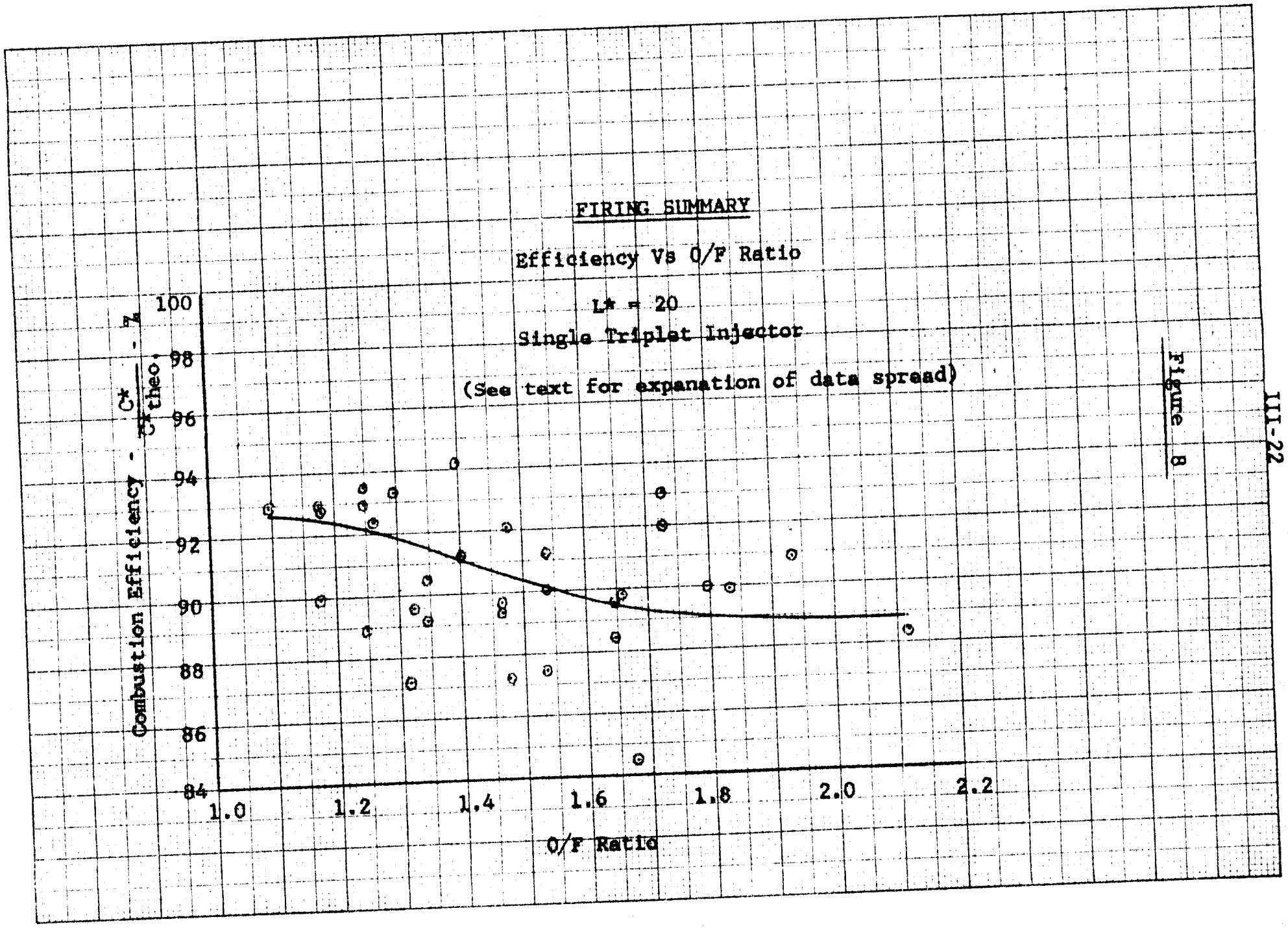

Figure 8

From the above named curves the following data was determined ideal to meet thrust, chamber pressure, and efficiency requirements for the single triplet injector with an L* of 20.

$$O/F \text{ ratio} = 1.2$$

$$\dot{\omega}_{ox} = .121 \text{ \#/sec}$$

$$\dot{\omega}_{fuel} = .101 \text{ \#/sec}$$

$$\dot{\omega}_{total} = .222 \text{ \#/sec}$$

For calculation of C* the following general equation was used

$$C^* = \frac{P_1 A_t g}{\dot{\omega}_T}$$

Since A_t, throat area, is impossible to measure accurately during a firing the following assumptions were made.

1. Erosion was negligible
2. The mean temperature of throat was 2600°F during firing. This is of course conservative.
3. The throat diameter therefore during firing equalled the diameter before firing plus thermal expansion based on 2500°F ΔT.

Since $\alpha_{TaCWC} = 4.0 \times 10^{-6}$ at 2500°F

$$A_{t_{2600}} = \frac{\pi}{4} \left\{ d_{t_{100}} \left[1 + (4.0 \times 10^{-6})(2500) \right] \right\}^2$$

$$A_{t_{2600}} = \frac{\pi}{4} (1.02)(d_{t_{100}})^2$$

This factor for throat area calculation was used to revise all C* values on the firing history table. (Note: C* values listed in progress reports #4 and #5 under this contract do not contain this temperature correction and will appear slightly low.)

Combustion Shell Erosion

Combustion chamber shell erosion was noted early in the firing program. The shell material is Stackpole 331 high density graphite.

Erosion was measured by weight loss. After 30 second steady state firings, gross weight loss was negligible, but a slight localized erosion pattern was observed. This pattern was determined to be caused by propellant impingement on the hot shell wall. The single triplet spray pattern results in a fan spray as shown below which explains the impingement on the shell wall and the localized erosion.

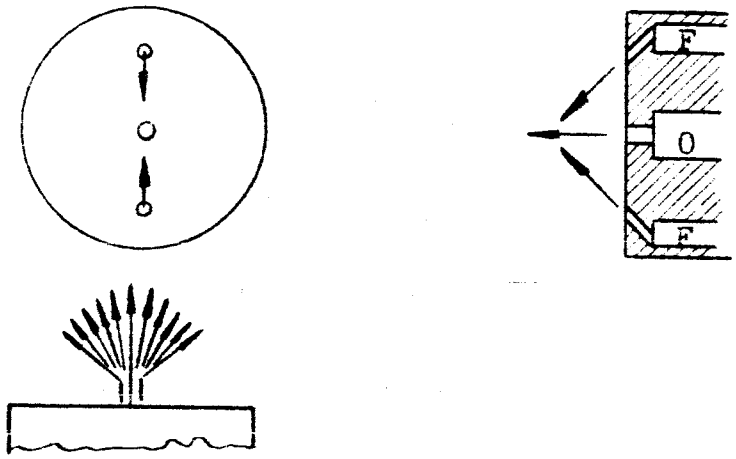

Figure 8A

Single Triplet Injection Fan Spray Pattern

One minute firings later in the program pointed up this shell erosion as a potential trouble spot with 4 to 5% weight loss over the one minute steady firing. Firing 60-23 on December 28 confirmed the weakness: erosion failure of the graphite shell after 411 seconds (6.85 minutes) total firing time.

Two approaches were considered to reduce erosion: (1) change the injector design to achieve a symmetrical, non-impinging spray pattern; and (2) provide erosion resistance through material changes or coatings to the combustion chamber shell.

After consideration it was decided not to change the injector design. The integrated valve body injector hardware had already been built and much test data already accumulated on it. Contract timing

would have been considerably set back by such a major change. In addition, the probability of sufficient improvement in firing life by such a change was not assured.

Improvement in erosion resistance was thus the goal set upon.

Table 6 lists the material changes and compares erosion resistance to high density graphite.

Table 6

Combustion Shell Erosion

Material	Steady State Firing Time	Firing #	% Weight Loss	Comments
High Density Graphite-331	68 sec	#60-20	4.7	Severe Local Erosion
H.D. Graphite with .004 TaC Plasma Sprayed	58 sec	60-25	7.9	TaC Lost After 15 sec.
H.D. Graphite Infiltrated with Pyrolytic graphite	61 sec	60-26	4.9%	Local Erosion Less Severe
Low Density Graphite Infiltrated with Pyrolytic Graphite	61 sec	60-29	7.3	Severe Erosion
.025 Tungsten Sheet Hot Wrapped as a Liner for H.D. Graphite	66 sec	60-31	1.96	Satisfactory

Several other materials were obtained and ready for firing evaluation but were not tested because of the success of the tungsten liner and because the contract completion deadline was close.

Among these were .010 tungsten vapor deposit on high density graphite and some experimental graphite and graphite-cermet mix materials.

At the contract completion the required 10 minute, 10 cps, equal on-off, pulse firing had been achieved but it was still the combustion chamber shell erosion which limited the life to ten minutes. At the time of this writing, under company sponsored development, Vickers has essentially eliminated this erosion problem.

Fabrication of Tungsten Sheet Liner

The dimensional requirements of the liner fabricated were: 1.5 inches in diameter and 2 inches long. The material used was a recrystallized tungsten sheet measuring 2 inches by 7 inches and .023 to .027 thick.

The furnace temperature range required to form the tungsten was between 700 to 1000°F. Temperatures below 700°F caused the material to revert back to a brittle condition and temperatures above 1000°F caused the material to oxidize. This left no choice but to form the

liner directly in the furnace using extension tools. To accomplish this, 2 fixtures (Figure 9) were designed and fabricated.

Liner forming sequence was accomplished, as follows, with reference to Figure 10.

Operation 1 formed a lip ¼ inch wide at one end of sheet to be used for attachment to the forming arbor.

Operation 2 clamped prebent sheet into forming arbor and placed in the furnace. Temperature of 1000°F was maintained for 1¼ hrs.

Operation 3 formed the sheet around the arbor by reaching into furnace with an extension handle and rotating the forming bar "C" clockwise as shown.

Operation 4 consist of trimming the liner as shown to obtain an overlap condition. One end of liner was chamfered to conform with inside angle of the nozzle to establish a smooth transition for the gas flows.

To install the liner into the graphite chamber, a hose clamp was employed to collapse the liner uniformally. Clamp was removed after starting the liner into chamber after which the liner was pushed into proper location.

Tungsten Liner Forming Fixture

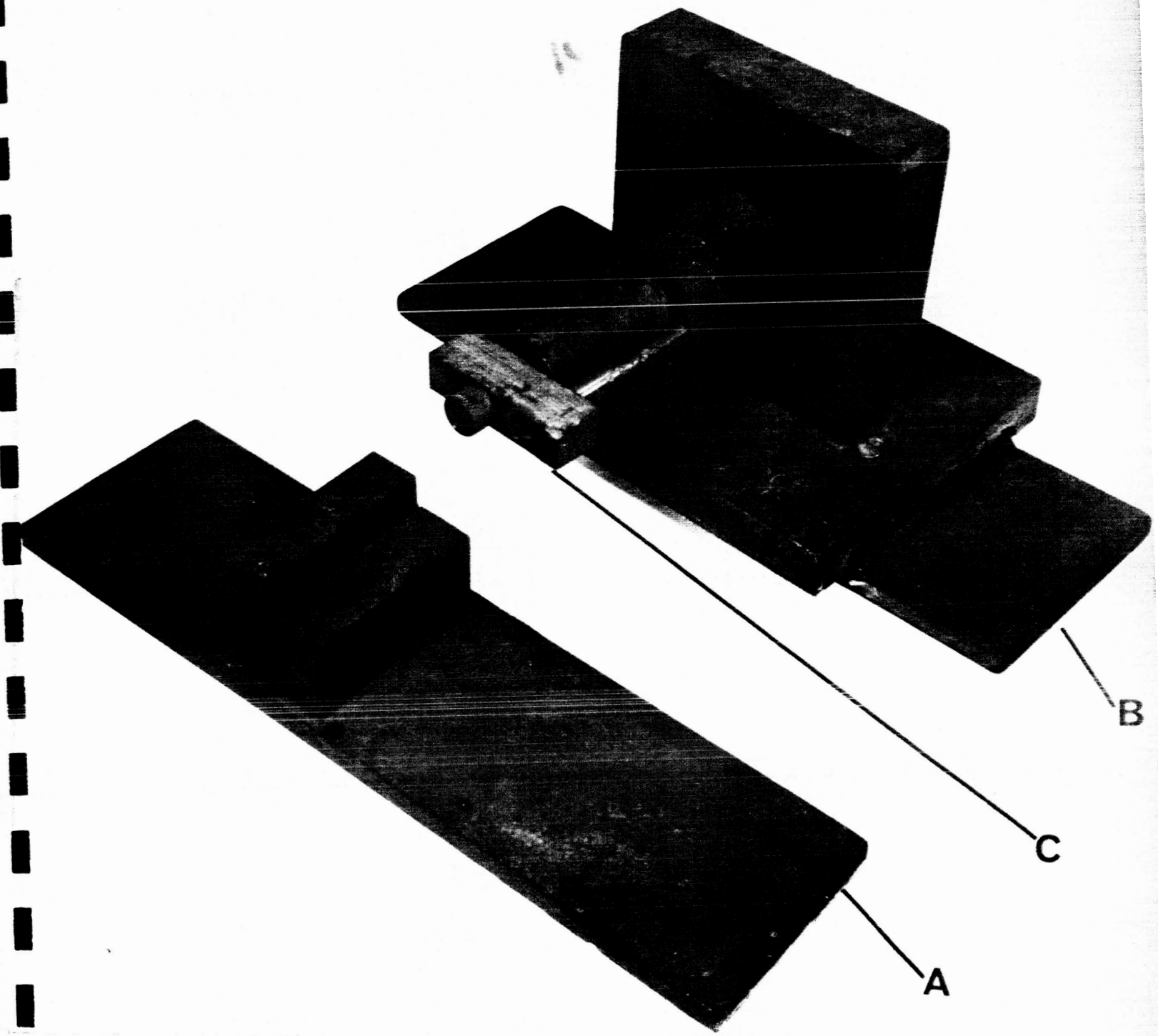

Figure 9

Tungsten Liner Forming Sequence

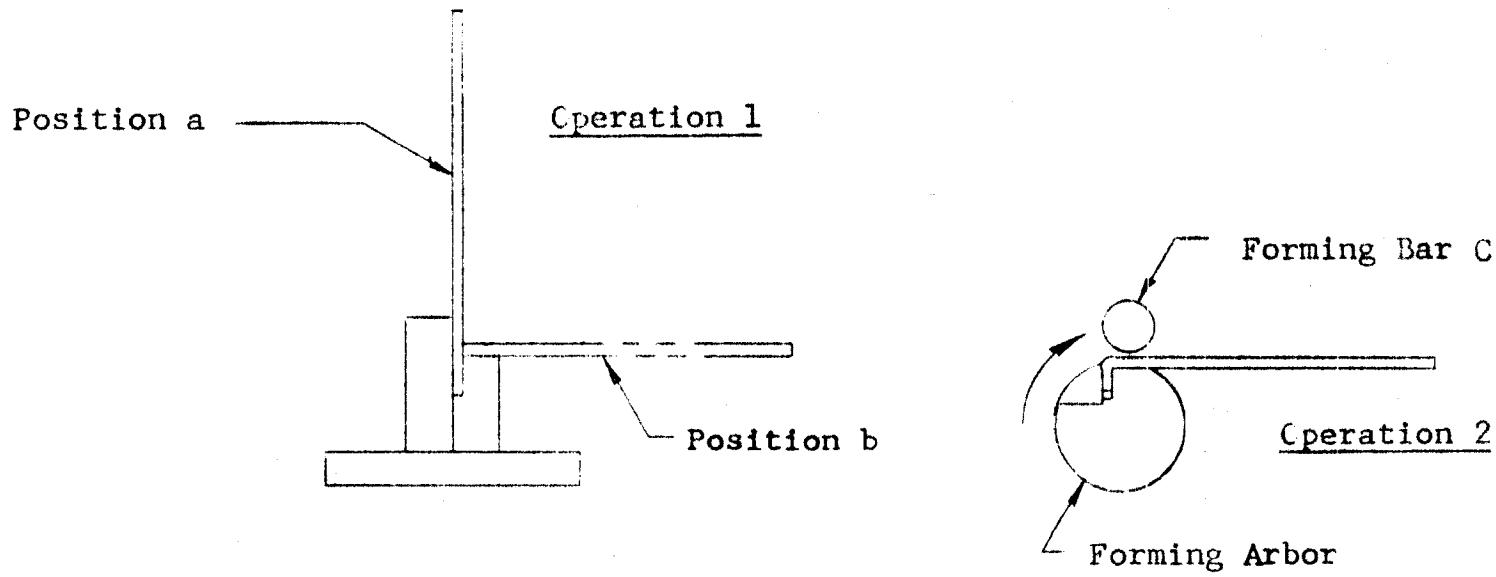

Fixture A (Figure

Fixture B (Figure

Fixture B (Figure

Figure 10

VICKERS INCORPORATED
research and development department

Heat Soak-Back

Measurement of "hot-Spot" temperature during firing and heat soak-back at that point after firing is summarized in Figure 11 . The reasons for controlling heat soak-back, and the maximum desired temperature of 500°F at the point of measurement were discussed previously.

Referring to the curve for steady state firings of Figure 11, it can be seen that soak-back temperatures of the original thrust chamber assembly were too high. Two modifications incorporating high temperature insulating spacers between the graphite shell and the injector plate were effective but had limited life. The final acceptable modification utilized the properties of high heat conductivity and high emissivity possessed by anisotropic pyrolytic graphite oriented parallel to the injector face. A 0.5 inch thick spacer proved effective in reducing final steady state temperatures to 450°F or below (at the "hot-spot" point of measurement).

The 10 cps firings shown in Figure 11 incorporated the pyrolytic spacer. It is significant that firing and soak-back temperatures saturate out at about the same temperature magnitude whether the firing mode is steady state or pulsing. The only difference between the two modes of firing is the time required to reach saturation temperature.

HEAT SOAK-BACK

Steady State and 10 cps Equal On-Off Time Firings

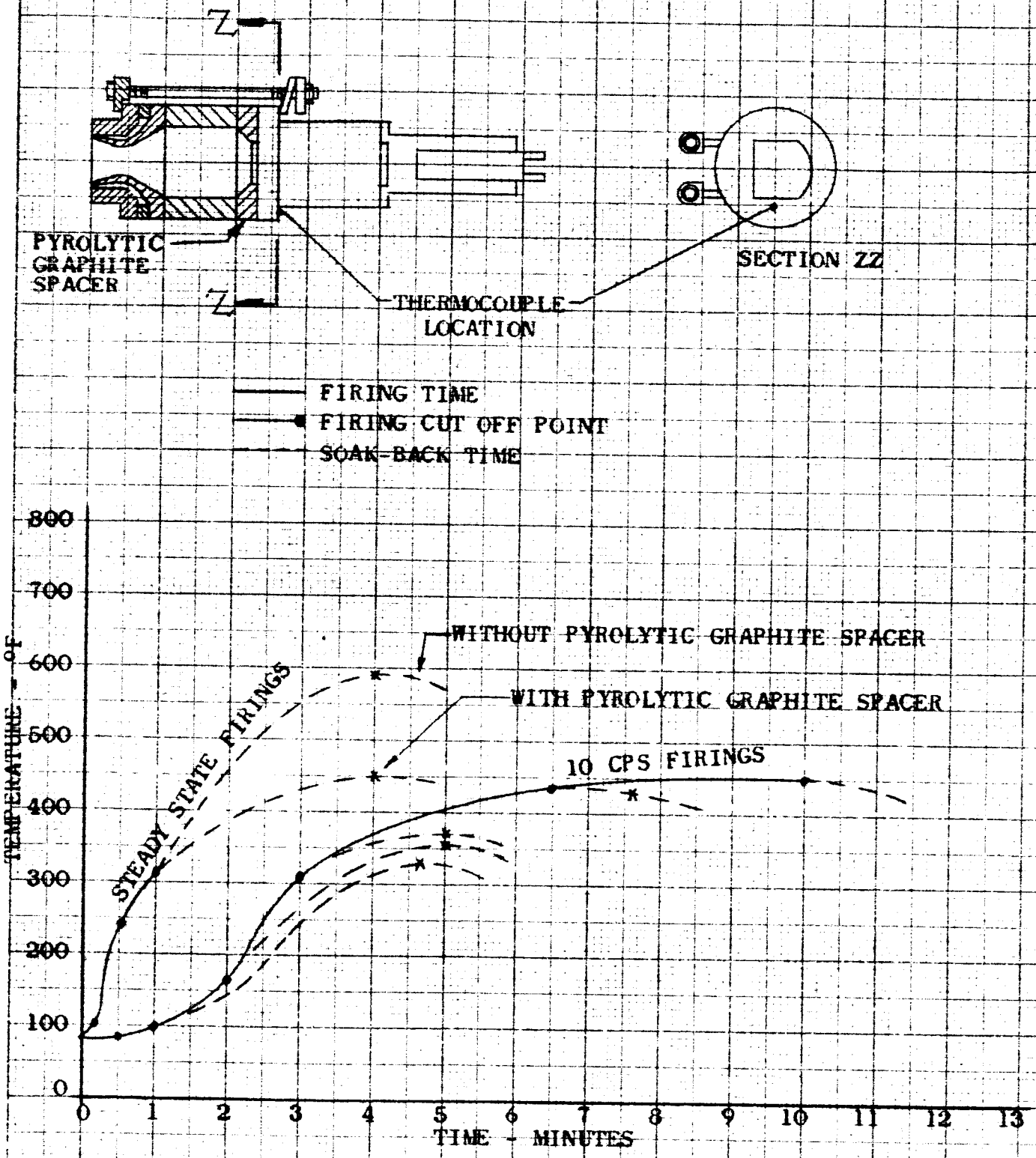

Figure 11

K+E 10 X 10 TO THE ½ INCH 359T-12 KEUFFEL & ESSER CO.

Combustion temperature is influenced by O/F ratio and combustion efficiency. Therefore a radical change in desired O/F ratio or an increase in desired combustion efficiency might require additional control of heat soak-back.

Ablative Nozzle Extension

The large 40:1 area ratio nozzle was not fired at Vickers because vacuum firing facilities were not yet available. Sea level firings did however allow evaluation of the nozzle extension material by incorporating a partial nozzle extension, cutoff at the sea level nozzle exit. Comparison photographs of vacuum and sea level test assemblies, Figures 1 and 3 , show the vacuum nozzle and sea-level extension. Figure 12 below shows the cutoff nozzle extension still in good condition after 467 seconds firing time.

Tayloron PA6

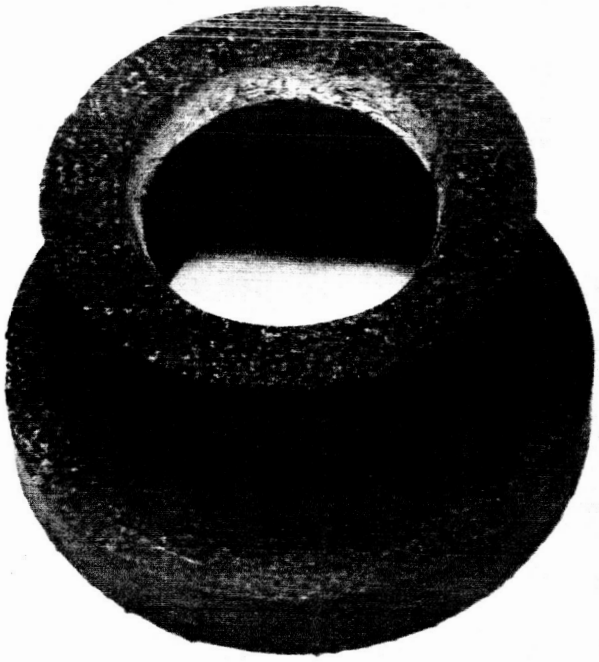

Tayloron PG

Cut-Off Nozzle Extensions After Firing

Figure 12

Both materials, Tayloron PA6 and PG, evaluated for this part proved satisfactory. The materials were chosen for lightness, ablative qualities, and resistance to mechanical shock. The PA6 was chosen for the final assembly because it formed a heavier protective charr layer.

Firing test results showed the effective life of the ablative nozzle extension to be about 13 minutes accumulated over 16 firings, with no attempt to control after-burning. Life-limit was determined by the extent of charring from both the inside and outside to cause porosity. One part, PA6#2, failed prematurely after 2½ minutes accumulated time, but failure was accelerated by a combustion chamber leak causing very high localized heat flux and asymmetrical loading on the extension flange.

Material limitations which require care in design were discovered during the test program, as discussed below.

One, in sea level firings, the phenolic binder will burn when exposed to air in the absence of a good charr layer. This burning occurs for sometime after shutdown of a duration firing where temperatures are high enough to cause combustion but not high enough to build up a protective charr on the outside surfaces. Repeated after-burning eventually weakens the structure and causes localized porosity. After-burning would not occur in space and is thus only a test problem. To obtain maximum test life from sea

level firings with this material, an external means of extinguishing the after-flame is desirable; a pair of nitrogen jets aimed at the external surface near the nozzle exit and actuated after shut-down is effective.

Two, because the carbonized charr layer, which builds up adjacent to high heat flux areas, is less dense than its original structure, some shrinkage occurs in the charred areas. This shrinkage proved troublesome in early firings by exceeding the assembled compression of the belleville spring, causing loss of compression and combustion gas leakage at flange seals. The high compression flange joint was required between the ablative extension and carbide nozzle to maintain gas tight sealing for full gas expansion to vacuum environment. Further testing showed that the ablative shrinkage rate tapers off exponentially with time. Thus pre-firing a new part and then re-torquing the assembly nuts to take-up the shrinkage provided enough belleville spring flexibility to handle further shrinkage for long duration firings.

In later developmental firings it was found that by reducing the heat flux in the flange area where the extension contacted the hot nozzle, shrinkage could be halved. Heat flux was reduced by adding a .23 inch thick anisotropic spacer between the PA6 extension and the

carbide nozzle, which held the PA6 contact temperature to 1055°F (firing #60-26).

In the final week of the contract an ablative material was received which Vickers considers somewhat superior to either Tayoloron PA6 or PG. It is a high silica phenolic with a nylon additive that should possess higher resistance to oxidation, somewhat better ablative properties, and possibly superior erosion resistance. Time was not available for test evaluation of this material under the contract.

Nozzle Erosion

Nozzle erosion, as was discussed previously, is difficult to separate from oxidation in sea level test firings. The only oxidation which is troublesome occurs in the throat area after shut down from the hot nozzle being exposed to atmosphere. Measurements of throat diameter before and after one minute steady firings show generally less than .0005 loss in diameter. Sandblasting the nozzle to remove loose oxide scale results in an additional .003 to .004 loss in throat diameter.

Probably the most significant conclusion that can be made regarding throat erosion is that with regard to causing changes in thrust during firings, nozzle throat erosion is insignificant compared to thermal expansion of the throat.

Figure 13 shows overall percentage weight loss with firing time. Since most of the oxidation scale occurs on external surfaces of the nozzle, most of the weight loss is confined to the external surfaces.

Some nozzle erosion was clearly definable in instances where out-of-roundness was measured in the throat area by means of 30:1 comparator traces before and after firing. The increase in throat area attributable to this out-of-round was, however, insignificant.

Nozzle Efficiency (Thrust Level)

Ideal sea level thrust comparable to 60# vacuum thrust is 43.5#. Initial sea level firings were short of optimum thrust because the vacuum nozzle throat section, 91687-X, was used. This nozzle was deliberatly overexpanding to provide flow continuity with the 40:1 vacuum "bell" nozzle extension. Later firings used a later designed nozzle, 92472-X, with optimum expansion for sea level. The two nozzles are shown in Figure 14.

Figure 13

Nozzle Weight Loss Due To Erosion and Oxidation Scale

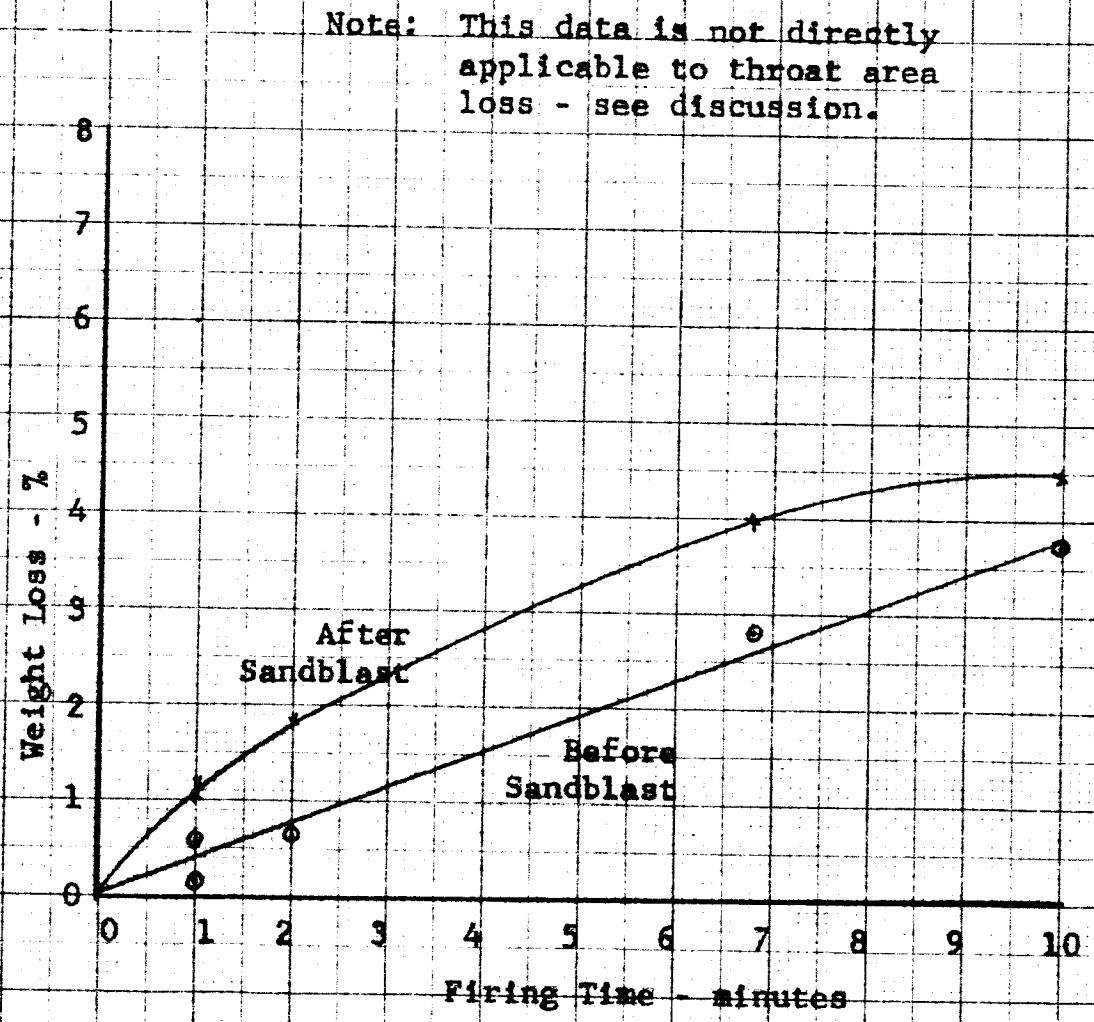

Overexpanding Nozzle For Continuity With 40:1 Vacuum "Bell" Nozzle

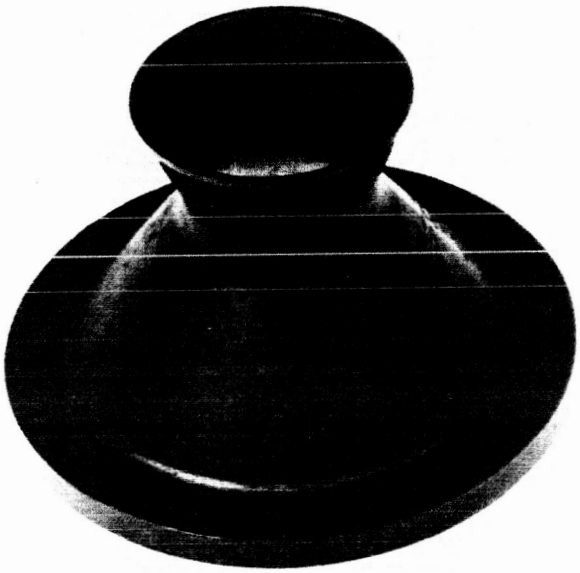

91687-X

Optimum Expansion For Sea Level

92644-X

Figure 14

Figures 15 and 16 show comparisons of the flame for optimum and over expansion nozzles. Visual monitoring of the flame during firings of the sea-level nozzle showed 5 to 7 clear shock diamonds depending upon conditions of the firing.

The integrated pulse rocket delivered under the contract was assembled with a sea level nozzle and cut-off extension. The vacuum nozzle and extension were delivered as additional parts.

Nozzle Reliability

Initial test firings brought out two trouble spots that required design changes to bring about maximum nozzle reliability.

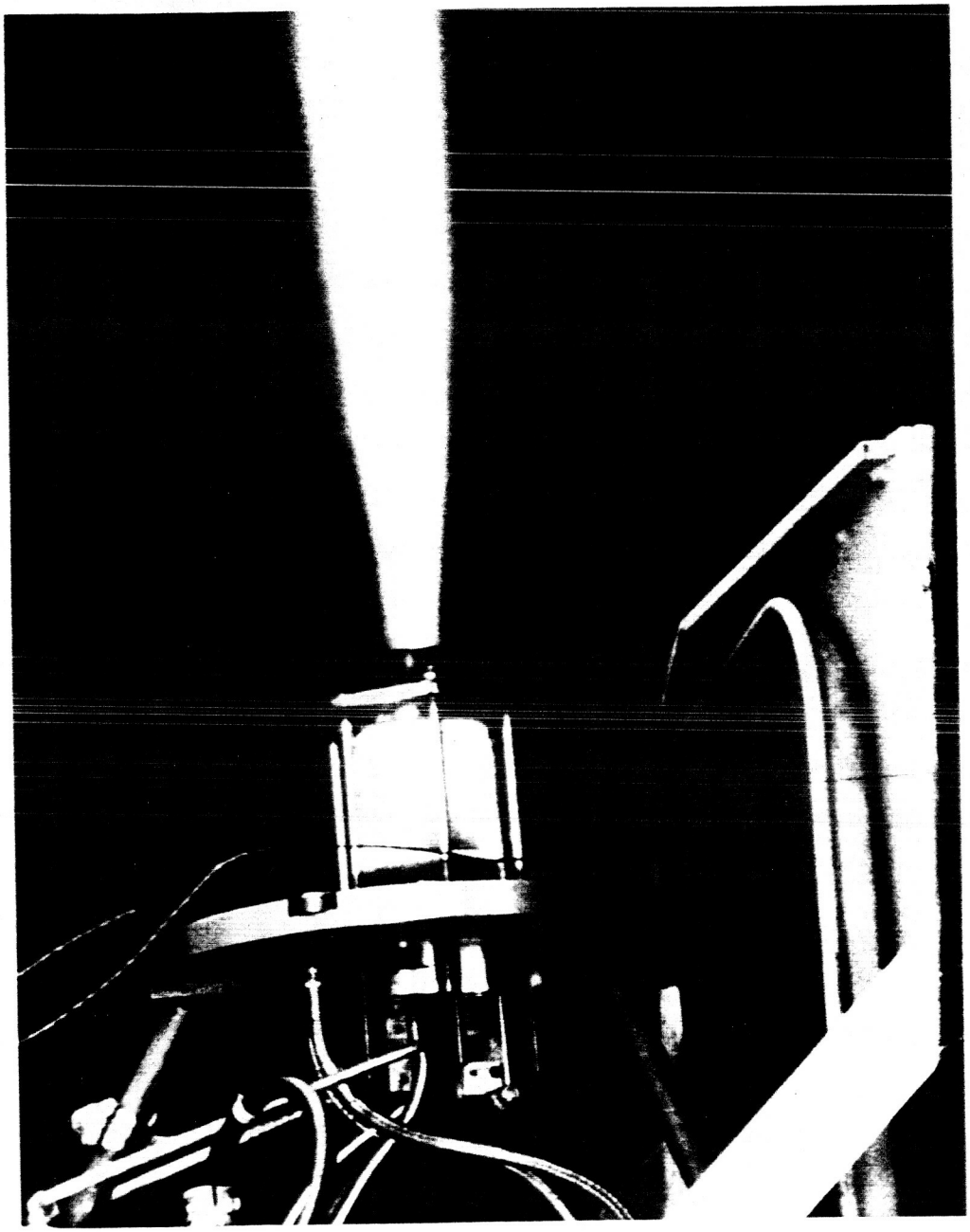

Overexpanded Nozzle (For Smooth Continuity With 40:1 Vacuum "Bell" Nozzle)

Sea Level Firing

Figure 15

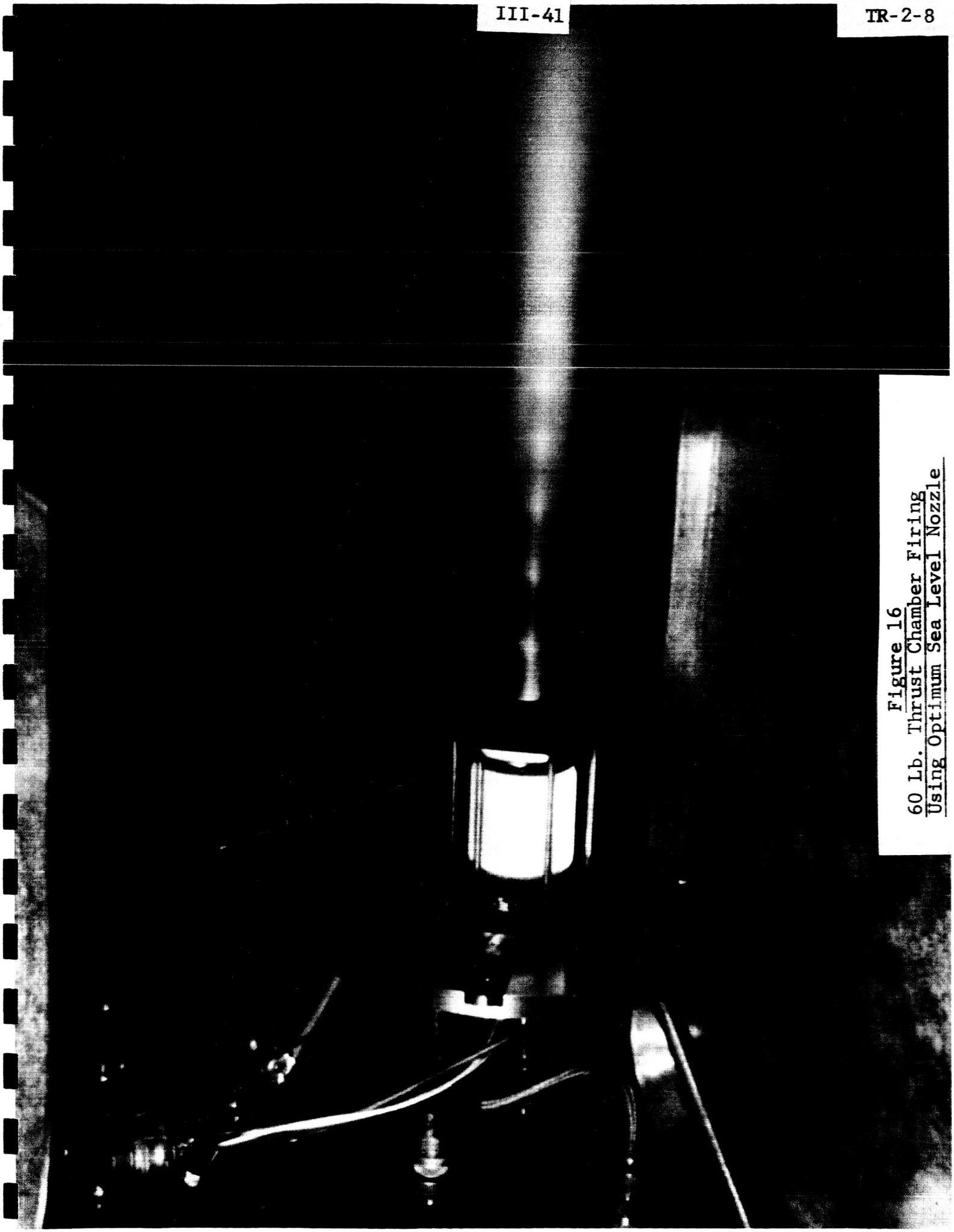

Figure 16
60 Lb. Thrust Chamber Firing
Using Optimum Sea Level Nozzle

One, with an ablative nozzle extension shrouding the carbide nozzle, good radiation cooling of the latter was hindered. The additional heat flux concentrated in the carbide nozzle raised the mean temperature to the point where chamber pressure forces acting on the diverging section exceeded the hoop strength of the material. At the temperatures involved a ductile failure occurred, similar to rupture of a pressure vessel. Increasing the wall thickness of this section of the nozzle to a proper size eliminated these failures.

Two, since the 50-50 TaC-WC material is somewhat thermal shock sensitive, one failure occurred from injection of cold oxidizer on a hot nozzle although the nozzle crack was superficial and the nozzle continued to perform throughout the remainder of the firing. The injection of cold propellant was traced to a malfunction of the bi-propellant valve which in turn was caused by high stiction and improper adjustment of the poppet linkage. The improper linkage adjustment allowed the oxidizer poppet to open before the fuel poppet and the high stiction in the linkage held the poppet open. The latter condition was corrected by a minor design modifiction. No further problems occurred with thermal shock throughout the test program.

Valve Poppet and Seat

The basic problem in establishing the poppet and seat configuration was in obtaining a combination that would be relatively leakproof. Of equal importance was the compatibility of the materials with the specified propellants (N_2O_4 and UDMH Hydrazine) and vacuum environments at elevated temperatures.

A series of poppet and seats were designed and in discussing development of the poppet and seat configurations, it will be noted that these were single poppet and single seat arrangements, employed in a test fixture, Section IV. Whereas the final valve design required dual seats and poppets. This approach was used to facilitate testing and to conserve development and fabrication costs while still obtaining desired results.

It is noted that the poppet and seat designs studied and tested by Vickers were mostly of the spherical shape used in various combinations.

It was felt that Vickers past experience in obtaining a high degree of accuracy and performance using spherical mating surfaces for valve components, would result in a successful effort in meeting the design requirements of this valve.

Valve Test Requirements

1. Solenoid operation with a frequency of 10 cycles/sec.
2. Downstream valve seat orifice of .130 in. diameter. (nominal)
3. Valve stroke .015 - .017 in.
4. Working pressure 260 psig.
5. Leakage rate not to exceed 0.1 cc/hr. (liquid)

Figure 17 shows the bench testing rig for the poppets and seats with tests carried out at room temperature using dry nitrogen as the test fluid.

The conversion of the propellant fluids to nitrogen gas with conformance to the maximum leakage allowed, is covered in Appendix A.

There is considerable experience and data available in regards to the compatibility of poppet and seat materials with the propellants used in this system. With the additional knowledge gained through material testing at Vickers, covered in this section, a limited number of materials were selected for testing. Outstanding among these materials is "Teflon" TFE - fluorocarbon resin which is familiar to many throughout industry. It's retention of mechanical properties at elevated temperatures and chemical inertness make this material very attractive for valve application.

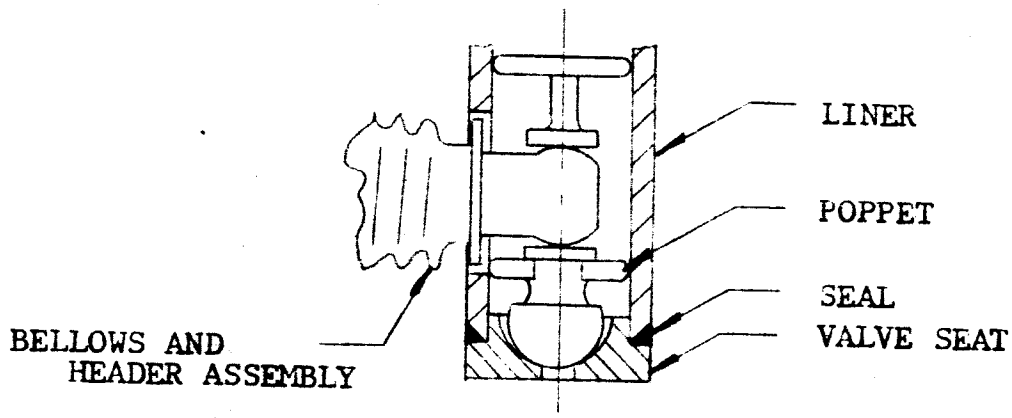

Figure 17

Figure 17 shows the poppet and seat sub-assembly and basic design principle that was carried throughout the valve development work. The poppet was made of 440C stainless steel and heat treated to a hardness of 36-40 Rockwell "C" which "toughened" the overall poppet to minimized the wear rate at the guide flanges and header-poppet engagement area. Aside from the nose configuration which was tested through many variations, the poppet remained the same.

The seat was also tested in many variations and was always located in alignment with the poppet through a hardened stainless steel liner.

Figure 18 illustrates the first approach in test hardware consisting of a stainless steel spherical poppet accurately machined with an application of sprayed teflon coating over the ball surface approximately .001 to .0015 inches thick.

The mating seat was spherical and made of a high density ceramic (AL_2O_3) with a hardness of MOH9. (Diamond hardness is MOH10) This material is chemically inert and vacuum tight down to pressures of 1×10^{-10}.

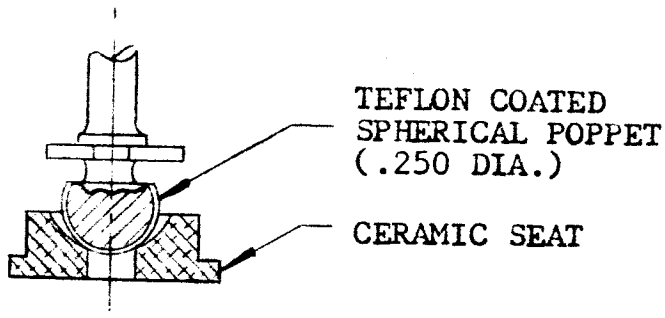

Figure 18

Machining the ceramic was limited to lapping and grinding using diamond paste and diamond faced grinding wheels. A conical entrance tangential to the spherical seat provided better alignment and larger flow entrance area for the same valve stroke. The spherical seat was lapped to a high finish and sized to the poppet ball. In preparing this hardware for testing, closer examination of the teflon coating under a microscope revealed a very rough surface. An attempt to smoothen the surface by burnishing was unsuccessful and only caused flaking and separation of the teflon from the ball, exposing areas of the base metal.

Upon discussing the teflon coating application with the vendor, it was learned that the rough surface was caused by the sintering operation in the oven at 750°F and a heavier coating would only deteriorate the bond between the teflon and the base metal. Further efforts with this approach were abandoned in view of other promising concepts.

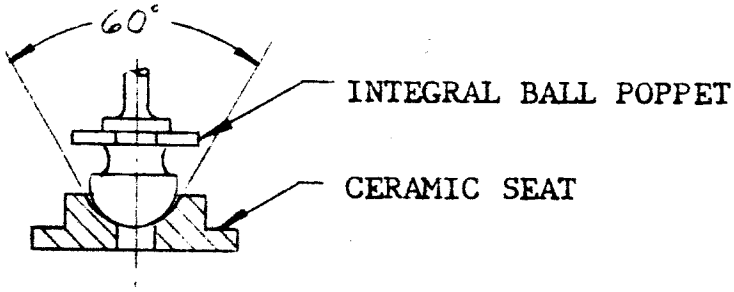

Figure 19

The second configuration tested, shown in Figure 19 consisted of using the same ceramic seat prepared for the first test and a stainless steel spherical poppet accurately machined and fitted to the ceramic seat. Testing this concept produced only moderately successful results and since a metal-to-metal type condition existed due to the hardness of the seat, leakage requirements were not met. With evidence of abrasion on the poppet surface, and the limited machinability of ceramic due to chipping and cracking, further development work with the ceramic material was stopped.

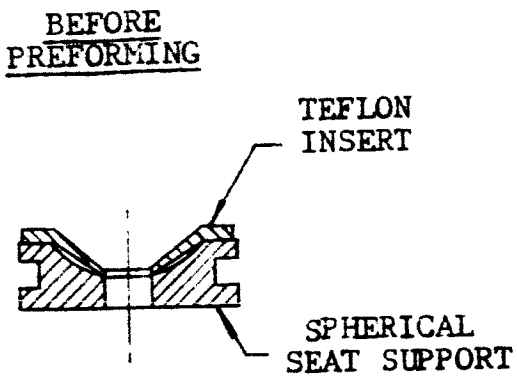

Figure 20

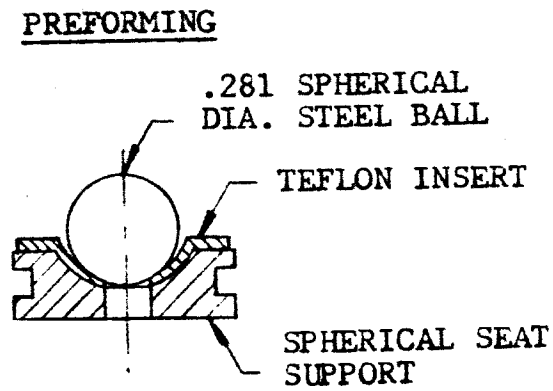

Figure 21

Another approach, shown in Figure 20 , incorporated a thin walled (.010 inch thick) conical insert of teflon with a stainless steel spherical support fitted together to make-up the seat assembly. Prior to installation into the test fixture, the teflon insert was preformed under load with a .281 inch diameter steel ball as shown in Figure 21 . The preloaded setup was installed into a furnace that was set at 250°F and heated for 24 hours. The conical insert and preforming approach was taken rather than machining a spherical teflon insert. The latter would be a more difficult and time consuming to manufacture accurately. A mating poppet was machined with an integral spherical ball .250 inches in diameter with a 4-8 micro inch finish.

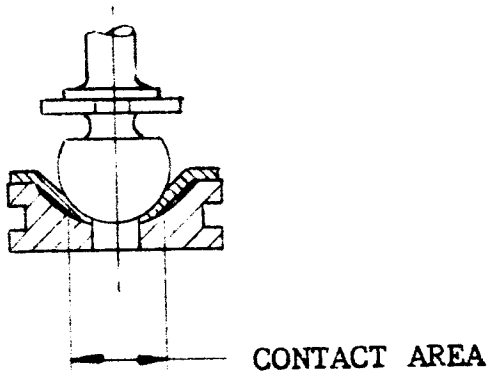

Figure 22

After the preforming operation, an impression was taken of the contact area between the poppet ball and teflon seat using prussian blue. Upon examination, this area was greater than desired and was caused by the preformed seat returning partially to it's original form Figure 22 . The prime purpose in using the .250 and .280 spherical diameters was to obtain a line contact around the periphery of the .130 diameter seat orifice. Thus, the theoretical effective seat area and the orifice area are identical and represent the ideal condition.

Figure 23 shows the valve closing forces that can be realized with a given seat area and valve inlet pressure. Continuous efforts were directed towards maintaining minimum effective seat areas with good sealing characteristics throughout the design and development program.

Although the seat area shown in Figure 22 was too great, it was decided to test this configuration since much could be learned of sealing characteristics under actual operation. The valve was installed into the test fixture shown in Section IV and a bench setup made illustrated in Figure 24 . This setup was used throughout the poppet and seat development program.

Figure 23

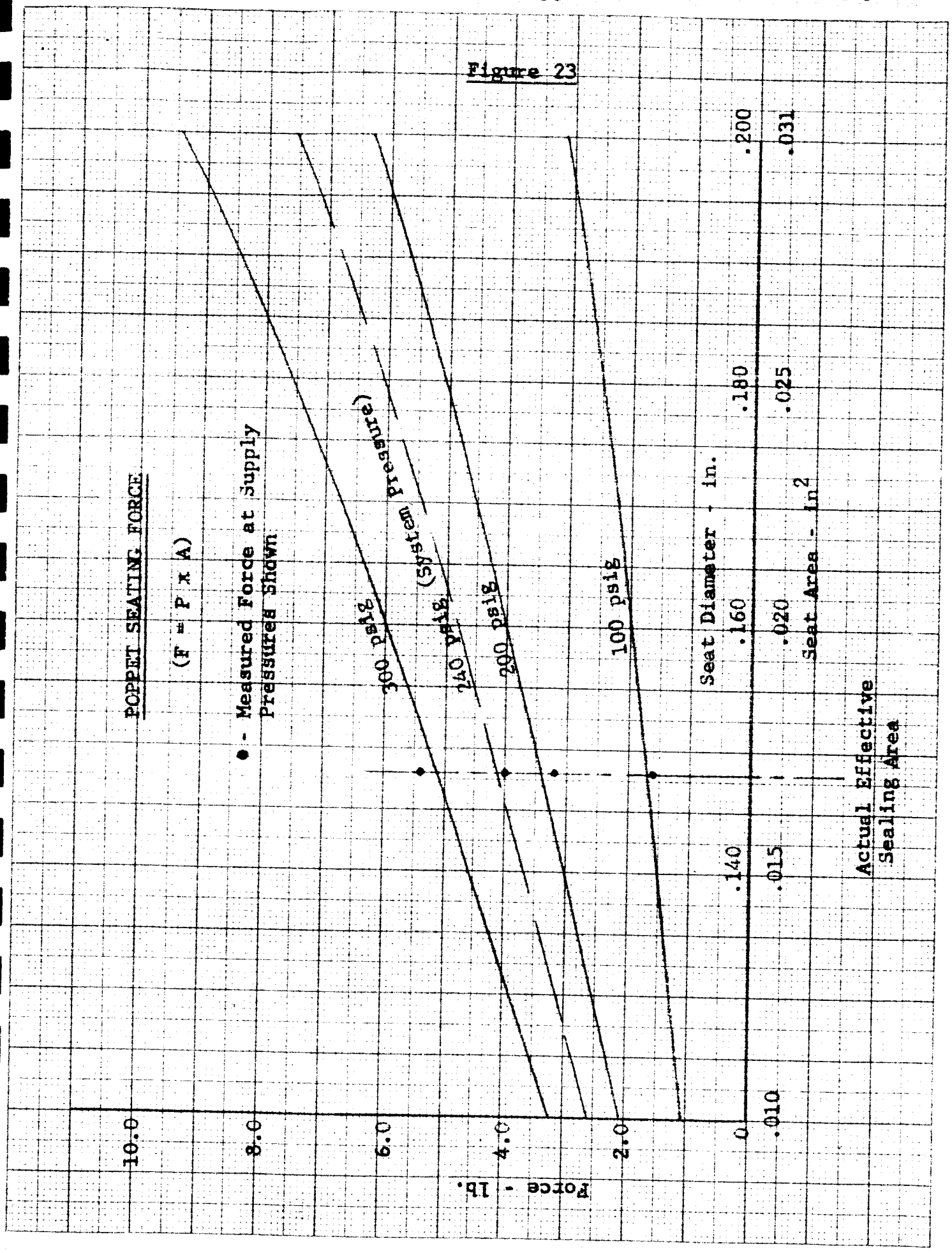
POPPET SEATING FORCE
(F = P x A)
● - Measured Force at Supply Pressures Shown
300 psig
240 psig (System Pressure)
200 psig
100 psig
Seat Diameter - in.
Seat Area - in^2
Actual Effective Sealing Area
Force - lb.
10.0
8.0
6.0
4.0
2.0
0
.010
.015
.020
.025
.031
.140
.160
.180
.200

Figure 24

Bench Test Setup

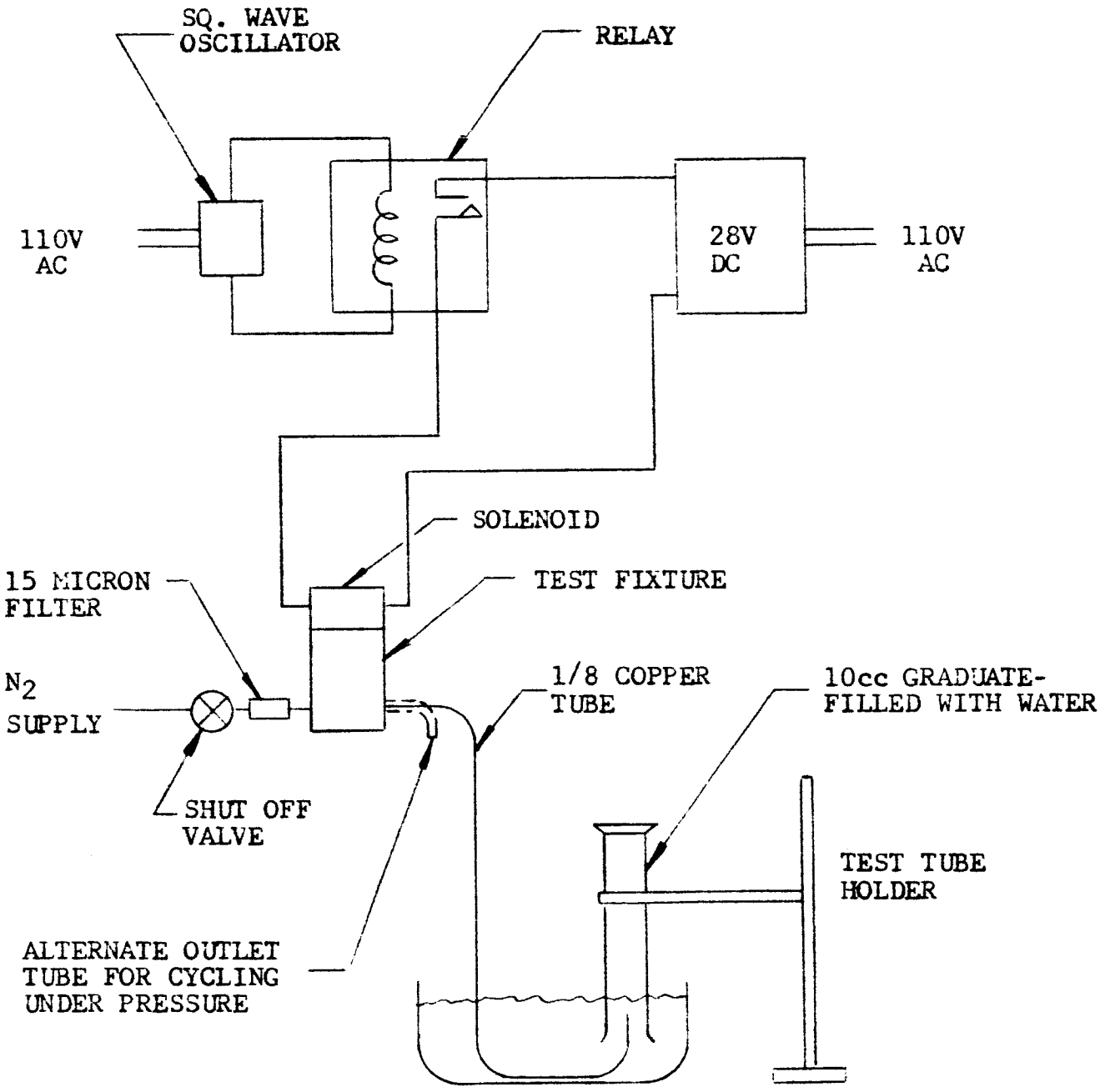

Table 7

Test Results with Valve Seat Configuration (Fig. 22)

Test Results

(Solenoid operating on one coil) 23-25 volts

1. Cycling 10 minutes on
   5 minutes off } Total cycling time - 40 minutes
   0 - pressure
   (Observing solenoid coil temperature)

2. Cycling 10 minutes on
   2 minutes off } Total cycling time - 50 minutes
   at 100 psi pressure Total leakage 2 bubbles

3. 20 minutes stand-by leakage check under pressure - 0 leakage

4. Cycling continuously under pressure
   stopped at 16 minutes - Coil hot
   0 - leakage

5. Cycling approx. 1 sec. on Total cycling time - 100 sec.
   2 minutes off } Total leakage 10 bubbles
   at 100 psi pressure

6. Readjust linkage for longer valve stroke.

7. Cycling 10 minutes on Total cycling time 30 minutes
   2 minutes off } Leakage - 0
   at 100 psi pressure

8. 15 hour stand-by leakage test (Figure 24)
   0 - leakage at 100 psi

9. Cycling 10 minutes on Total cycling time 82 minutes
   2 minutes off } Total leakage - 10 bubbles
   at 100 psi pressure

10. Disassembled valve for inspection and observed a well seated teflon seat with a contact diameter of approximately 0.220. This is considerably more than desired since the seat orifice

Table 7 Continued

diameter is 0.128 inches.

11. Reassembled valve to check repeatability in alignment of the poppet and seat. There was some difficulty before good alignment was established and assembly technique developed. The second coil was also wired into the circuit of the solenoid.

(Solenoid operating with both coils)

12. Cycling 20 minutes on
2 minutes off } Total cycling time 3 hours
at 100 psi pressure Total leakage - 0

13. Second 15 hour standby leakage test (Figure 24) was setup. 1 bubble of gas was trapped in graduate after 15 hours. This could have occurred by the expansion of gas trapped between the valve and the water barrier. Valve was cycled for 15 minutes directly after above text with zero leakage in 2 minutes.

Total accumulated cycling time - 74 hours

Total cycles at 10 cycles/sec. = 266,400

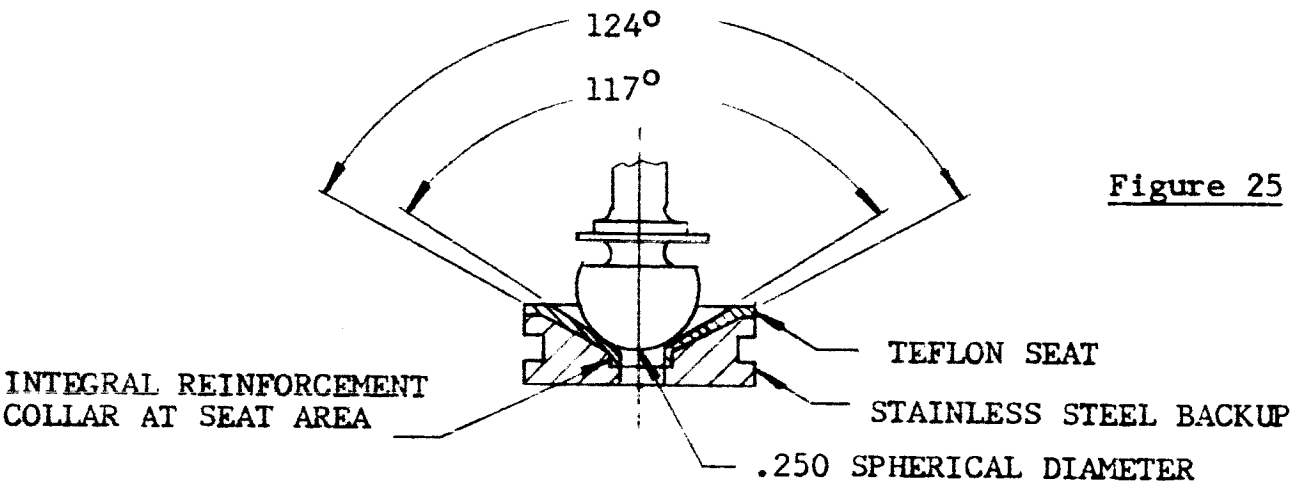

Figure 25

Illustrated in Figure 25 is another seat approach taken towards maintaining a minimum effective seat area. With a .250 spherical poppet ball diameter and a 117° conical teflon seat, produced a line contact around the periphery of the .130 diameter seat orifice. An integral collar at the seat area was machined integrally to serve as a reinforcement for the seat lip. The combined conical angles of 117° and 124° produced a tapered cross section and resulted in additional ridgidity to the seat.

The valve configuration was bench tested with results shown in Table 8.

No attempt to record leakages were made at this time since the main purpose was to obtain data showing the rate of increase in the effective seat area by cycling under system pressure.

Table 8

Cycles 10 cps	Effective Seat Dia.	Seat Area in^2	% Area Increase
-0-	.130 (theo.)	.0133	--
36,000	.162	.0206	55
36,000	.179	.0251	89

72,000 Total Cycles

The test results, in Table 8, showed promise and a set of poppets and seats were fabricated and fitted into the bipropellant valve. There was 8.5 minutes accumulated in actual firings resulting in a total of 51,000 cycles. When the seats were examined, the effective seat diameters were found to be:

Oxidizer side = .174 Fuel side = .172

It is interesting to note that the increase in seat diameters from the initial line contact mentioned earlier, compared favorably with the bench test results shown in Table 8 . However, it appeared that the valve closing force would increase gradually by some factor of cycling time and therefore further testing was discontinued to direct our efforts towards additional new designs.

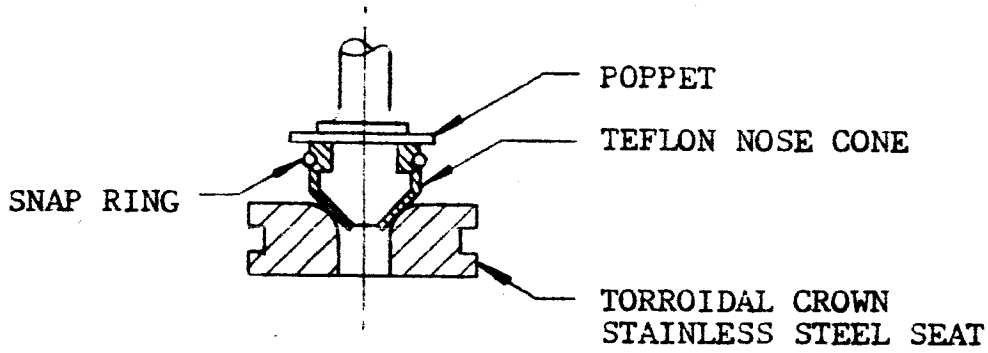

Figure 26

The next valve design was made and assembled as shown in Figure 26 It consisted of a 90° teflon conical nose cone fitted over a mating cone on the poppet. This was retained securely with a snap ring. The crowned seat was made of 347 stainless steel and polished to 8 micro inch finish at the seat area.

The valve was installed and cycled in the test fixture for three minutes. The stroke decreased considerably and with power off, leaked very badly. Disassembly showed nothing wrong and was re-assembled for another attempt. After approximately three minutes of cycling, the stroke decreased again and the valve leaked badly with power off.

After careful analysis, the leakage was found to be caused by a ballooning effect of the teflon nose cone. With nitrogen leaking under the teflon, the nose cone would separate from the poppet absorbing the stroke that had been initially adjusted into the valve.

Since other new poppet and seat design hardware were ready for testing, work was stopped on this design pending further study of the basic configuration.

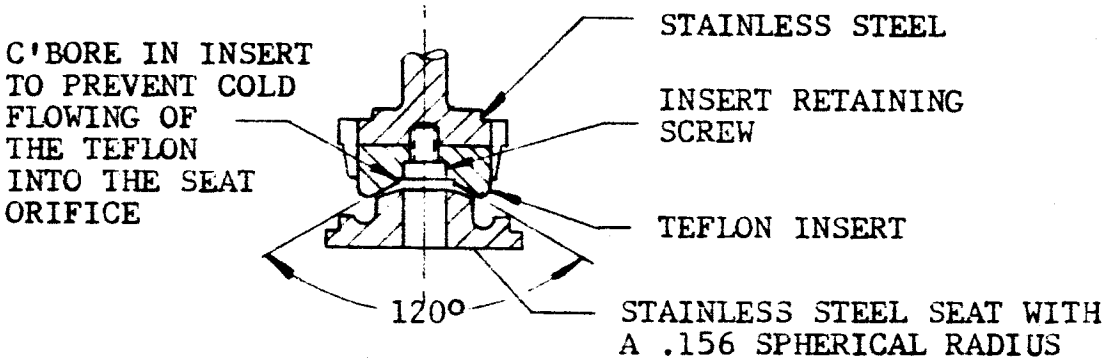

Figure 27

In Figure 27 is depicted a breadboard configuration which in principle is the reversal of Figure 25. The teflon contained a 120° concave conical seat with a central counterbore .010 greater in diameter than the seat orifice. This arragnement prevented the teflon from cold flowing into the orifice and effecting the sealing characteristics.

The stainless steel seat was machined with a .156 convex spherical radius which was polished to a 4 micro inch finish. This configuration permitted a line contact around the periphery of the counterbore of the teflon insert with a diameter of .140. Preliminary test results were very gratifying and it was decided to simplify the poppet and insert retaining the above mentioned features before continuing tests.

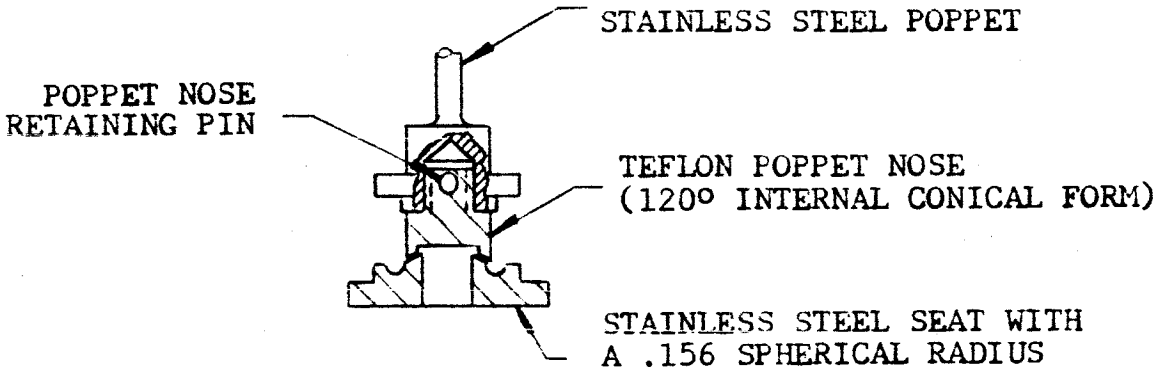

Figure 28

Figure 28 shows results of the design change in which the teflon insert was threaded into the poppet with a controlled torque of 70 gram inches. The insert was retained with a stainless steel roll pin preventing any movement in operation. The convex seat was used without any changes.

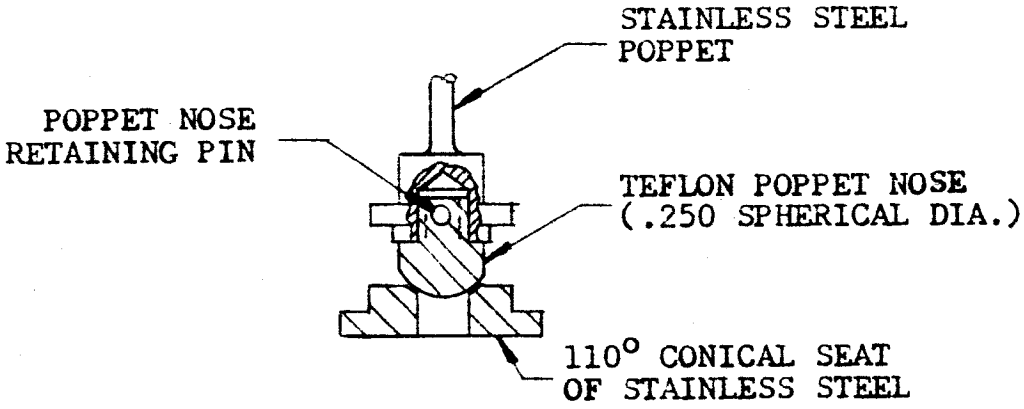

Figure 29

Valve configuration shown in Figure 29 was also fabricated at this time to take advantage of the identical manner employed in the poppet

nose assembly to the poppet proper. The teflon poppet nose was machined with a .250 spherical diameter and mated to a stainless steel seat having a 110° conical seat and polished to a 4 micro finish.

Preliminary tests employing Figure 29 also indicated a good potential valve and warranted further evaluation. A parallel test program was setup to bench test both Figure 28 and Figure 29 designs.

Tables 9 thru 13 display the type and manner of tests that were conducted and the results of these tests.

Table 9

Valve cycled for a total of ½ hr. with leakage checks taken after each 5 minute cycling period - N_2 test fluid, 250 psig	
Total leakage for ½ hr. taken for 1 minute each period.	
Valve Figure 28 -0- leakage	Valve Figure 29 -0- leakage

Valve cycled for 2 seconds and leakage checked for 5 minutes at each pressure level shown. - N_2 test fluid

Inlet Pressure	Valve Figure 28	Valve Figure 29
30 psig	-0- leakage	-0- leakage
100 psig	-0- leakage	-0- leakage
260 psig	-0- leakage	-0- leakage

Table 10

Valve Attitude Leakage Test

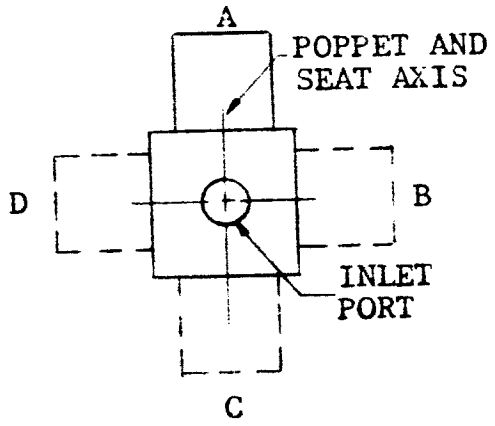

Fixture rotated about inlet and outlet port axis.
N_2 Test Fluid
Inlet Pressure - 250 psig

Leakage Test Cycle

1 minute cycling at 10 cps
1 minute leakage check

Fixture Position	Valve Figure 28	Valve Figure 29
A	-0- leakage	-0- leakage
B	-0- leakage	-0- leakage
C	-0- leakage	-0- leakage
D	-0- leakage	-0- leakage

Table 11

Table 12

Valve cycled for 2 seconds and leakage checked for 1 hr. periods.

Test setup (Figure 24)
N_2 Test Fluid
Inlet Pressure - 260 psig

Leakage Check Periods - hrs.	Valve Figure 28	Valve Figure 29
1	-0- leakage	-0- leakage
2	-0- leakage	-0- leakage
3	1 bubble	1 bubble
4	-0- leakage	1 bubble
5	-0- leakage	-0- leakage

Table 13

Extended time leakage test (steady state)
Test Setup (Figure 24)
N_2 Test Fluid
Inlet Pressure - 260 psig

Test Valve	Time Period	Leakage
Figure 28	19 hrs.	2 bubbles (estimated)
Figure 29	14 hrs.	3 bubbles (estimated)

Poppet and Seat Design Check

Disassembly and careful inspection of the poppets and seats (Figure 28 and 29) used in the preceding series of tests, revealed no permanent deformation of the teflon poppets or any damage to the seats. This series of tests substantiates in part the design objective of maintaining a nominal force load on the poppet within the elastic limits of the teflon material.

Further tests were conducted on these two valve designs and are covered in other sections of this report.

Bellows Sub-Assembly

In the early stages of the valve design, the problem of establishing a "zero leak" highly reliable and flexible seal between the poppet valve chamber and the external operating linkage presented itself. The propellants to be used in the system pointed to a seal of non-organic material. A survey was made and the metal bellows was selected which met the requirements of the valve design. With Vickers' past experience in using metal bellows as a sealing member on similar installations it was felt that no serious problems would arise in their use at this time.

Figure 30 , next page, shows the manner in which the bellows were employed. The bellows and subsequent processing in part was furnished by *B. F. Goodrich. A slotted header which engages and operates the poppet, was welded to one end of the bellows. To the other end of the bellows, a flange was welded which locates this sub-assembly in the valve body. A teflon "O" ring was installed between the inner face of the flange and valve body.

The performance of the bellows assembly is covered in other sections of this report under - Pulsating Endurance, and Environmental Testing.

* The bellows and welding operations were furnished by:
B. F. Goodrich
Aero Space and Defense Products - Dept. 1817
Akron, Ohio

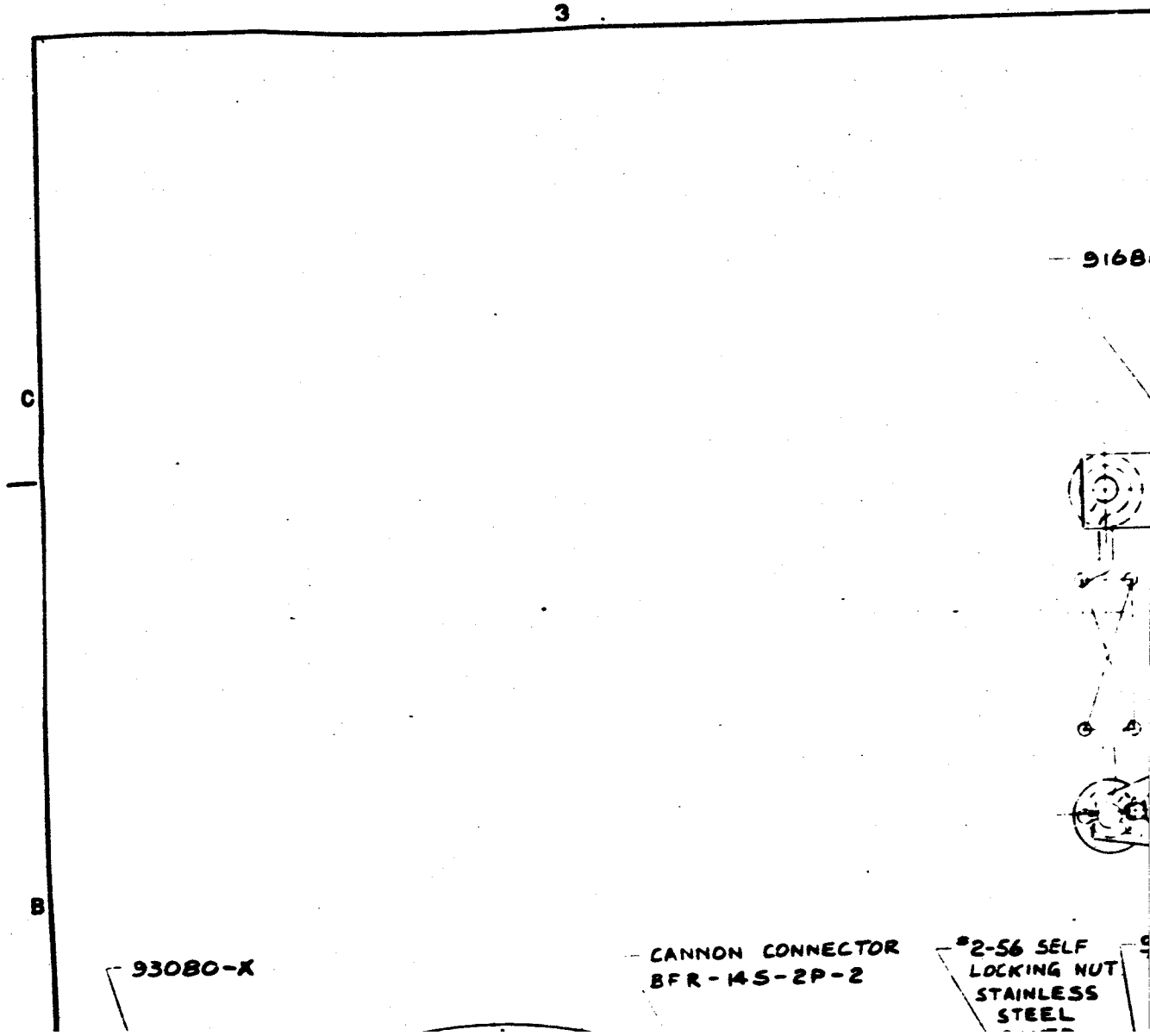
3
C
B
9168
93080-X
CANNON CONNECTOR
BFR-14S-2P-2
#2-56 SELF
LOCKING NUT
STAINLESS
STEEL

2

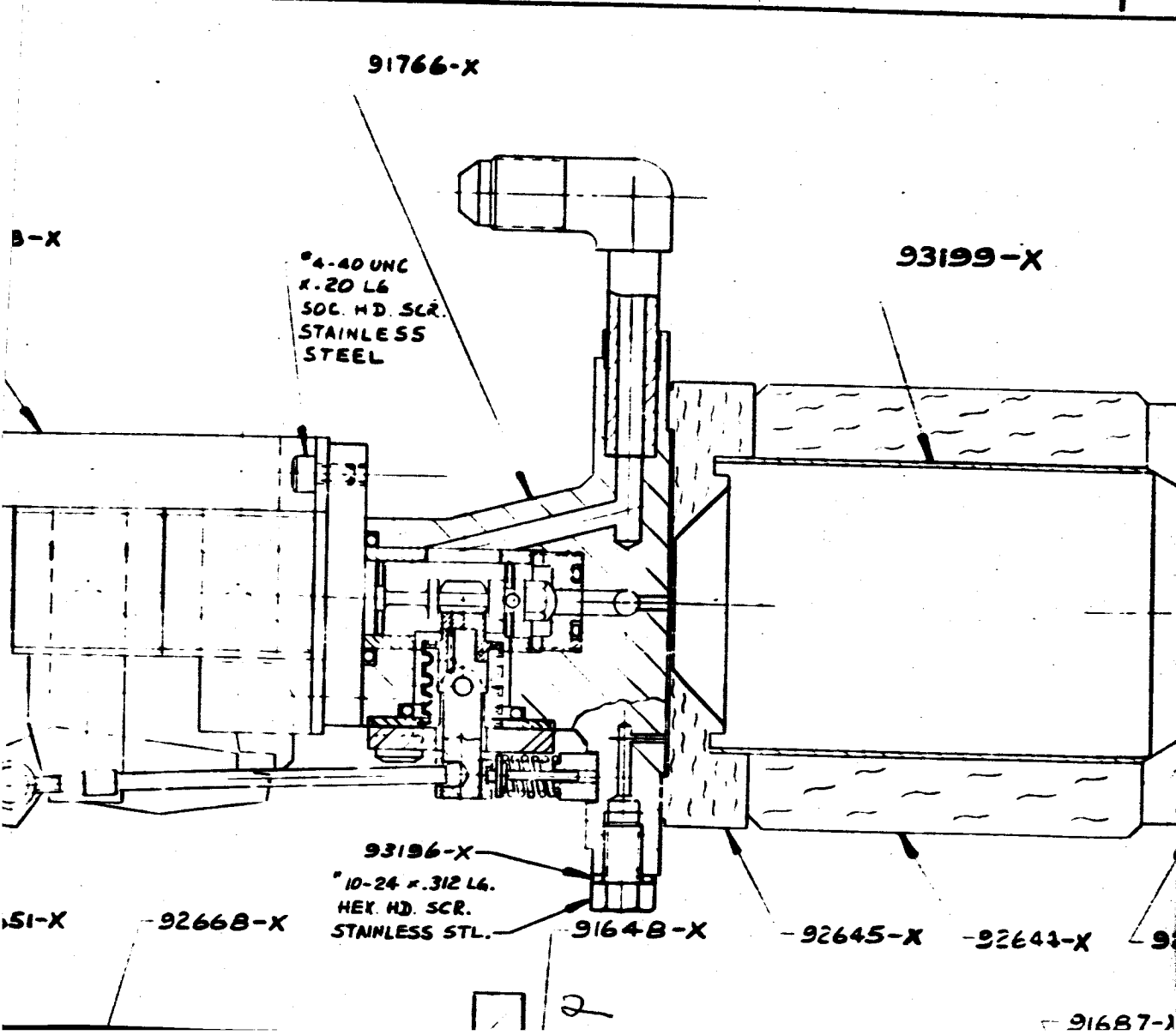
2
91766-X
B-X
#4-40 UNC
x .20 LG
SOC. HD. SCR.
STAINLESS
STEEL
93199-X
93196-X
#10-24 x .312 LG.
HEX. HD. SCR.
STAINLESS STL.
51-X
92668-X
91648-X
92645-X
92643-X
91687-1

3

Figure 30

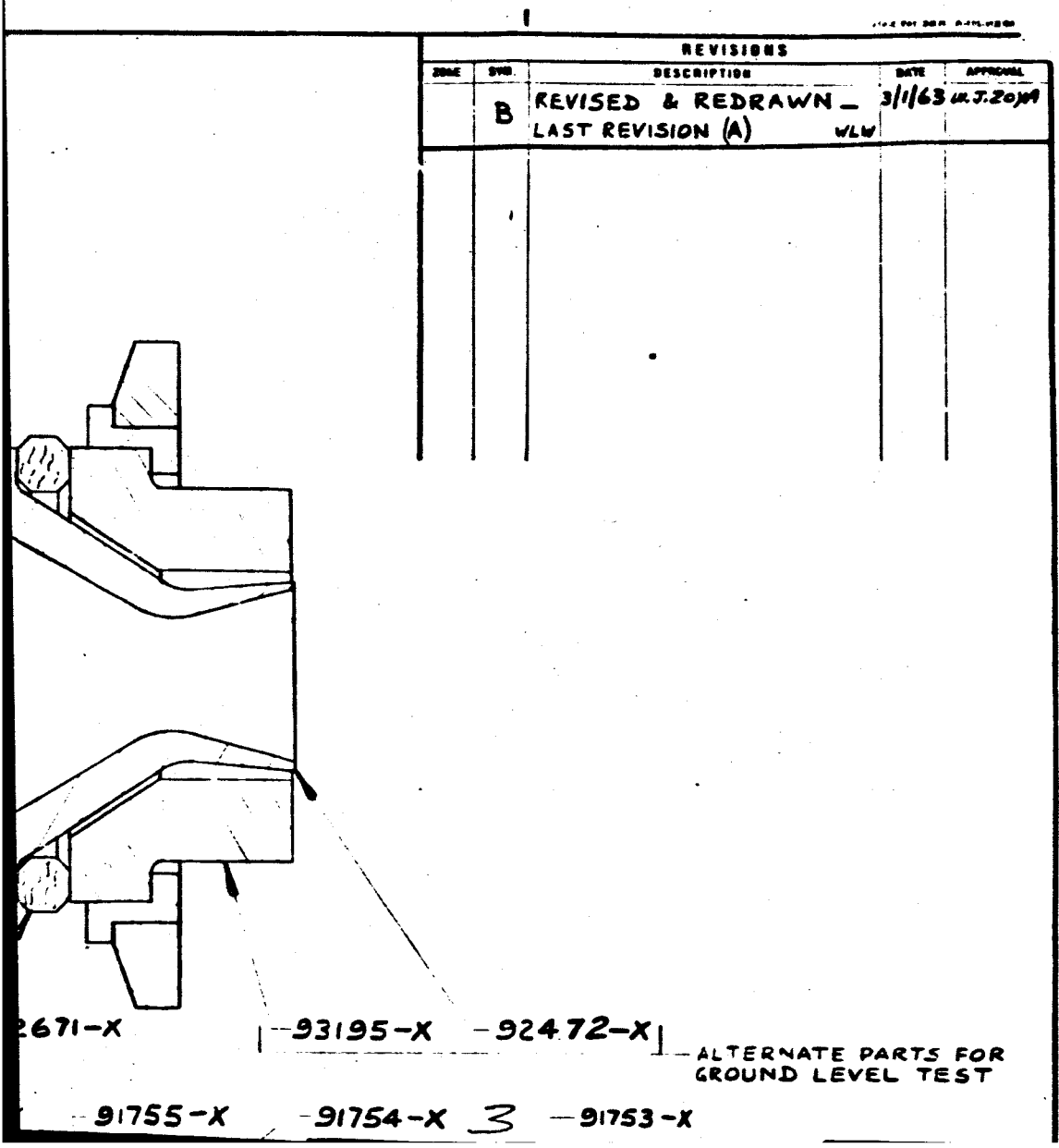
REVISIONS
ZONE
SYM.
DESCRIPTION
DATE
APPROVAL
B
REVISED & REDRAWN _
LAST REVISION (A) WLW
3/1/63
C
B
2671-X
93195-X
92472-X
ALTERNATE PARTS FOR
GROUND LEVEL TEST
91755-X
91754-X
3
91753-X

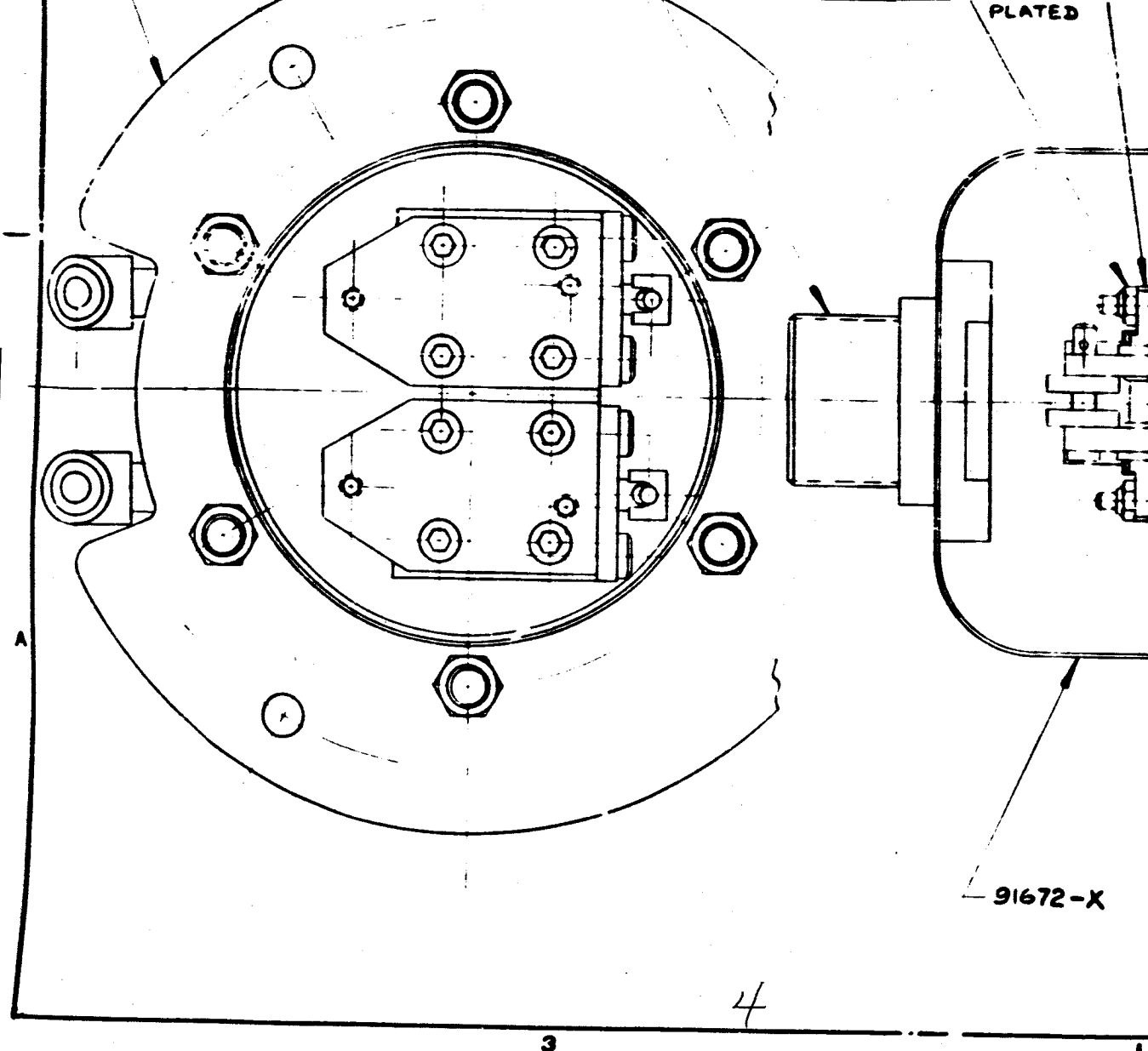

REI

4

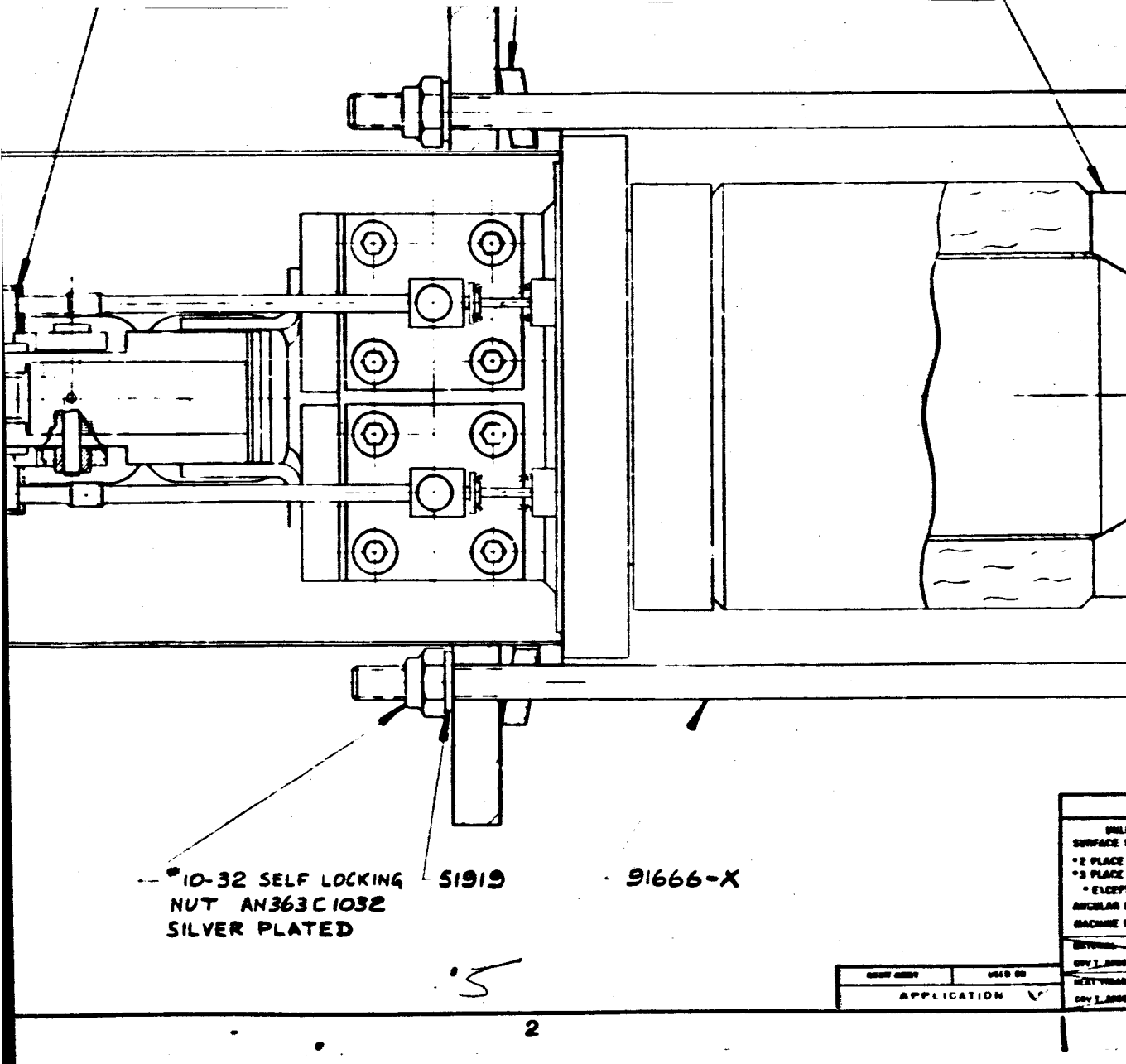

2

DUCED COPY - NOT TO SCALE SHO

5

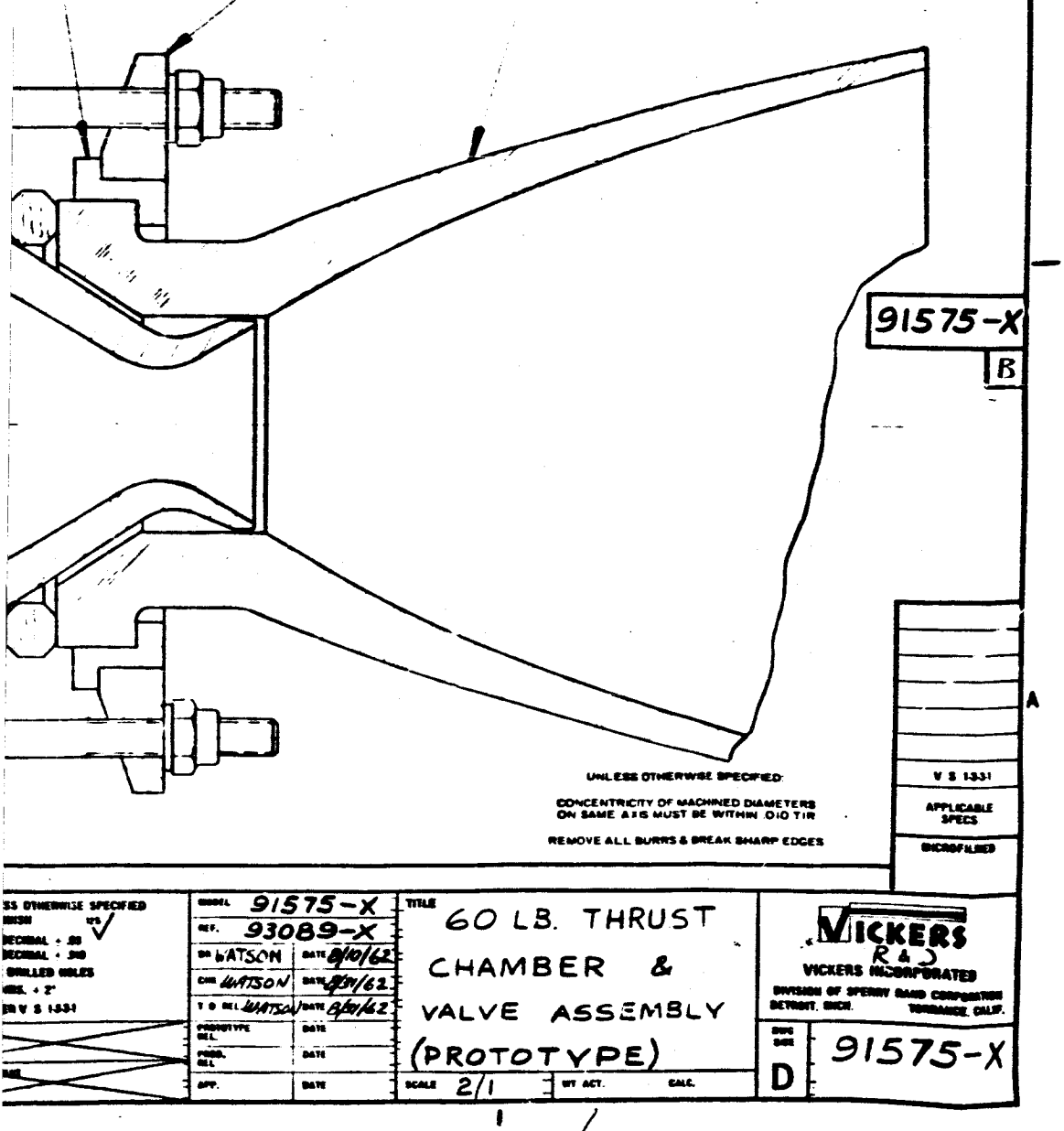
91575-X
B
A
UNLESS OTHERWISE SPECIFIED:
CONCENTRICITY OF MACHINED DIAMETERS ON SAME AXIS MUST BE WITHIN .010 TIR
REMOVE ALL BURRS & BREAK SHARP EDGES
V S 1-331
APPLICABLE SPECS
MICROFILMED
SS OTHERWISE SPECIFIED
DRILLED HOLES
MODEL 91575-X
REF. 93089-X
DR WATSON DATE 8/10/62
CHK WATSON DATE 8/31/62
T O REL WATSON DATE 8/31/62
PROTOTYPE REL.
PROD. REL.
APP.
DATE
TITLE
60 LB. THRUST CHAMBER & VALVE ASSEMBLY (PROTOTYPE)
SCALE 2/1
WT ACT.
CALC.
VICKERS
R&D
VICKERS INCORPORATED
DIVISION OF SPERRY RAND CORPORATION
DETROIT, MICH.
TORRANCE, CALIF.
SIZE D
91575-X

6

DWN

6

Static Seals

In the final design of the valve assembly, static seals were required in 6 areas. However, there are only 3 basic areas requiring static seals for each valve. These of course were doubled for the twin valve configuration. (Figure 30)

1. 2 required at one end of each chamber liner.
2. 2 required located at the inner face of each bellows flange.
3. 2 required located at the opposite face of each poppet seat.

In the studies of various static seals, many new design concepts have appeared in attempt to improve and refine the present state-of-the-art.

Time did not permit development work in this area and it was felt that using commercially available "O" rings made of teflon would meet the environmental conditions imposed upon the seals.

Emphasis was placed on several points with repect to the use of the teflon "O" rings for optimum results.

1. Individual inspection of the "O" rings to establish a high degree of quality with regards to dimensions and surface finish.

2. Designing the "O" ring grooves to obtain adequate installed squeeze and remain within the elastic limits of the teflon material.
3. Machining the "O" ring grooves and associated surfaces to obtain a surface finish in the range of 8-10 micro inches.

B. SOLENOID (OR TORQUE MOTOR) DEVELOPMENT

Summary of Development

1. The developed torque motor produced the designed torque.

2. Modifications to the torque motor increased the developed torque to meet added load requirements imposed by the valve.

3. The response of the torque motor was adequate to meet the pulse bit target specifications.

4. Investigations have disclosed where the torque motor design can be improved. These are primarily in the areas of minimization of saturation and dynamic balance.

Description of characteristics and factors affecting response:

The magnetic circuit of the torque motor is similar to a core type transformer made of "U" and "I" laminations. A coil is mounted on each leg of the "U" lamination and these coils are connected in parallel-aiding. The "I" laminations form the armature which is positioned to bridge across the ends of the "U" laminations. One end of the armature is fitted with a fixed pivot point relative to the "U" core. The opposite end is free to rotate and represents the output of the torque motor.

The gap between the core and armature at the pivot end is called the back gap and its permeance (or reluctance) is relatively constant over the operating range of armature rotation. The gap between the output end of the armature and the core is variable. This is called the working gap because the magnetic forces created in this gap generates the working torque needed to actuate the armature and its connected load. The "U" and "I" laminations at the output ends are fitted with crowns that form a compound type of working gap consisting of two linear and two inverse gaps.

The principle of operation of a torque motor can be summed by stating that any magnetic circuit composed of more than one part, which are

allowed to re-orient themselves with respect to each other, will assume a configuration tending to establish the largest magnetic flux under the influence of a magnetizing force. This is another way of saying the air gaps between the ferromagnetic parts will tend to become smaller, or the air gaps will tend to their minimum values.

The developed torque of the motor is directly proportional to product of the rate of change of the working gap permeance per radian of armature rotation and the square of the ampere-turns across the working gap. The ampere-turns across the working gap are directly proportional to the flux spanning the working gap and inversely proportional to the working gap permeance. Therefore, the developed torque is directly proportional to the product of the rate of change of permeance with angular position and the square of the air gap flux and inversely proportional to the square of the air gap permeance.

The coil ampere-turns constitute the magnetizing force. Not all the coil ampere-turns are available across the working gap because some ampere-turns are required to establish the flux in the iron portions of the magnetic circuit and across the back gap. The ampere-turns needed for the iron and back gap should be negligible with respect to those of the working gap to produce an efficient design. Low ampere-turns requirement for the iron portions is readily achieved

by proper selection of the type of steel and using a sufficiently large cross-sectional area to insure the maximum flux does not saturate the iron.

The "U" laminated cores must carry the working gap flux and the leakage flux which is established between the two legs on which the coils are mounted. The leakage flux is not available across the working gap and therefore does not contribute to developed force but only tends to saturate the core.

In our torque motor the required torque was greatly increased above the originally design valve by increasing the width of the working and back gap. A corresponding increase in core cross-sectional area was not permitted. The resulting increase in working gap flux caused the iron portions of the magnetic circuit to become saturated at the higher ampere-turn inputs.

In the compound working gap construction, the two types of gaps compliment each other over the working range. When the gap is fully open, the linear gaps are predominant and when the gap is near the closed portion, the inverse gaps are now predominant in creating the developed torque. The rate of change of permeance of the linear gap sections are essentially constant whereas the rate of change of permeance of the inverse gap sections continually increases and attains a relatively high value in the closed position. The overall effect is

a gradual increase in permeance as the working gap closes over the greatest portion of the armature stroke, but as the gap approaches the closed position, the rate of change is extremely large.

When the coil current is low, practically all the coil ampere-turns are available to produce flux across the working gap and therefore all the ampere-turns are producing torque. As the current is increased, the iron begins to saturate and most of the additional ampere-turns are assumed by the iron portion of the circuit with very few added ampere-turns for the working gap. Therefore, the developed torque does not increase appreciably after saturation of the iron occurs.

In our design, a fraction of the steady-state current is sufficient to produce saturation and the developed torque will actually decrease as the armature is moved over its mid-range of travel. This operating characteristic can be explained in the following manner. Assume that the armature is in the open position and the current is held constant at a value which either produces core saturation or just below that value. As the armature is moved into the mid-range of operation, the permeance of the working gap is increased. This would tend to increase the working gap flux except that the iron portions are saturated, causing some of the ampere-turns formerly available for the working gap, being used for the iron. The effect of the decreasing working gap ampere-turns is not completely

compensated for by the increasing rate of change of permeance and the developed torque will be lowered. As the armature is moved beyond the mid-range towards the closed position, the effect of the increasing rate of change of permeance will become dominant and more than off-set the fall-off in working gap ampere-turns. The developed torque continues to increase as the armature approaches the closed position, and the torque at the closed position will be more than double that at the open position with the same coil current.

Summarizing, the developed torque at a constant current will initially tend to decrease as the armature is closed due to working gap ampere-turns being lost to the iron portions, but as the armature continues through the mid-range, the developed torque increases by the over-riding effect of the increased rate of change of permeance, and in the closed position the developed torque greatly exceeds that of the open position.

The decrease in torque through the mid-range of armature travel is detrimental because the accelerating torque is correspondingly reduced, resulting in slower dynamic response. In the closed position, practically all of the ampere-turns are required for the iron portions of the circuit and relatively few are across the working gap. Therefore, in shut down where the armature is returned to the open position by the return spring torque, the current must drop down to an exceeding low

value before the core can be unsaturated and the working gap flux and hence, developed torque decrease. The return spring torque can not be effective in opening the armature until the developed motor torque is below this return torque. Thus, no return action is possible during the time interval required to reduce the current to the necessary value to unsaturate the core.

The magnetic circuit which is coupled to the electric circuit of the coil has permeances which produce the inductance in the coil circuit. The effect of inductance in an electrical circuit is to prevent any instantaneous change in current. When the current is constant, the inductive effects are not operative, but any attempt to increase or decrease the current will be opposed by the storing or releasing the energy of the magnetic field associated with the coil. The overall inductive effect forces all current changes to be expotential in form. Any change in current tends to be directly proportional to the magnitude of change in applied voltage and inversely proportional to the circuit inductance.

The developed torque of the motor is a current device because the ampere-turns supply the magnetizing force. Therefore, the speed of response of the motor is also limited to that of the response of current controlled by the applied voltage. The magnitude of the

change in current after a given time interval of voltage change can be increased by either using a large incremental voltage, reduction of inductance or both.

Another factor of importance in limiting the transient response concerns the eddy current and hysteresis losses of the iron portions of the magnetic circuit. The current (and therefore ampere-turns) of the coils consists of two components. One component of current is necessary to supply the core losses in the core and the other component is the magnetizing current required to establish the magnetic field. These two currents tend to be 90 electrical degrees out of phase with respect to each other. The loss component will lead and the magnetizing component will lag the total coil current. Since the magnetizing component of current establishes the flux and torque, any time lag between the coil current and this component appears as a time lag between the developed torque and the coil current. Small core losses tend to reduce this time lag to a minimum because the total current will approach the magnetizing current as the core losses are decreased.

The major sections of the iron portions of the magnetic circuit are laminated to keep the eddy current losses to a minimum and transformer grade steel is used to insure low core losses. Appendix C lists values of electrical and mechanical parameters and basic magnetic equations pertaining to solenoid design.

Solenoid - Discussion of Modifications

Initial tests showed developed torque was less than designed torque by about 20%. The reason was the permeance of the back gap was too low and some saturation of armature iron was occurring adjacent to the pulling gap. Modifications were made as follows. The two back brackets were made into one piece and the length of the back gap reduced. Armature thickness was increased and the crown on the pulling gap replaced by a two-step gap.

Later tests showed a relatively high power and hence high current level was required for response and to overcome losses due to coil heating. The 35 watts power input was objectionable to NASA's requirements at that time so two modifications were incorporated to achieve the same performance with about 18 watts power. The coil wire size and the number of turns were increased, and the armature width at the working gap was increased to equal the pole piece width.

Later modifications to coils and the armature return spring involved response for minimum pulse bit operation and will be discussed in that section.

SECTION IV

ENDURANCE AND RELIABILITY

SECTION IV

ENDURANCE AND RELIABILITY

Bench Pulsing Endurance

To establish a reasonable factor of reliability for the integrated bipropellant valve design, a series of tests were conducted which covered the various sub components making up the integrated valve assembly.

1. Solenoid Assembly - (mechanical)
2. Valve Poppet and Seat
3. Bellows Assembly

Test I

A test system was setup using the test fixture Figure 31 assembled with the following sub-assemblies which were identical to those used in the integrated unit shipped to NASA-Houston on February 19, 1963.

1. Solenoid Assembly - 91688-X
2. Bellows Assembly - 91464-X (Figure 32)
3. Valve Poppet and Seat (Figure 33)
    a. Poppet Sub-Assembly - 92678-X
    b. Valve Seat - 92232-X

3

C

B

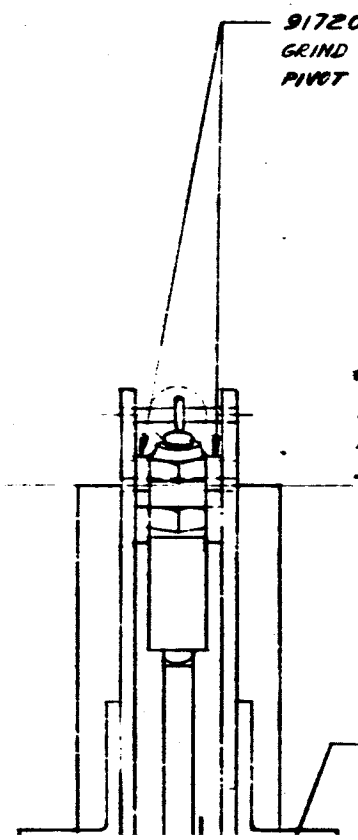
91720-X - FITTING SPACER
GRIND AT ASSEMBLY TO CENTRALIZ
PIVOT ARM WITH .0003/.0005 CLE
201584
NUT
#4-40 UNC HEX. NUT
GRIND HEAD HEIGHT AT
ASSY. FOR .0001 TO
.0005 TOTAL CLEARANCE
91724-X
CONNECTOR
91723-X
LINK
#4-40 UNC-X .312
SOC. HD. CAP SCREW

2

1 2

RANCE.

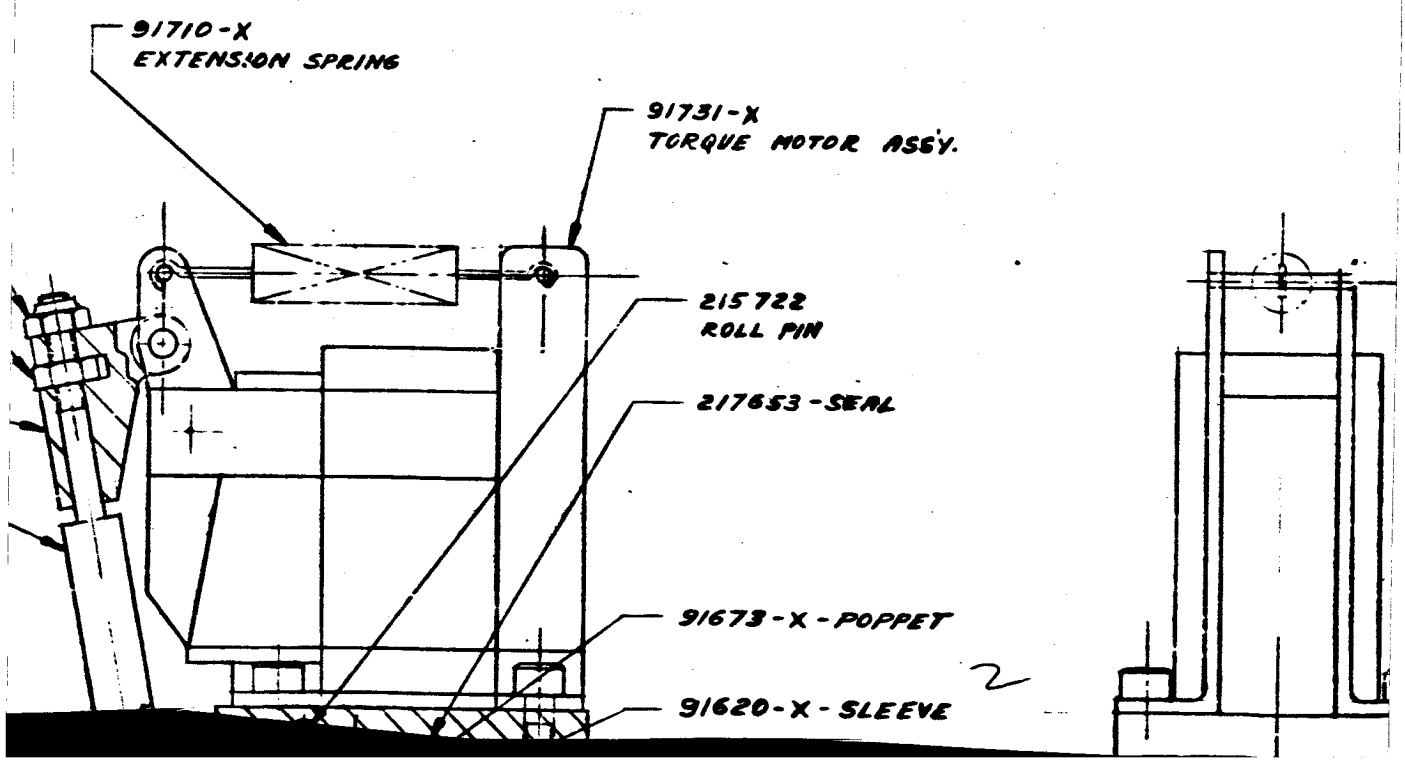
91710-X
EXTENSION SPRING
91731-X
TORQUE MOTOR ASSY.
215722
ROLL PIN
217653-SEAL
91673-X-POPPET
91620-X-SLEEVE
2

3

Figure 31

REVISIONS				
ZONE	SYM.	DESCRIPTION	DATE	APPROVAL

C

B

#4-40 UNC X.437
SOC. HD. CAP SCREW

91623-X
END PLATE

3

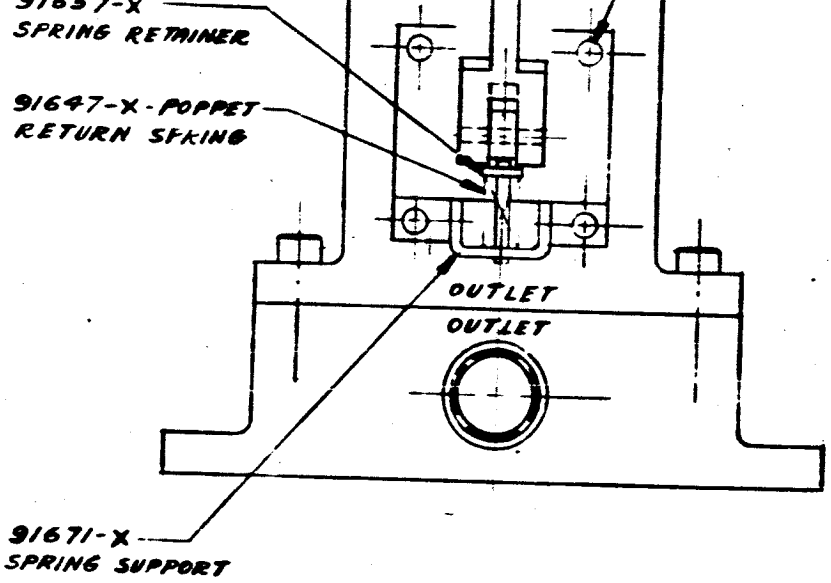
91637-X
SPRING RETAINER
91647-X - POPPET
RETURN SPRING
OUTLET
OUTLET
91671-X
SPRING SUPPORT
PIVOT PIN
91722-X
PIVOT ARI
9166
PIVO
2176
9140
BEL

A

3

4

4

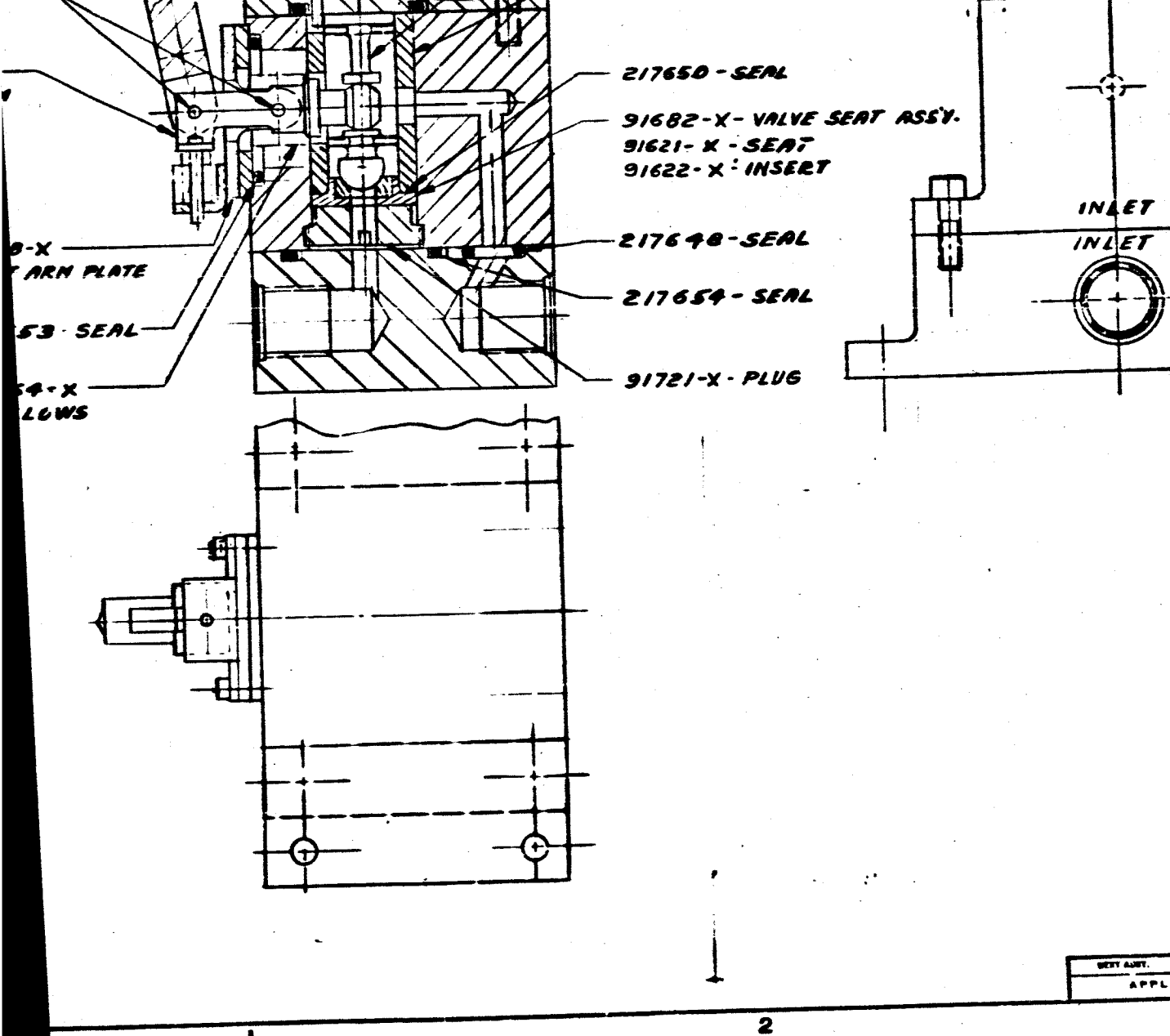

2

REDUCED COPY - NOT TO SCALE S

5 5

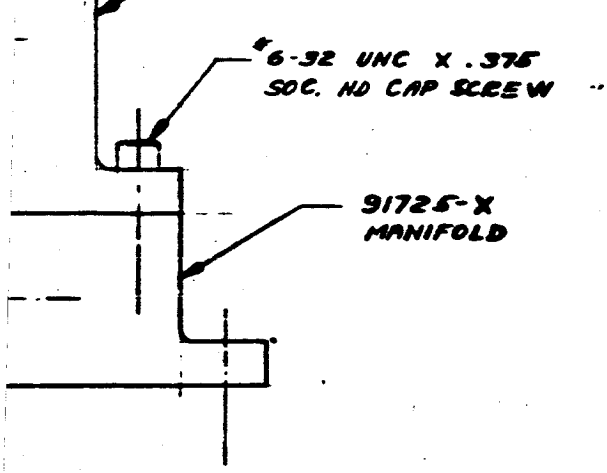

91617-X

UNLESS OTHERWISE SPECIFIED:

CONCENTRICITY OF MACHINED DIAMETERS ON SAME AXIS MUST BE WITHIN .010 T.I.R.

REMOVE ALL BURRS & BREAK SHARP EDGES

A

V S 1-3-84

APPLICABLE SPECS

MICROFILMED

UNLESS OTHERWISE SPECIFIED
SURFACE FINISH
*2 PLACE DECIMAL ± .03
*3 PLACE DECIMAL ± .010
* EXCEPT DRILLED HOLES
ANGULAR DIMS. ± 2°
MACHINE PER V S 1-3-84

MATERIAL
GOV'T SPEC
HEAT TREATMENT
GOV'T. SPEC

MODEL 91617-X

REF.

DR. KOVALSKY DATE 8/16/62
CHK. HK DATE 8/30/62
T.O. NO. 20119 DATE 8-30-62
PROTOTYPE REL. DATE
PROD. REL. DATE
APP. DATE

TITLE
TEST VALVE FIXTURE

SCALE 2/1 WT. ACT. CALC.

VICKERS
R&D
VICKERS INCORPORATED
DIVISION OF SPERRY RAND CORPORATION
DETROIT, MICH. TORRANCE, CALIF.

DWG SIZE D 91617-X

CATION

91617-X

SHOWN

6 6

NO OF CYCLES - 10,000 MIN.

OUTSIDE PRESSURE - 250 PSI (B1)

WORKING PRESSURE - 250 PSI
(CONSTANT DURING OPER

MAX. PRESSURE - 375 PSI (B2)

AXIAL COMPRESSIVE SPRING RATE
(250 PSI WORKING PRESSUR
COMPRESS BELLOWS TO IN
LENGTH AS SHOWN)

MAX TORQUE AT PIVOT POINT TO
BELLOWS 1°50' AS SHOWN

B

MARK
LATES
LETT

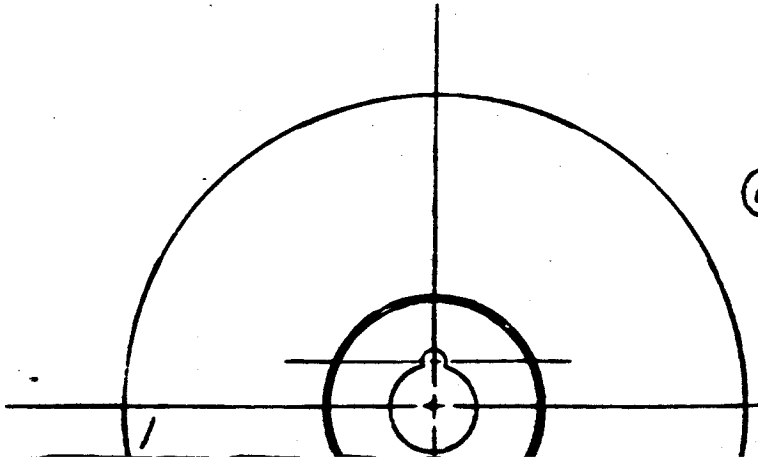

2

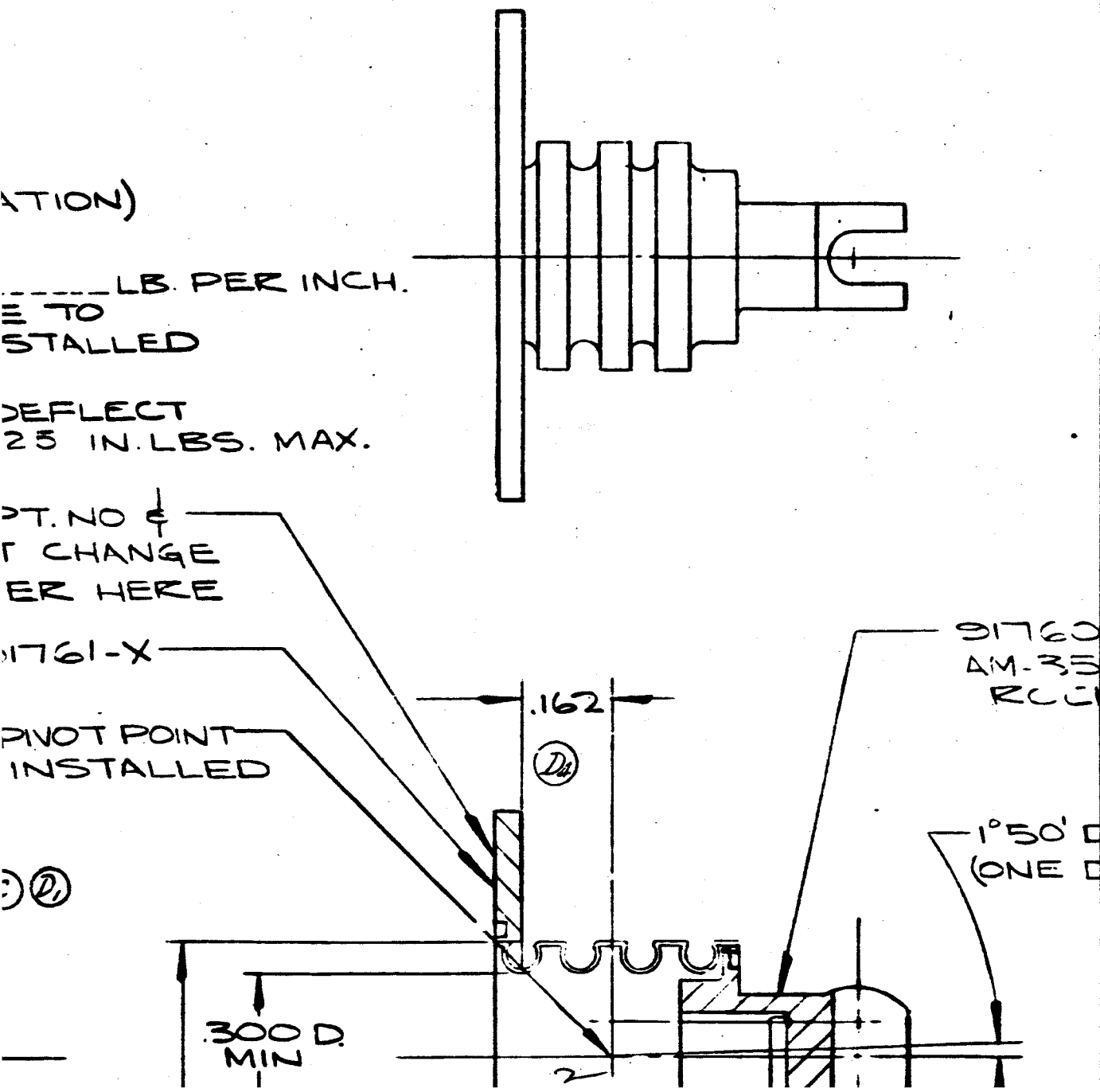

ATION)
LB. PER INCH.
E TO
STALLED
DEFLECT
25 IN. LBS. MAX.
PT. NO ¢
T CHANGE
ER HERE
1761-X
PIVOT POINT
INSTALLED
.162
91760
AM-35
1°50'
(ONE
.300 D.
MIN

3

REVISIONS				
ZONE	SYM.	DESCRIPTION	DATE	APPROVAL
1-B 1-A 2-A	A	(1) VS 1-1-B-15 REMOVED (2) 235/.230 CENT. REMOVED (3) & (4) PICTURE CORRECTED WLW	9/21/62	W J Zoya 9-21-62
2-B 1-A	B	(1) WAS 370 PSI (2) WAS 425 PSI (3) WAS 370 PSI WLW	9/29/62	W J Zoya 10-29-62
2-B	C	PICTURE CHANGE .125 R. ADDED	12/28/62	W. J. Zoya
2-B 2-A 1-A 2-B	D1 D2 D3 D4	PICTURE CHG. -.125 R. REMOVED ADDED "INCONEL X" ADDED "ANNEALED" 32 FINISH REMOVED	2-25-63	W. J. Zoya

Figure 32

B

-X
O STAINLESS STEEL (A-1)
< 'C' 36-40

DEFLECTION
DIRECTION)

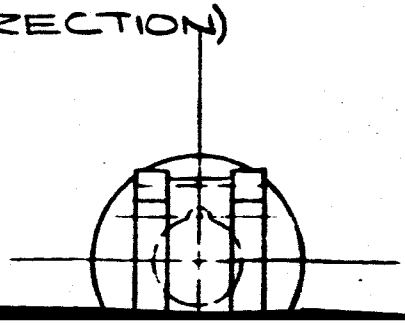

3

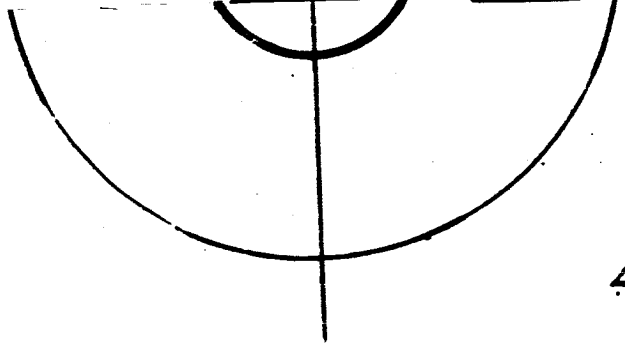

410
MA

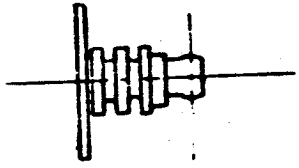

ACTUAL SIZE

4 4

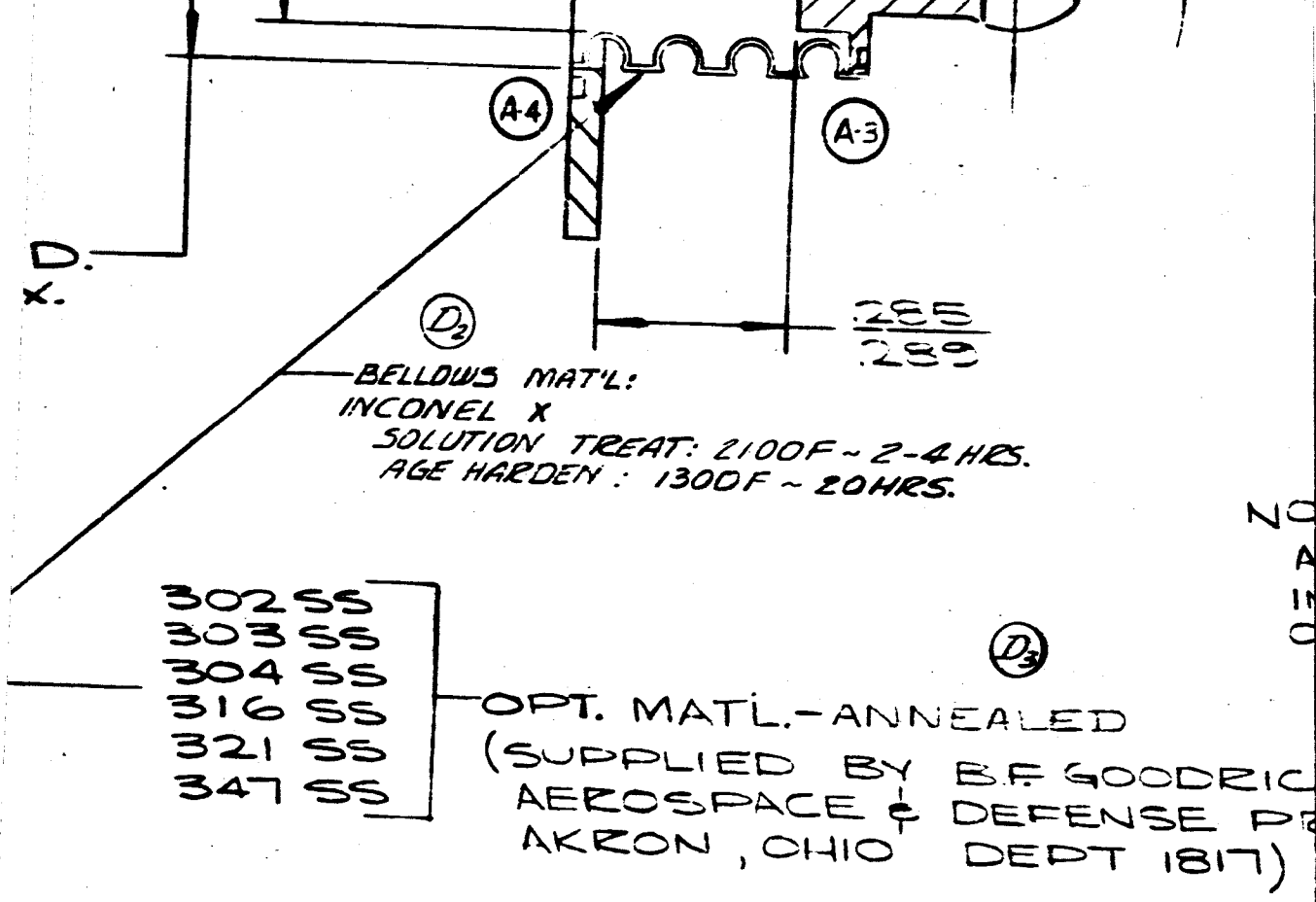

91766-X	91575-X
NEXT ASSY	USED ON
APPLICATION	

UNLESS OTHERWISE SPECIFIED

SURFACE FINISH 125 ✓

• 2 PLACE DECIMAL ± .03
• 3 PLACE DECIMAL ± .010
• EXCEPT DRILLED HOLES
ANGULAR DIMS ± 2°
MACHINE PER VS 1-3-3-1

MATERIAL GOV'T. SPEC. AS SHOWN

HEAT TREATMENT GOV'T SPEC. AS SHOWN

MODEL 91575	
REF. 7600	
DR. W FRANCIS	DA
CHK. [illegible]	DA
T. O. REL. ZOYA	DA
PROTOTYPE REL.	DA
PROD. REL	DA
APP.	DA

REDUCED COPY - NOT TO SCALE SHOWN

5 5

A-2

91464-X

D

TE:
LL DIMENSIONS SHOWN ARE
NSTALLED DIMENSIONS WITH
UTSIDE PRESSURE AT 250 PSI

B.3

H
ZODUCTS

UNLESS OTHERWISE SPECIFIED:

CONCENTRICITY OF MACHINED DIAMETERS ON SAME AXIS MUST BE WITHIN .010 TIR

REMOVE ALL BURRS & BREAK SHARP EDGES

A

VS 1-3-3-1

APPLICABLE SPECS.

MICROFILMED

11

-X	TITLE
D-X	BELLOWS -
TE 8-2-62	60 LB VALVE &
TE 8-3-62	NOZZLE
TE 8-3-62	SUB ASS'Y.
TE	
TE	
TE	
	SCALE 4/1 WT. ACT. CALC.

VICKERS
E&D
VICKERS INCORPORATED
DIVISION OF SPERRY RAND CORPORATION
DETROIT, MICH. TORRANCE, CALIF.

DWG SIZE C

91464-X

1

6

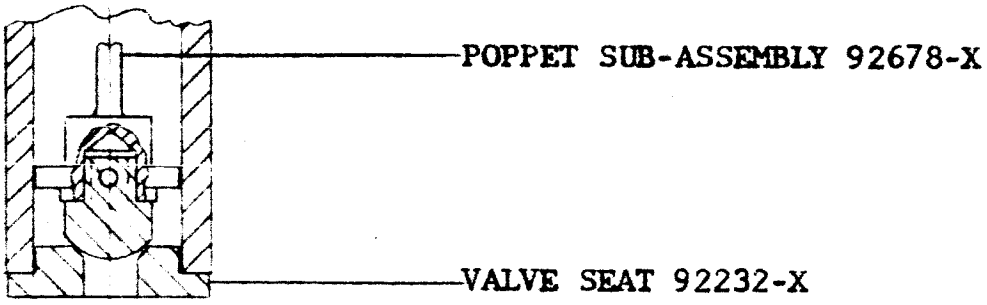

Figure 33A

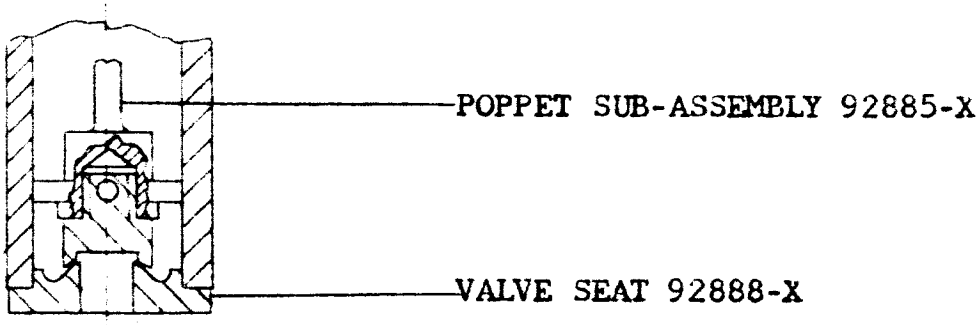

Figure 33B

Valve Poppet Sub-Assemblies

Figure 33

Test Conditions

Valve Stroke	.015 in
Cycling Frequency	10 cps
Input Current	.9 amps (28V) D-C
Test Fluid	N_2
Inlet Pressure	260 psig
Ambient Temperature	78°F
Test Duration	200,000 cycles

Test I - Procedure

With an inlet pressure of 260 psig and the discharge port open to atmosphere, the test fixture was cycled electrically at 10 cps. During this test, the afore mentioned sub-assemblies were monitored every 1/2 hr. for any signs of malfunction.

With the discharge port left open, and the electrical power momentarily shutoff, the fixture was submerged in water up to the solenoid and checked for leakage. Since more thorough and comprehensive tests were made as to the sealing capabilities of the poppet and seat, which is covered in another section of this report, a short time of 1/2 min. every 1/2 hr. under water was felt to be sufficient time to ascertain the sealing integrity of the poppet and seat as well as the bellows assembly.

Test I - Results

The test was terminated after completing 214,800 cycles due to the

erratic behavior of the solenoid. The 10 cps armature action was not being maintained, with skips to the normal pulsing observed. This erratic pulsing was caused by brinneling of the armature opening-stop and is described further in discussion of the solenoid performance below.

There was no indication of leakage or malfunction of the poppet, seat or the bellows assembly up to the shut down of the test.

Leakage of the poppet valve could of course be detected from the open discharge port and any leakage of the bellows could be seen at the slot in the pivot plate through which the lever arm is assembled. There was no leakage at any time during the test.

$$\frac{214{,}800 \text{ total cycles}}{18{,}000 \text{ cycles}/\tfrac{1}{2} \text{ hr.}} = 12 \text{ checking periods}$$

Inspection

The test fixture was completely dis-assembled and all the following parts examined carefully using a 30 power microscope.

Solenoid

For this test, the solenoid Figure 34, was assembled with a light spring attached to the armature and with power off would assist in returning the armature to full open position taking up all backlash in the linkage

IV-7

Endurance Test Solenoid

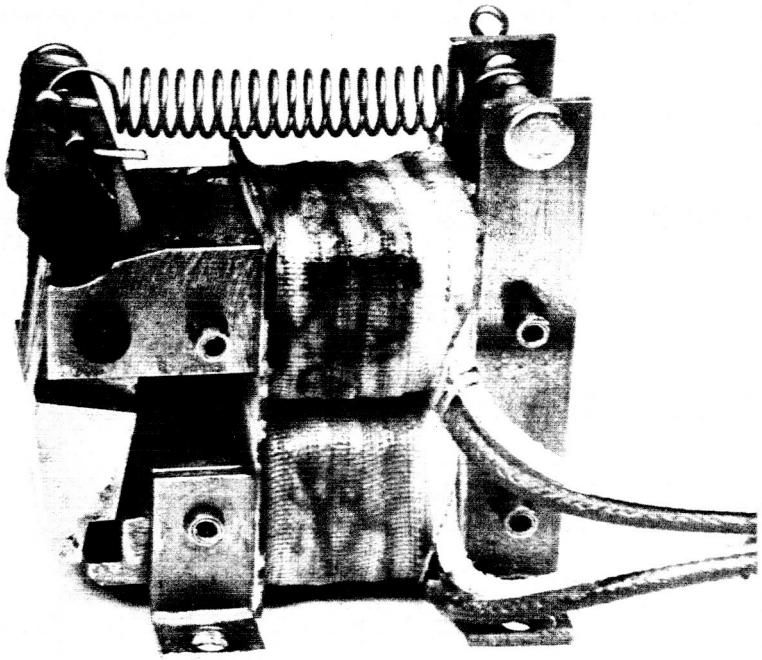

Figure 34

train. The stop for the armature was made-up of the armature support strap and the end of the pole piece. This stop dictates the open position and optimum corner-to-corner gap of the armature and pole piece. There is a ratio of approximately 5:1 in the distance between the armature stop and the opposite stepped end of the armature with reference to the pivot point. Therefore, with the armature stop located close to the pivot point, a small amount of brinneling can substantially increase the initial air gap beyond optimum corner-to-corner position.

It was this wear and increase in gap that caused the erratic operation of the solenoid, since pulling power to the solenoid decreases rapidly as the initial gap increases beyond corner-to-corner. A stop located at the stepped end of the armature would correct this condition. This was changed on Endurance Test II.

The copper graphite bearings (4 on each solenoid assembly), were in very good condition and indicated a minimum amount of wear.

The non-magnetic brass strip on the crown, drawing #91700-X, which serves both as the armature stop and flux gap in the closed position, showed normal wear and was in very good condition.

The two coils assembled on the pole piece loosened up slightly. However this is not serious and can be corrected in the future with the

FORM EN-201-A REV. 9-62 KSE 168 9-62

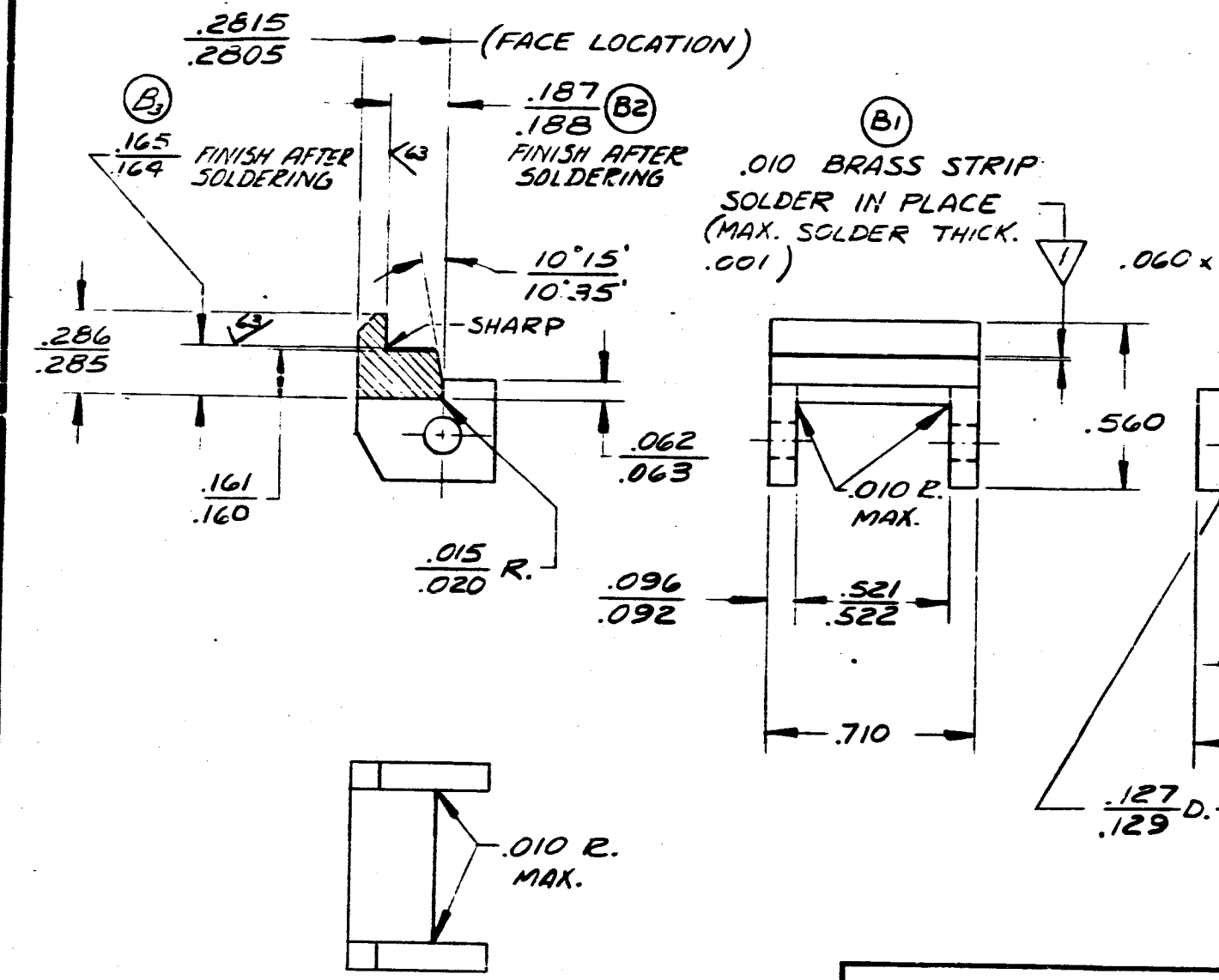

1 SOLDER WITH STAINTIN 157 PA
B4 (EUTECTIC WELDING ALLOYS CORP.)

91688-X	91688-X
NEXT ASSY	USED ON
APPLICATION	

UNLESS OTHERWISE SPECIFIED
SURFACE FINISH 125
2 PLACE DECIMALS ± .03
3 PLACE DECIMALS ± .010
ANGULAR DIMENSIONS ± 2°
CONCENTRICITY .010 TIR MAX.
REMOVE ALL BURRS & BREAK SHARP EDGES .010 MAX.
MACHINE PER VS 1-3-3-1
MATERIAL VS 1-1-7-1
HEAT TREATMENT

REDUCED COPY - NOT

91700-X B

REVISIONS

SYM	DESCRIPTION	DATE	APPROVED
A	REVISED & REDRAWN	1-14-63	[illegible]
B1	BRASS STRIP (SOLDERED) ADDED	2-22-63	
B2	.187 - .188 DIM. WAS .190 - .191	SARGO	W. J. ZOVA
B3	.165 - .164 DIM. WAS .1625 - .1615		
B4	SOLDER NOTE ADDED		

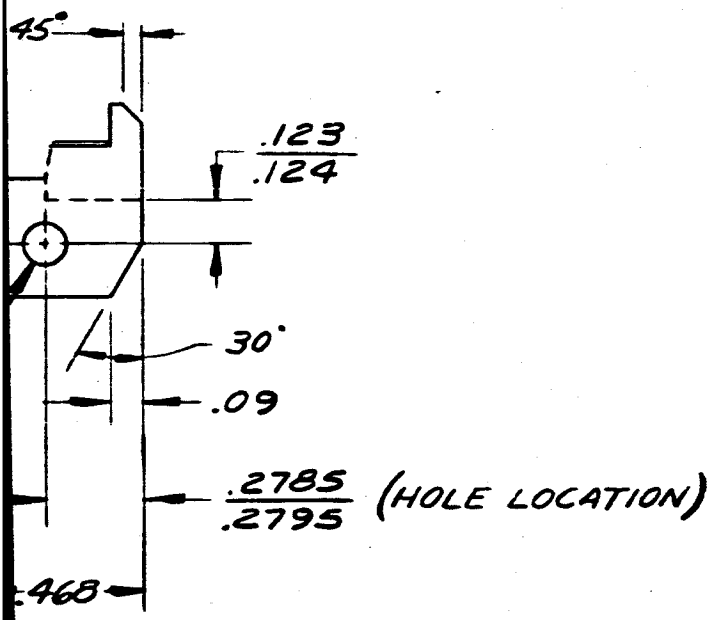

VS 1-1-7-1
VS 1-3-3-1
APPLICABLE SPECIFICATIONS

REF	
DR B. SARGO	DATE 8-8-62
CHK B. SARGO	DATE 8-17-62
T O REL ZOYA	DATE 8-27-62
PROTO REL	DATE
PROD. REL	DATE
STDS REVIEW	DATE
MFG REVIEW	DATE
ENGRG APP	DATE
PP	DATE

VICKERS
R : -

VICKERS INCORPORATED
DIVISION OF SPERRY RAND CORPORATION
DETROIT, MICH. TORRANCE, CALIF.

TITLE
CROWN

CODE IDENT NO.	DWG SIZE	
62983	B	91700-X
SCALE 2/1	WT ACT.	CALC	SHEET

TO SCALE SHOWN

2

use to an epoxy bond during the initial solenoid assembly.

Valve Poppet and Seat

The teflon ball and poppet sub-assembly tested with the stainless conical seat, were in excellent condition. The immediate seat area on the teflon had burnished to a high glossy finish with no discernable deformation. The concial seat appeared the same as when it was first assembled with no visible deterioration of the initial high polished surface.

Bellows Sub-Assembly

The bellows sub-assembly was removed from the test fixture and disassembled. There was no visible sign of fracturing of the bellows proper or the welds at each end. The header showed a minimum amount of wear in the area contacting the poppet. The pivot shaft which was installed as a free floating part showed signs of chafing inside the bellows. In future assemblies, the pivot shaft will be installed with a light interference fit in the lever to fix the location central within the inside diameter of the bellows.

Test II

A second endurance test was conducted that was primarily setup to test the "backup" poppet and seat design. The same fixture used in Test I was assembled with the following components.

1. Valve poppet and seat Figure 33A)
   a. Poppet sub-assembly #92885-X
   b. Valve Seat #92888-X
2. Solenoid Assembly - 91688-X

   The same solenoid assembly used in Test I, which had accumulated 214,800 cyles, was reassembled to the test fixture. It was felt that with an external armature stop (discussed after Test I) the solenoid would operate properly.

   A steel bracket Figure 36 was designed and made that contained 2-1/4-20 brass screws adjusted to optimum corner to corner conditions and locked in place to serve as the external armature stop. This bracket also served as a mounting base for the test fixture.
3. Bellows Assembly - 91464-X

   This same bellows assembly was also used in Test I, having accumulated 214,800 cycles.

Using the same solenoid and bellows assemblies from Test I in Test II, presented an opportunity to accumulate many more cycles and further establish the reliability of the design.

Test II Fixture - Armature Stop Setup

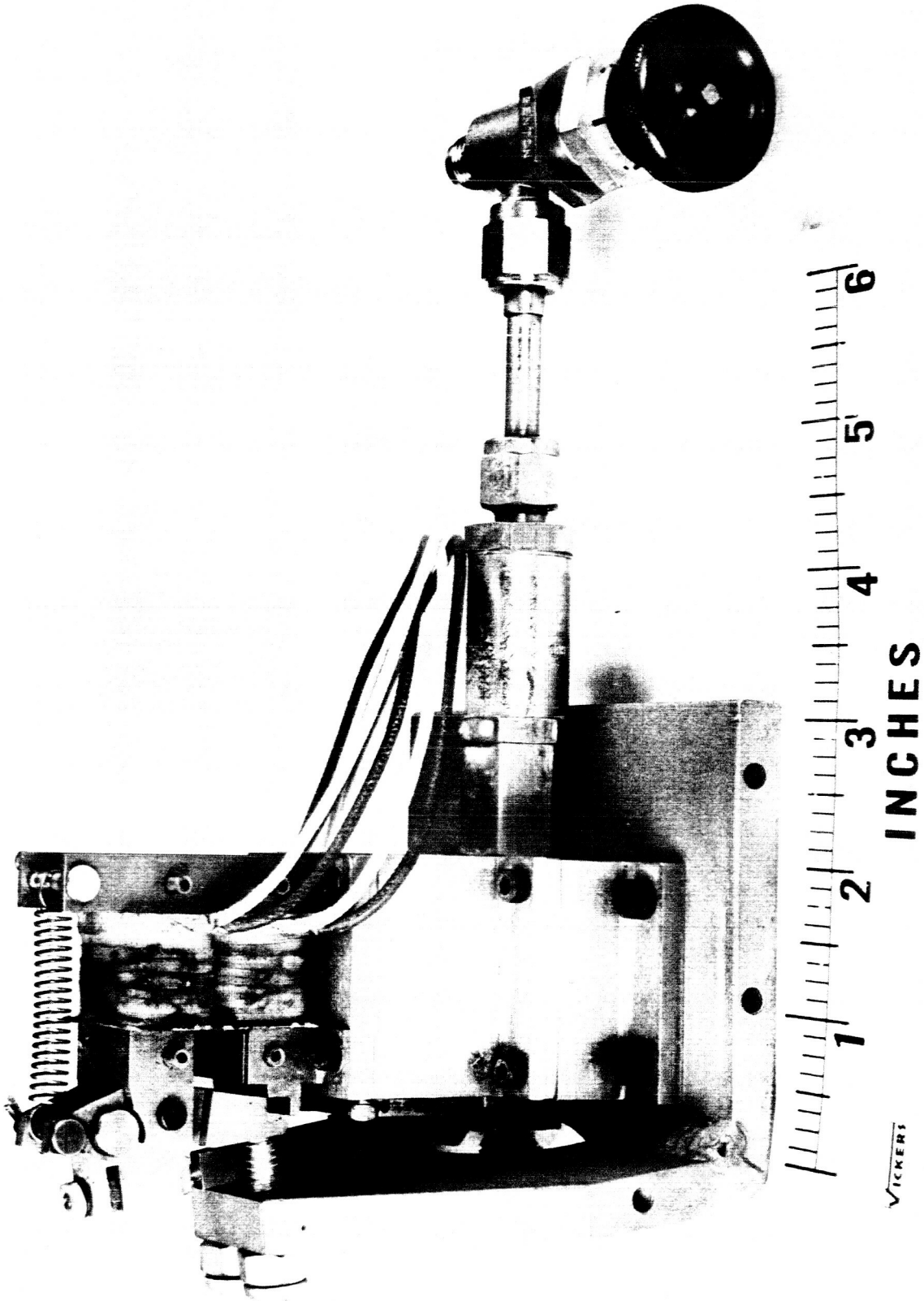

Figure 36

Test Conditions

Valve Stroke	.015 in
Cycling Frequency	10 cps
Input Current	.9 amps (28V) DC
Test Fluid	N_2
Inlet Pressure	260 psig
Ambient Temperature	76°F
Test Duration	250,000 cycles

Test II - Procedure

The test was conducted in the same manner as outlined in Test I procedure. The test was visually monitored every 1/2 hr. with leakage checks taken for 1/2 minute under water.

Test II - Results

The test was terminated after completing 252,000 cycles with no visible signs of leakage or malfunction.

$$\frac{252{,}000 \text{ total cycles}}{18{,}000 \text{ cycles}/\tfrac{1}{2} \text{ hr.}} = 14 \text{ checking periods}$$

A total of 466,800 cycles at 10 cps were accumulated by the solenoid and bellows assemblies in the endurance test series I and II.

Inspection

The test fixture was completely disassembled and all the following parts examined carefully, using a 30 power microscope.

Solenoid

The solenoid assembly operated very well during this test. The externally fitted armature stop has solved the problem of maintaining the optimum adjusted corner-to-corner gap position of the armature with respect to the pole piece. Future units would have a light-weight stop fitted to the solenoid and be part of the integrated assembly.

The four graphite and copper bearings were in excellent condition having smooth burnished surfaces and indicating a normal amount of wear.

The brass strip, installed as a combination air gap and armature stop (closed position) was also in excellent condition with no visible material deterioration.

Valve Poppet and Seat

The concave teflon and poppet sub-assembly with the stainless convex seat were in excellent condition. The contact area of the seat on the teflon was also burnished to a glossy finish with no deformation visible. The original polished finish on the stainless seat had been retained with no visible surface deterioration.

Bellows Sub-Assembly

The bellows was carefully inspected at the welded areas at each end and the bellows proper for any signs of fracturing or fatigue and was found to be in excellent condition.

Hot Firing Endurance and Reliability

The goal for endurance firing of the integrated pulse rocket was 10 minutes continuous firing at 10 cycles per second, equal on-off times. This goal was achieved. The first attempt was firing #60-23 on December 28, 1962, with a duration of 210 seconds. Some difficulties were encountered with linkage adjustments which required minor modifications. The combustion chamber shell failed from erosion (total accumulated time: 411 seconds) which prompted the accelerated development or erosion resistance in the combustion chamber.

Although the latter development was still in progress, firings 60-24 and 60-27 were made to evaluate modifications to the solenoid, poppets and linkage. Erosion failures of the combustion chamber were anticipated. Firing 60-24, which was witnessed by W. Karakulko of NASA, Houston performed well for 120 seconds at which time the test was shut down because of a combustion gas leak across a flange seal. The leak was caused by shrinkage of a new PA6 nozzle extension and resultant loss of assembly compression (discussed in the Combustion Chamber Section on Nozzle Extension.).

Other significant problem areas, based on these test results, are listed below along with modifications for incorporation in firing #60-27.

Problem Areas Encountered	Corrective Action Taken
1. Mounting flange of the pivot arm plate 91688-X shows signs of flexing at system pressure with a resulting distortion at the pivot arm pin, additional friction has been encountered.	1. Flange thickness has been increased. Location of #4-40 flange screws pulled in. Bellows chamber diameter has been decreased to facilitate relocation of the flange screws.
2. 91660-X pivot pin had been pressed into 91661-X lever arm at assembly. This could cause additional distortion to related parts.	2. Pin holes of related parts resized and pin length increased to establish full floating installation.
3. Oxidizer etching the inner surface of 91653-X plate. Fuel side o.k.	3. Material change from aluminum to a 300 series stainless to both plates.
4. 91651-X pin, supporting upper ends of push rods show evidence of fretting in the bearing area of the solenoid armature.	4. Armature side plates redesigned to facilitate installation of copper impregnated graphite bearings.
5. Fatigue failure of one link 91667-X at termination of threaded section.	5. None. Cause of failure was a combination of stress concentration produced by deep-cut threads coupled with a bending load imposed by improper alignment of solenoid, linkage and valve. The bending load oscillated with armature motion.

Firing #60-27 met all expectations of performance for 407 seconds including erosion failure of the graphite combustion shell as anticipated.

Firing #60-32, on February 4, 1963, incorporated the tested tungsten sheet liner to provide erosion resistance in the combustion chamber. This firing, witnessed by W. Karakulko and A. Watkins of NASA, Houston, cycled perfectly at 10 cps for 588 seconds and 48 seconds of minimum impulse bits (a total of 10 minutes and 36 seconds). Erosion failure of the combustion chamber did occur at the end of this firing, and while the life requirement was met, chamber erosion is recognized as the factor which limits reliable operation to 10 minutes. No other failures or degradation of performance occurred during the firing. Continued pursuit of the erosion problem through Vickers' funded research programs has, at the time of this writing, produced test data which would appear to have eliminated erosion as a problem.

Further development of endurance reliability under contract funding, beyond the attained goal, was not attempted in keeping with NASA's desires that greater emphasis be placed on achieving a minimum, repeatable impulse-bit.

power input. Electrical and valve response from command to poppets full open was .006 seconds and from valves open to 80% thrust was .010 seconds. Response from signal off to zero thrust was .005 seconds. Figure 37 illustrates these values from the final firing.

Considerable "bench" testing was performed on the integrated unit to determine what parameters most affected both "on" and "off" response. These tests were paralleled with a Vickers funded, generalized, dynamic analysis of the integrated unit and its driving pulse circuit. The dynamic analysis is not fully completed at this writing, and was really undertaken for Vickers use in optimizing future components and subsystems through analog studies. However, information gleaned from this section of the analysis coupled with bench test data, provided a rather thorough knowledge of what physically determined good response. Nitrogen supply bench test setup is shown in Figure 38.

Time was not available under this contract to fully apply the knowledge gained to the delivered hardware. Major changes to the prototype torque motor, for instance, were out of the question at this point in the program.

For a given solenoid and torque load, "on" response may be made faster by increased power input. Since torque load actuation is satisfied

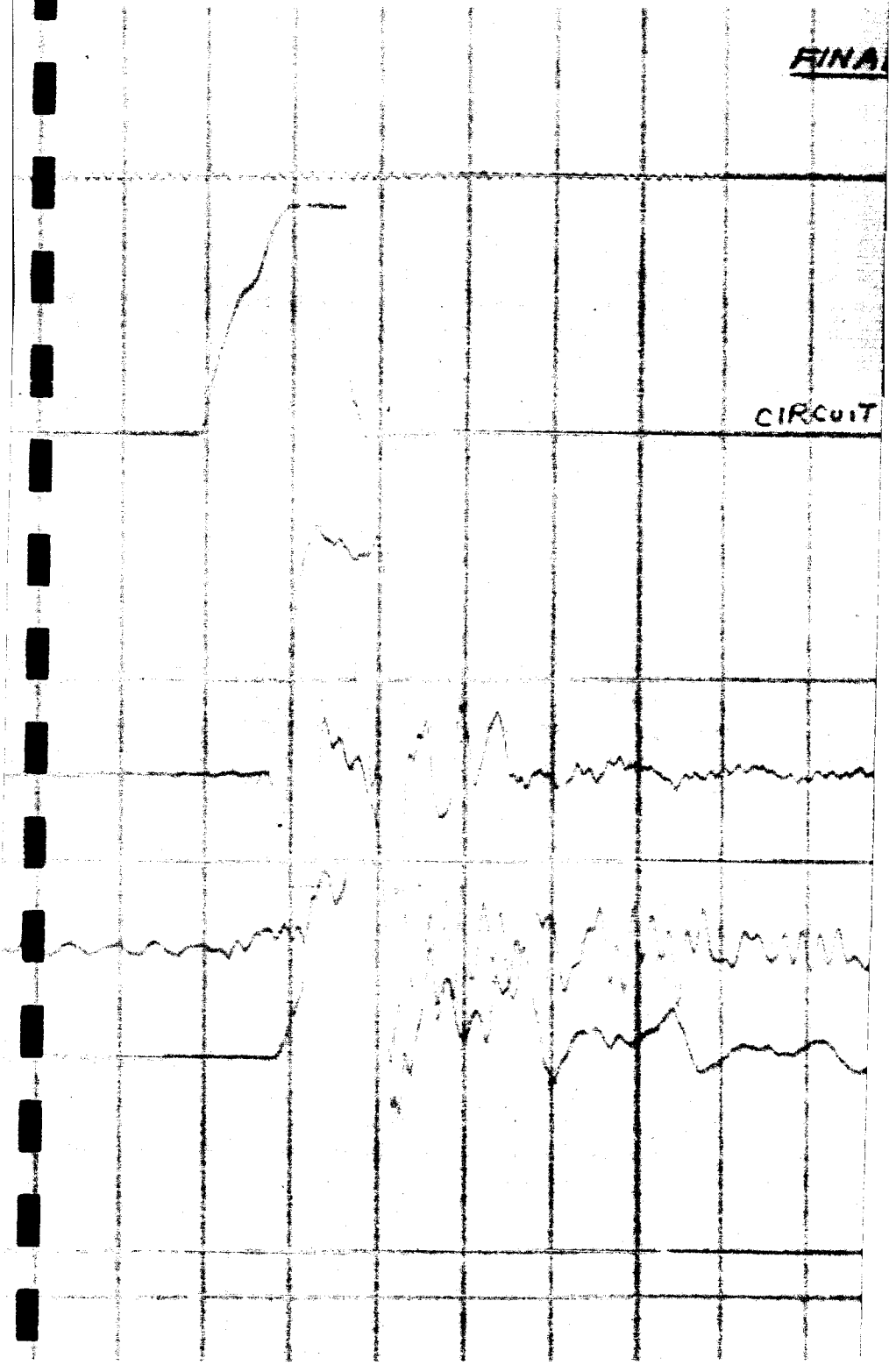
FINA
CIRCUIT

FIRING 60-34

P_{OX} = 235 PSI

P_F = 235 PSI

E = 40 VOLTS

CURRENT 1.5" = 1.0 AMPS

CALCULATED IMPULSE SI = .177 #-SEC

FUEL FLOW - SEE VENTURI CA

THRUST 1" = 20 #

OX FLOW - SEE VENTURI CALIBRA

.010 SEC

✓

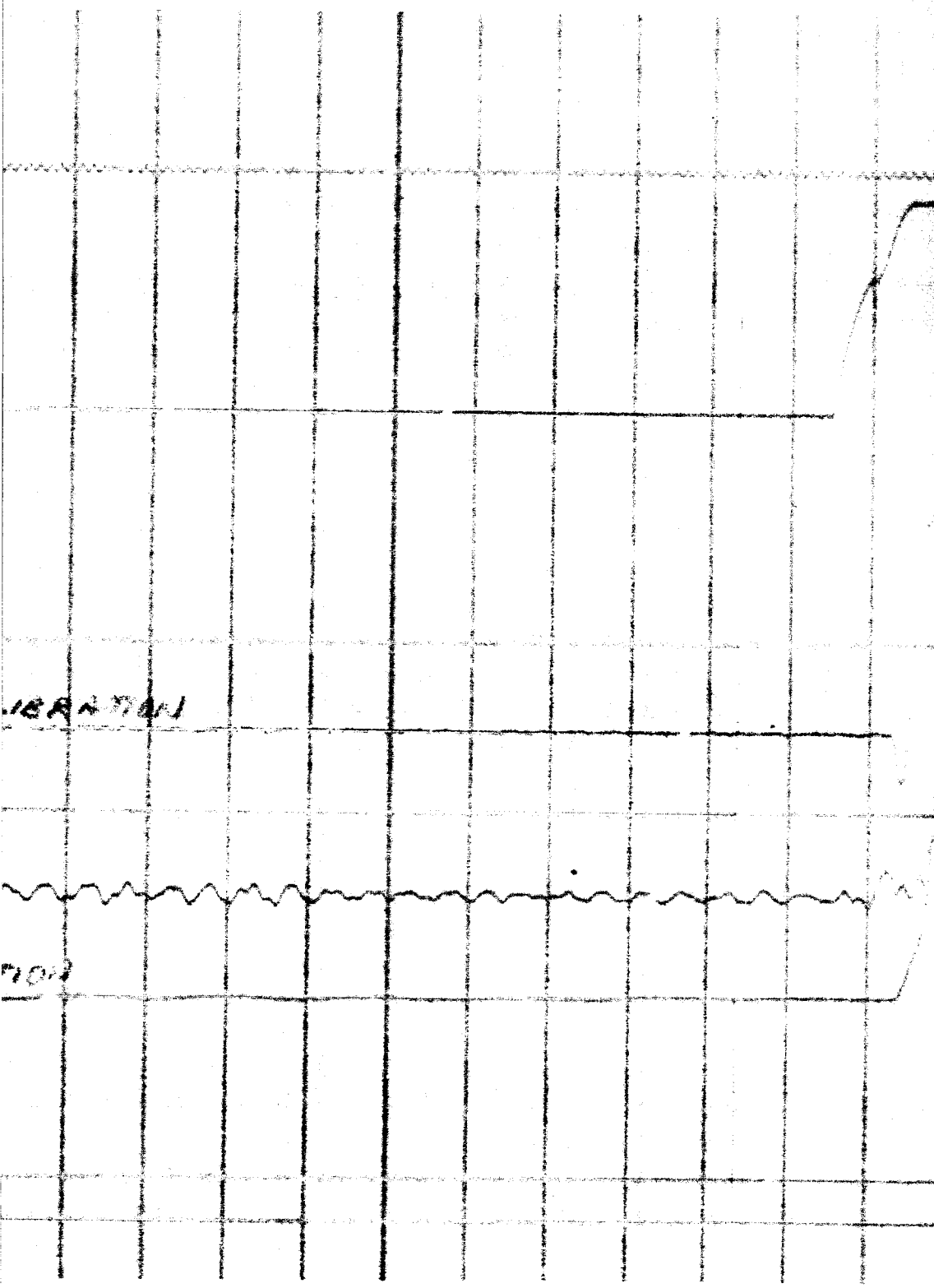

3

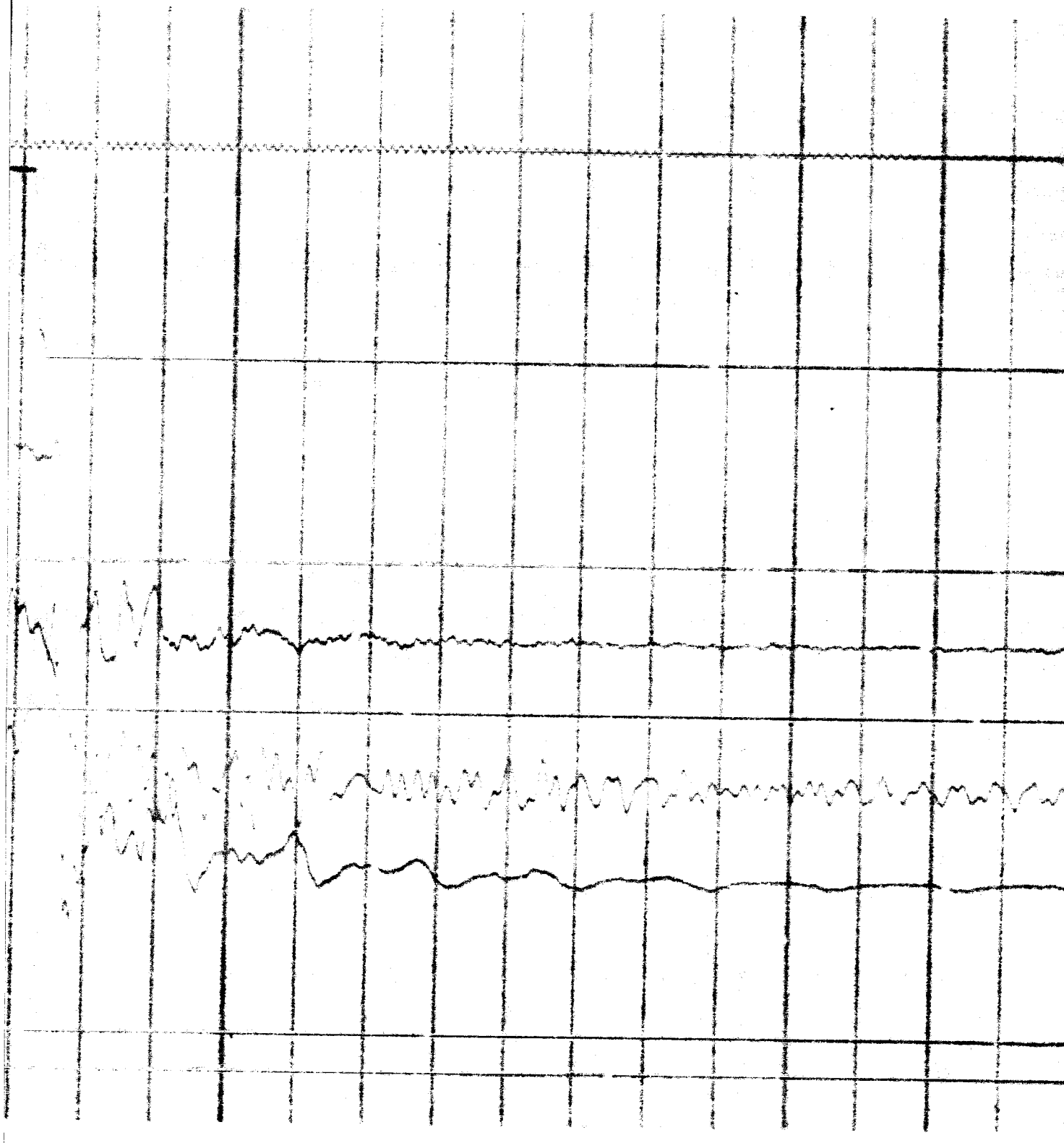

4

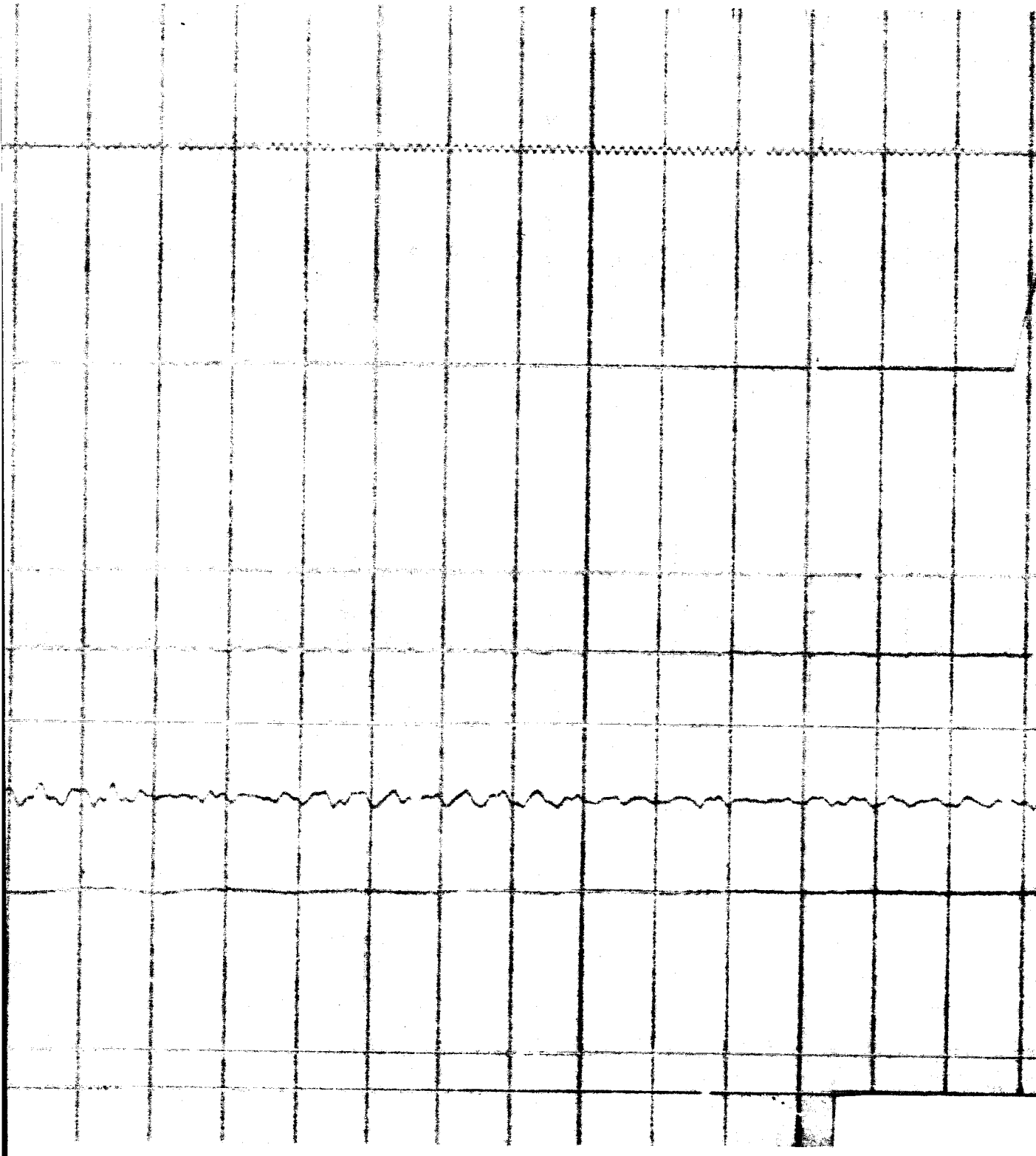

5

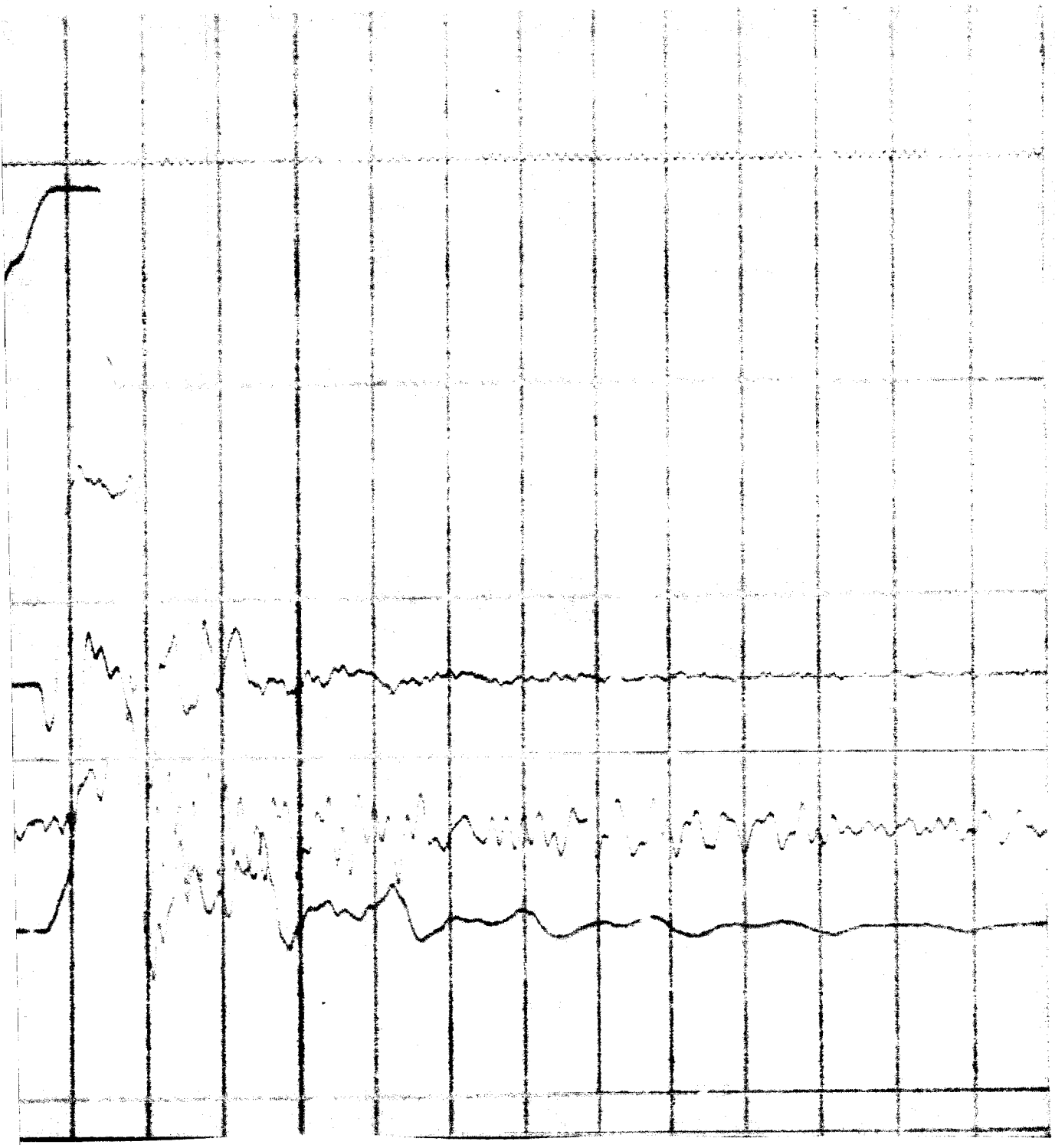

Final Firing Response Traces

Figure 37

Figure 36
Response Bench Testing

by a fixed value of ampere turns, it is undesirable to increase coil current beyond what is required because additional I^2R losses, in the form of heat, must then be dissipated by the coils. An external resistor of good wattage dissipation capability allows power input to be increased without unnecessary coil heating. To be consistent with redundant coil operation the external resistor must be equal to ½ the resistance of one coil circuit leg and be by-passed for single coil operation.

Figure 39 shows the affect of power on "on" response and demonstrates the principles stated above.

"On" response can also be improved by reducing circuit inductance relative to circuit resistance. For a given solenoid design and load configuration only a limited amount of juggling of $\frac{L}{R}$ can be done.

The coils shipped to NASA on the delivered unit were designed for 40 volt supply operation. Since NASA stated preference for 28 volt coils they are returning the unit for a coil change. Time was available in the interim to design the 28 volt coils such that a somewhat reduced $\frac{L}{R}$ could be realized.

"On"response,while important to closed loop system dynamics, does not affect attainment of a minimum impulse bit. Since the time lag

Figure 39

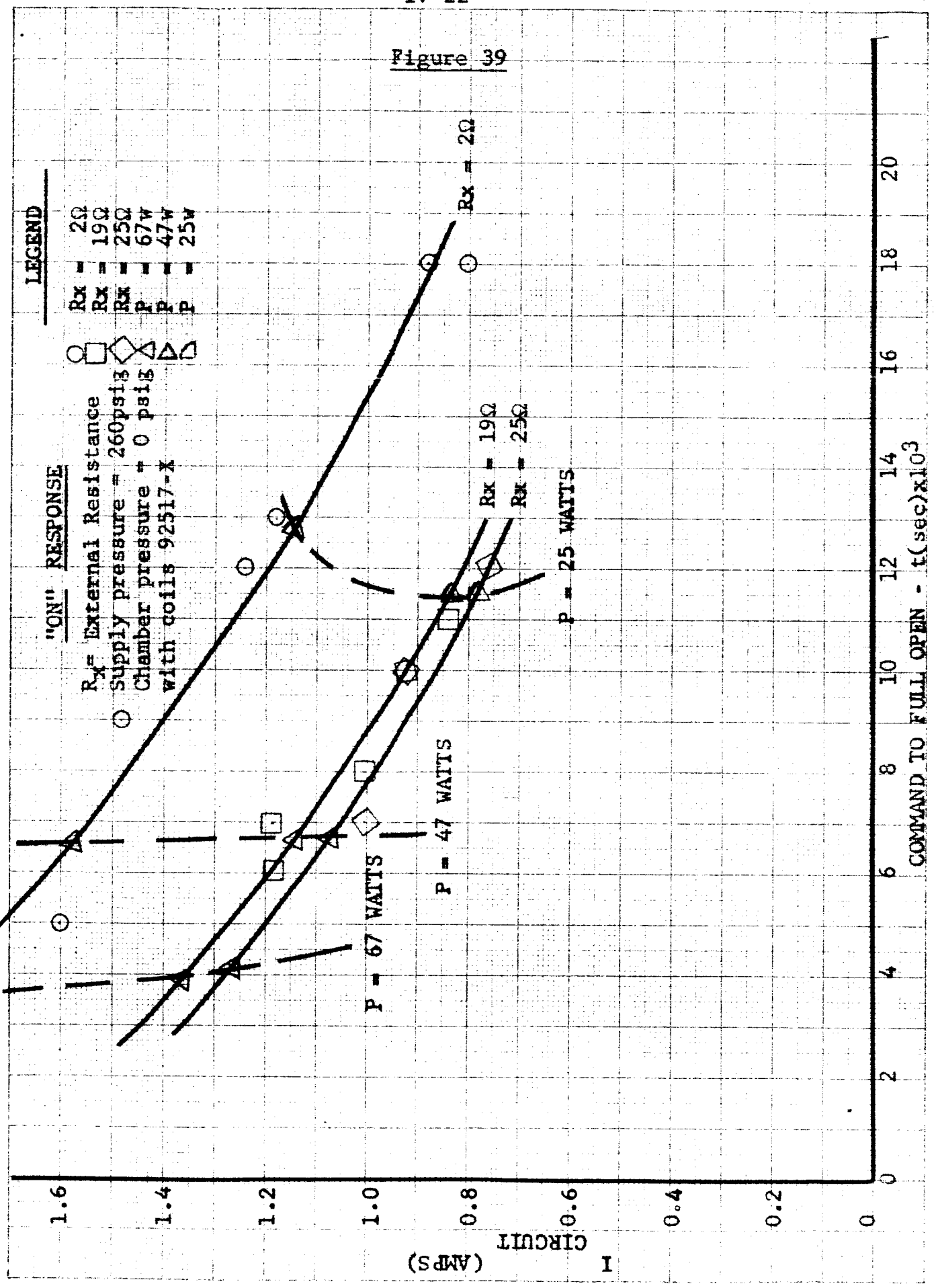
"ON" RESPONSE
Rx = External Resistance
Supply pressure = 260psig
Chamber pressure = 0 psig
with coils 92517-X
LEGEND
Rx = 2Ω
Rx = 19Ω
Rx = 25Ω
P = 67w
P = 47w
P = 25w
Rx = 2Ω
Rx = 19Ω
Rx = 25Ω
P = 25 WATTS
P = 47 WATTS
P = 67 WATTS
I CIRCUIT (AMPS)
1.6
1.4
1.2
1.0
0.8
0.6
0.4
0.2
0
0
2
4
6
8
10
12
14
16
18
20
COMMAND TO FULL OPEN - t(sec)x10^-3

between "off" command and "zero" chamber pressure represents a non-reduceable impulse (for a full stroking valve), this lag represents the minimum attainable impulse bit. Thus fast "off" response is of the utmost importance.

The existing solenoid design has a fast rising torque characteristic as the inverse working gap approaches zero (poppets open). This means that for good "off" response the current must decay to near zero rapidly because a very small current will hold the armature in its "in" position. Again, maintaining low inductance in the circuit becomes important to minimize current tail-off. To counteract current tail-off can be accomplished by an additional decay circuit, but more components are required and the high negative voltage transients tend to break down the transistor pulse switch. On the delivered unit, a last minute modification solved the problem through use of a high rate armature return spring which did not become engaged until a point in armature stroke after the initial poppet unseating forces had been overcome. Contract delivery deadline precluded application of other solutions to reduction of "off" time.

It is important to mention here that the circuit pulse switch itself can greatly influence current decay (and hence "off" response). When voltage is cut off in an inductive circuit a back emf is generated proportional to the time rate of current decay. A proper solid state switching circuit to provide fast decay and yet handle the large back emf generated without

component damage or transient current "leaks" requires careful design.

It is worth considering that for an optimum flyable pulse type reaction control, the switching circuit should be designed integral with a particular solenoid design. Thus, a single pulse rocket module could incorporate the solid state power switch, the solenoid, the bipropellant valve and injector, and the thrust chamber. For maximum system reliability a separate power switch would be used with each pulse rocket anyway. Thus each pulse rocket module would take two electrical plug-ins; (1) the low voltage command line from the pulse generator to trigger the solid state power switch circuit, and (2) the power supply line. Vickers has the capability to provide such a complete module.

SECTION V

CALIBRATION CURVES, INSTRUMENTATION, AND SCHEMATICS

SECTION V

CALIBRATION CURVES, INSTRUMENTATION, AND SCHEMATICS

The following figures are presented to illustrate propellant, nitrogen, and basic electrical circuits used by Vickers for firing thrust chambers and pulse rocket engines and to show specially developed thrust and flow pickups. Also presented in this section are calibration curves.

Figure 40 - Temporary Switching Circuit For Minimum Impulse Bit
This circuit is called temporary because repeatable "on" pulse widths could not be maintained in the .008 to .012 seconds range. A Tektronix pulse width modulator which can supply repeatable "on" pulses as short as .001 seconds is in operation at the time of this writing.

Figure 41 - Schematic - Firing Pad - Cell 2

Figure 42 - Schematic - Firing Pad - Cell 1

Figure 43 - Schematic - Instrumentation Circuit

Figure 44 - Vickers High Response Strain Bridge Load Cell
0 - 100# Thrust

Figure 45 - Vickers High Response Venturi Flow Meter

Figure 46 - Load Cell Calibration

Figure 47 - OX and Fuel Venturi Flow Meters Calibration

Figure 48 - Injector-Valve Calibration Poppet Stroke vs Propellant Flow

Figure 49 - Water Calibration of Injector - $\dot{\omega}$ vs ΔP

ADDITIONAL DESCRIPTIONS OF EQUIPMENT

The temporary switching circuit in figure 40 requires further explanation of its ability to maintain repeatable "on" pulse widths. Actually, repeatability of small impulse bits could be established for a given "on" width command (see figure 37, page IV-19). The test problem was that the Hewlett Packard Pulse Generator, which was modified with breadboard circuits to allow unbalancing of the "on" and "off" time widths, produced short "on" pulses which randomly varied plus of minus 2 milliseconds from a 10 millisecond nominal "on" pulse. Anywhere from 2 to 5 consistent "on" times would be generated before a change occurred. From any given set of consistent "on" times, however, a repeatable impulse was recorded. As was mentioned, a pulse generator is now in operation that supplied consistent "on" pulses as short as .001 second.

Vickers load cell shown in figure 44 is a high response thrust measuring device with a natural frequency of 715 cycles per second. The load is supported on 4 structural webs each of which are instrumented with 4 strain gages. Complete compensation is effected to cancel the effects of side loads and temperature. Output is linear and is read from a standard strain bridge circuit.

Vickers high response venturi flow meters, figure 45, are basically venturi meters designed for propellant flows of 0.1 to 1.0 gpm. Throat and upstream pressure taps are sensed by a unique sandwich diaphragm transducer with a natural frequency of 180,000 cps.

Strain gages within the diaphragm are protected from propellant contact.

The schematic of the electrical load circuit showing proper values for external resistance with the redesigned 28 volt coils is shown in Appendix C.

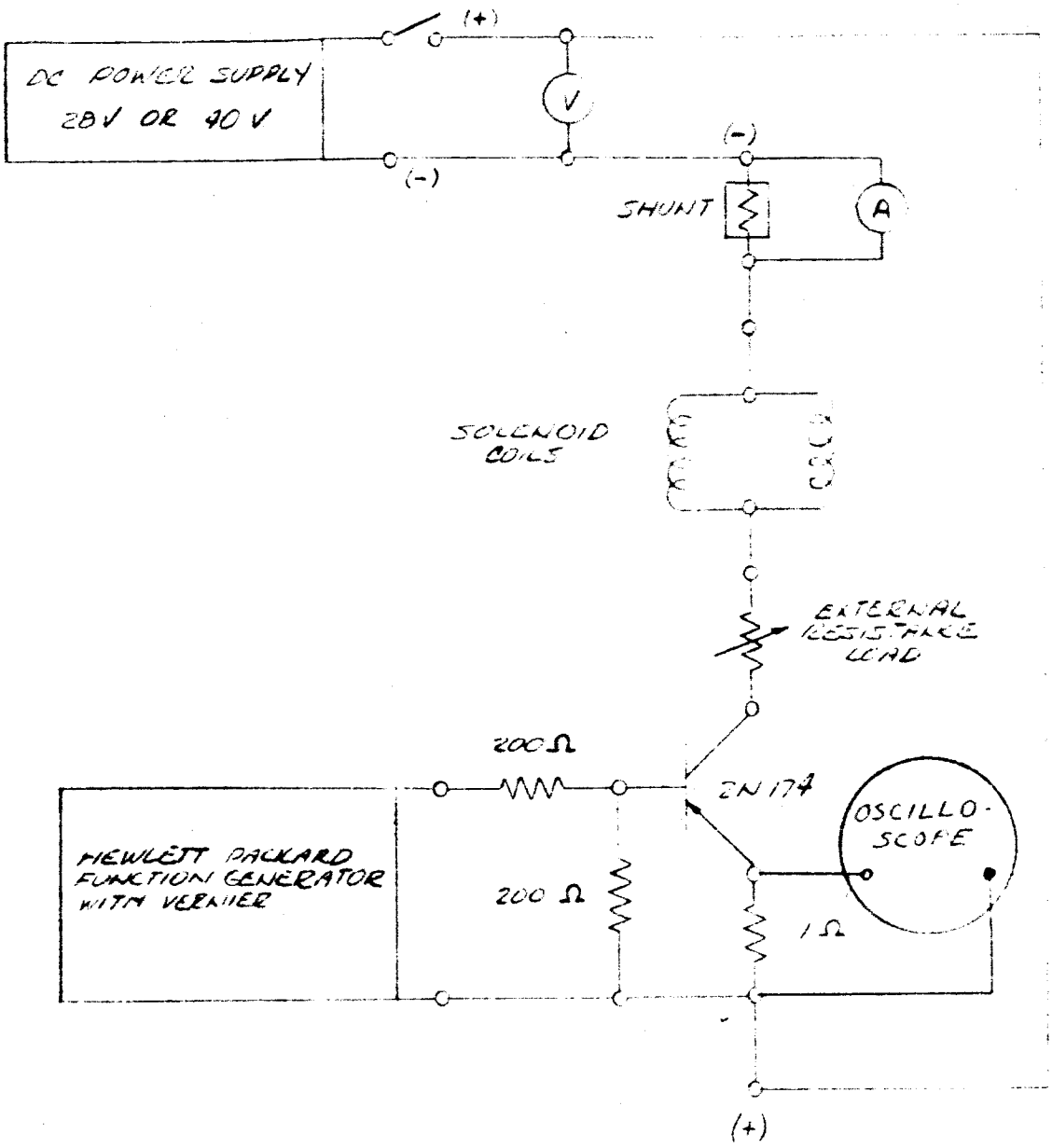

VICKERS INCORPORATED

RESEARCH & DEVELOPMENT

TEMPORARY SWITCHING CIRCUIT FOR MINIMUM IMPULSE BIT

FIGURE 40

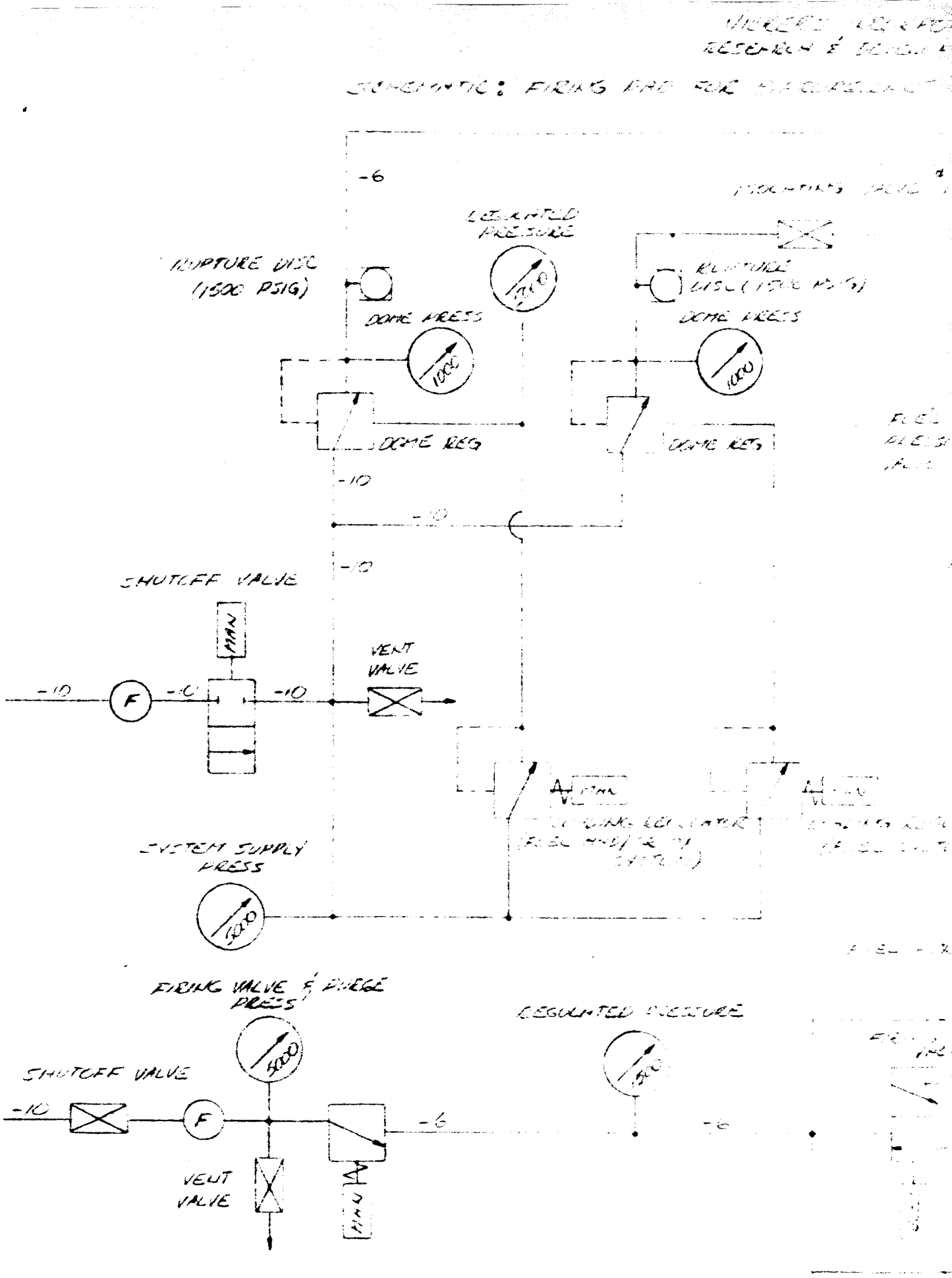

SCHEMATIC: FIRING PAD FOR
-6
REGULATED PRESSURE
RUPTURE DISC (1500 PSIG)
DOME PRESS
1000
DOME REG
-10
SHUTOFF VALVE
MAN
VENT VALVE
F
SYSTEM SUPPLY PRESS
5000
FIRING VALVE & PURGE PRESS
REGULATED PRESSURE
SHUTOFF VALVE
VENT VALVE

2

V - 3

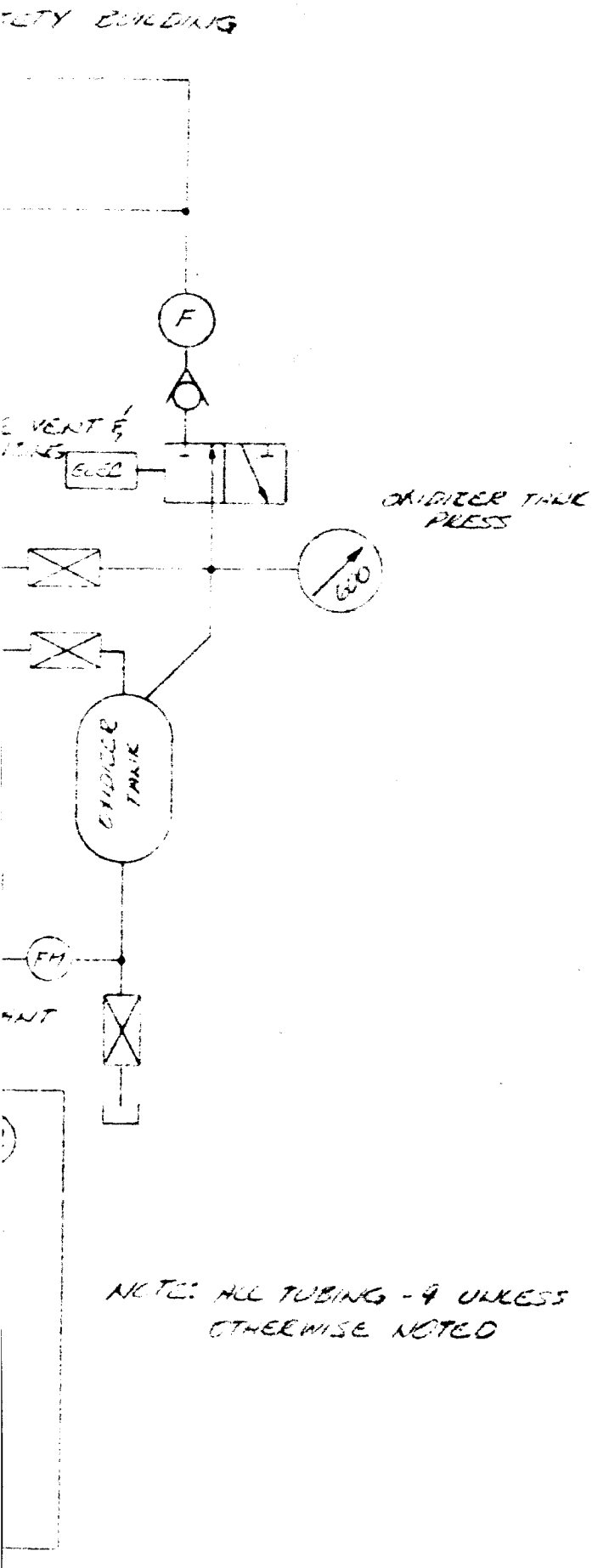

FIGURE 41

3

J.L. Coiac
E&D 2-15-3

1. DAHL VALVE, 539 P4/303 + L 1.6 + B + RC 15
2. SKINNER VALVE, V 53 DB 2 150
3. DAHL VALVE, 501 P4/303 + G 0.63 + RC [illegible]
4. TELEDYNE
5. TANK (91287-[illegible])
6. 1/8" HOKE HAND VALVE
7. AN 827-4C, CROSS
8. MS 20819-4C, SLEEVE
9. AN 818-4C, COUPLING NUT
10. AN 924-4C, BLKD NUT
11. AN 832-4C, BLKD UNION
12. AN 818-6C, COUPLING NUT
12A. AN 860-6-4C, REDUCER
13. AN 816-4C, PIPE-TUBE NIPPLE
14. FLOWMETER (FUEL)
15. FLOWMETER (OX)
16. AN 826-4C, TEE, PIPE RUN
17. AN 824-4C, TEE
18. AN 815-4C, UNION
19. AN 6227-4, O-RING
20. AN 820-4C, CAP
21. AN 824-6C, TEE
22. MS 20819-6C, SLEEVE
23. AN 820-6C, CAP
24. CHECK VALVE
25. AN 806-4C, PLUG

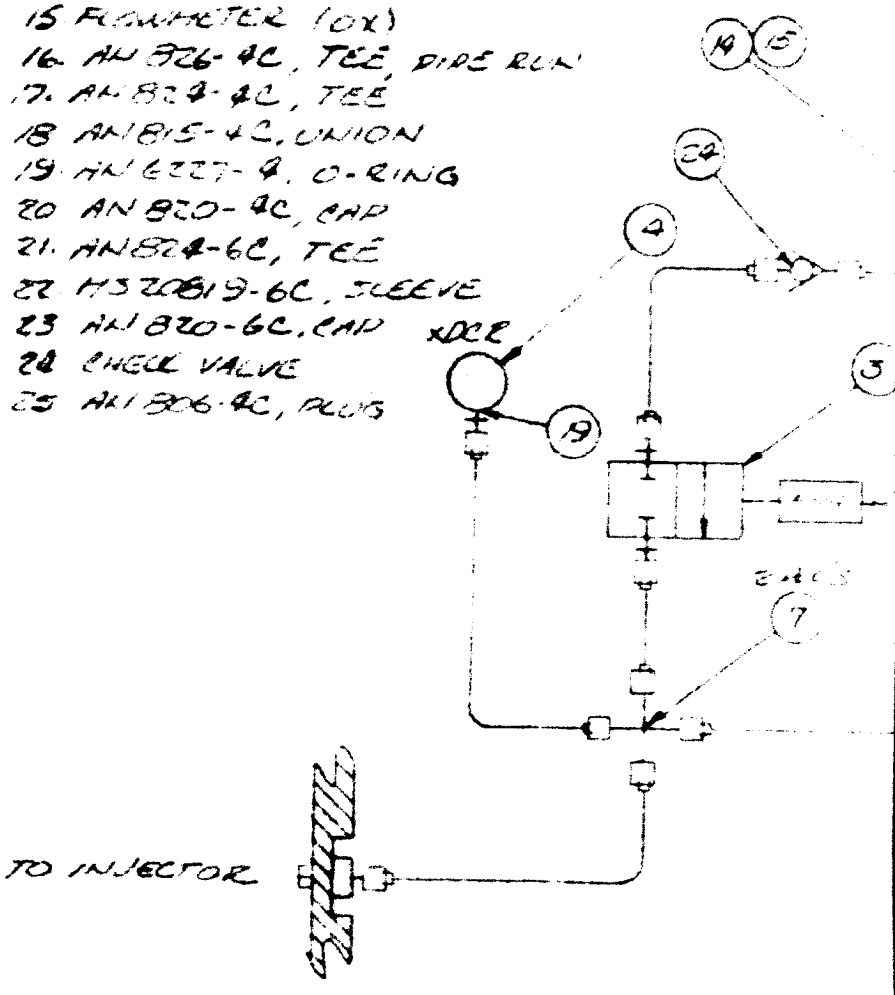

VICKERS
RESEARCH AND D

FUEL & OXIDIZ

FIRING PAD

1

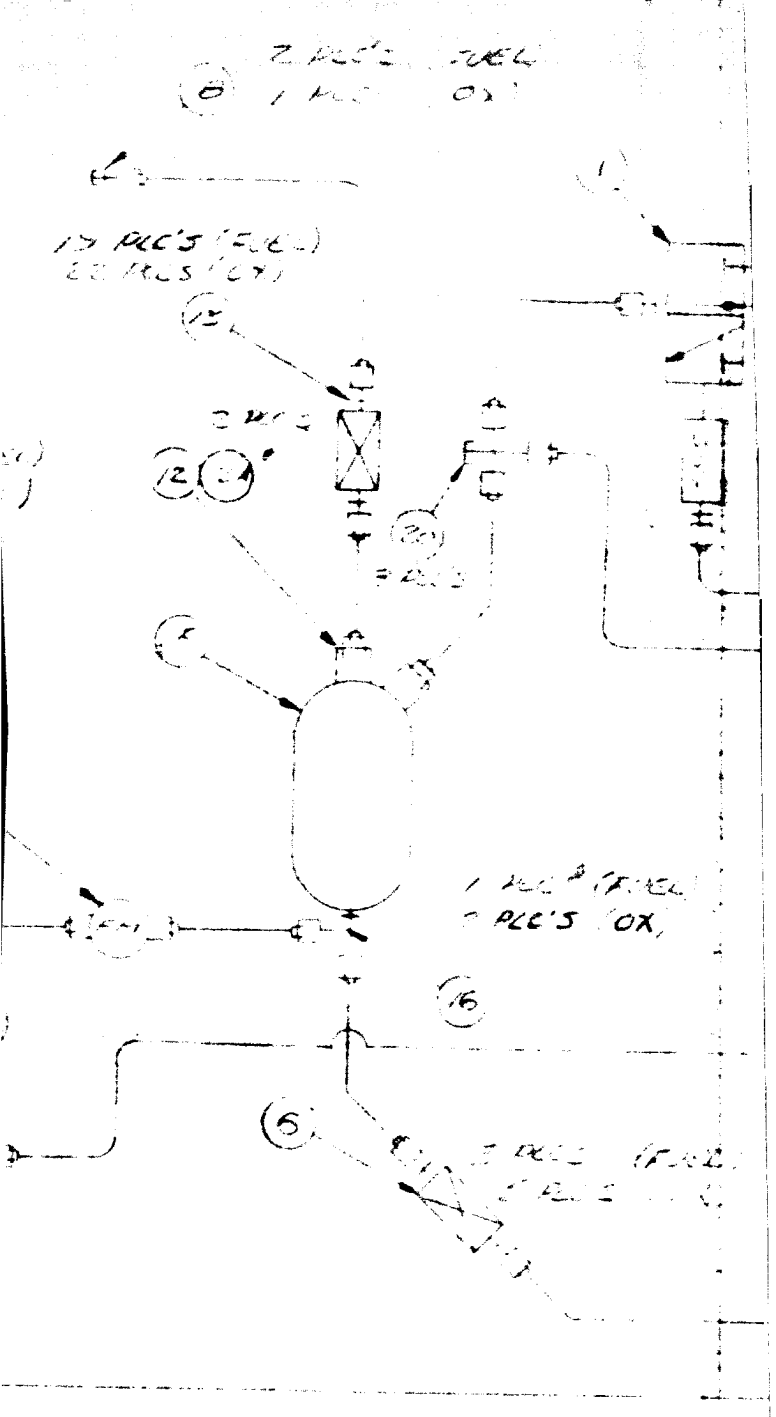

Inc
EVELOPMENT

1 MAXIMUM SAFETY BLDG.

2

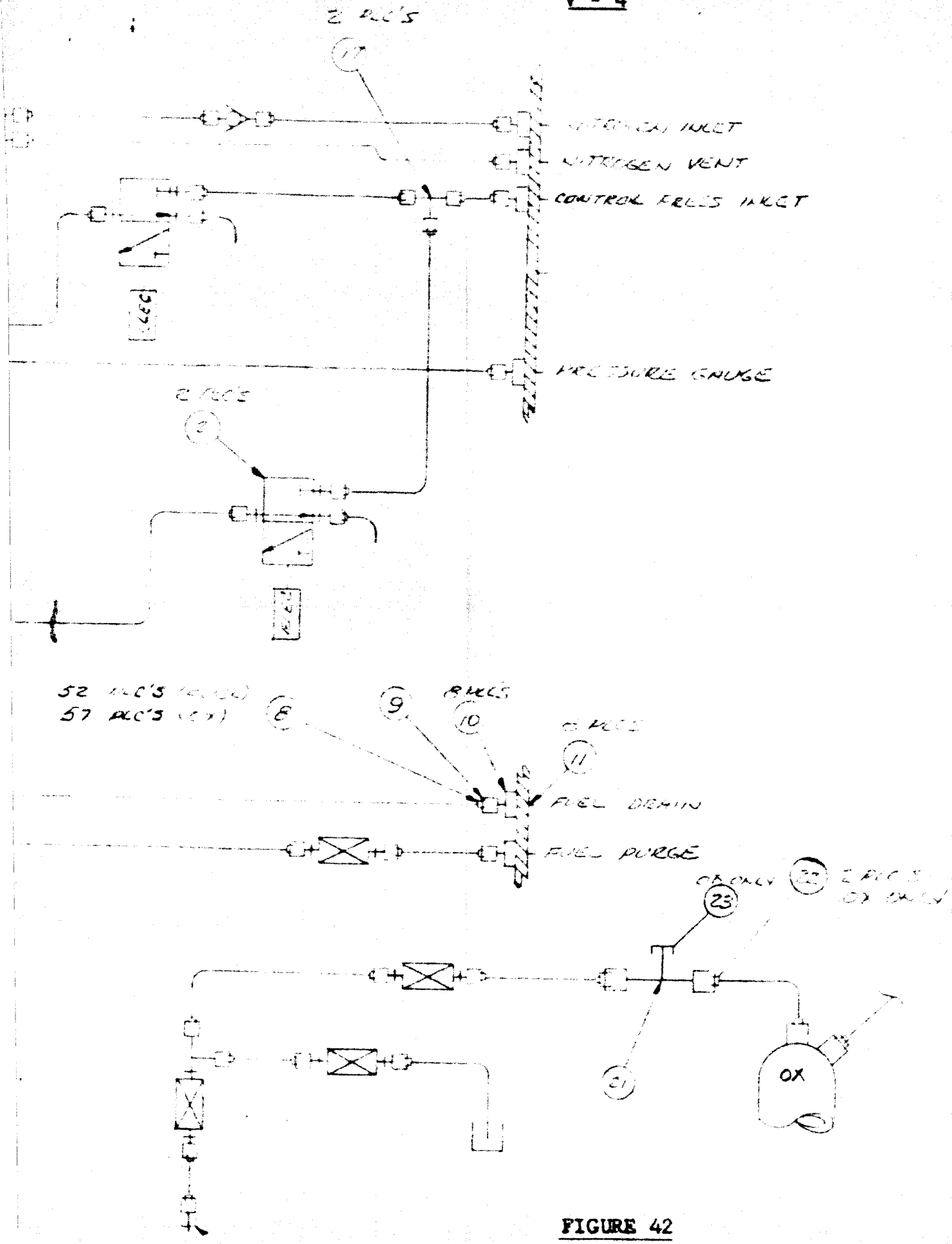
2 PLC'S
17
NITROGEN INLET
NITROGEN VENT
CONTROL FRLCS INLET
PRESSURE GAUGE
2 PLC'S
52 PLC'S
57 PLC'S
8
9
8 PLC'S
10
2 PLC'S
11
FUEL DRAIN
FUEL PURGE
OX ONLY
23
2 PLC'S
OX ONLY
31
OX
OX ONLY

FIGURE 42

Figure 43

Schematic - Instrumentation Circuit

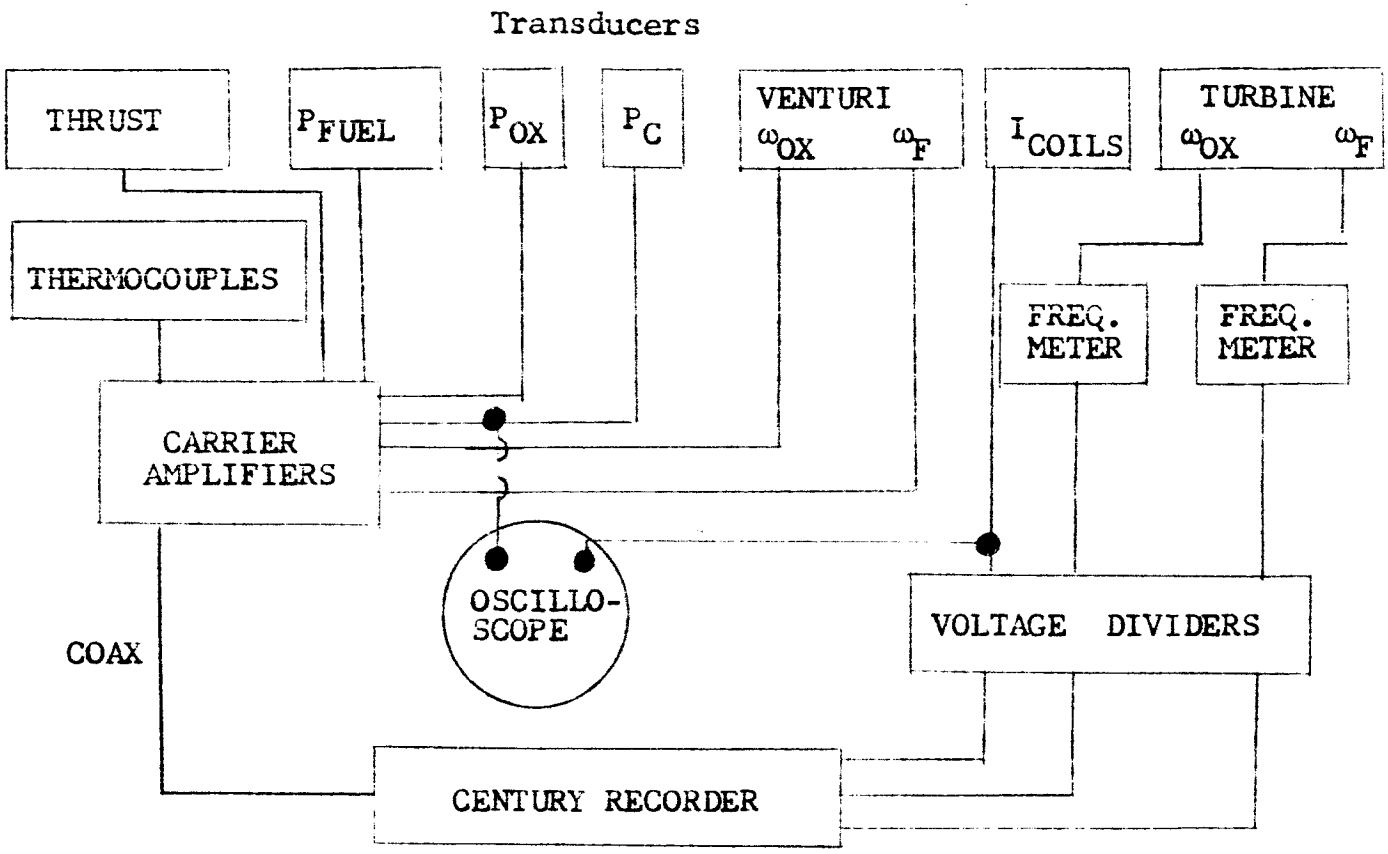

1. Pressure Transducers

   P_{ox}, P_f Taber type 176 0 - 1000 psi

   P_c - Dynisco Pt 31 0 - 1000 psi

2. Recorder - Century Model 408 Oscillograph Galvo Natural Frequency 500 cps

3. Amplifiers - Century Model 507 Carrier Amplifier Static and Dynamic Phenomena up to 500 cps

4. Flow - Fisher Porter Turbine, Vickers High Response Venturi

5. Thrust - Vickers High Response Strain Bridge Load Cell

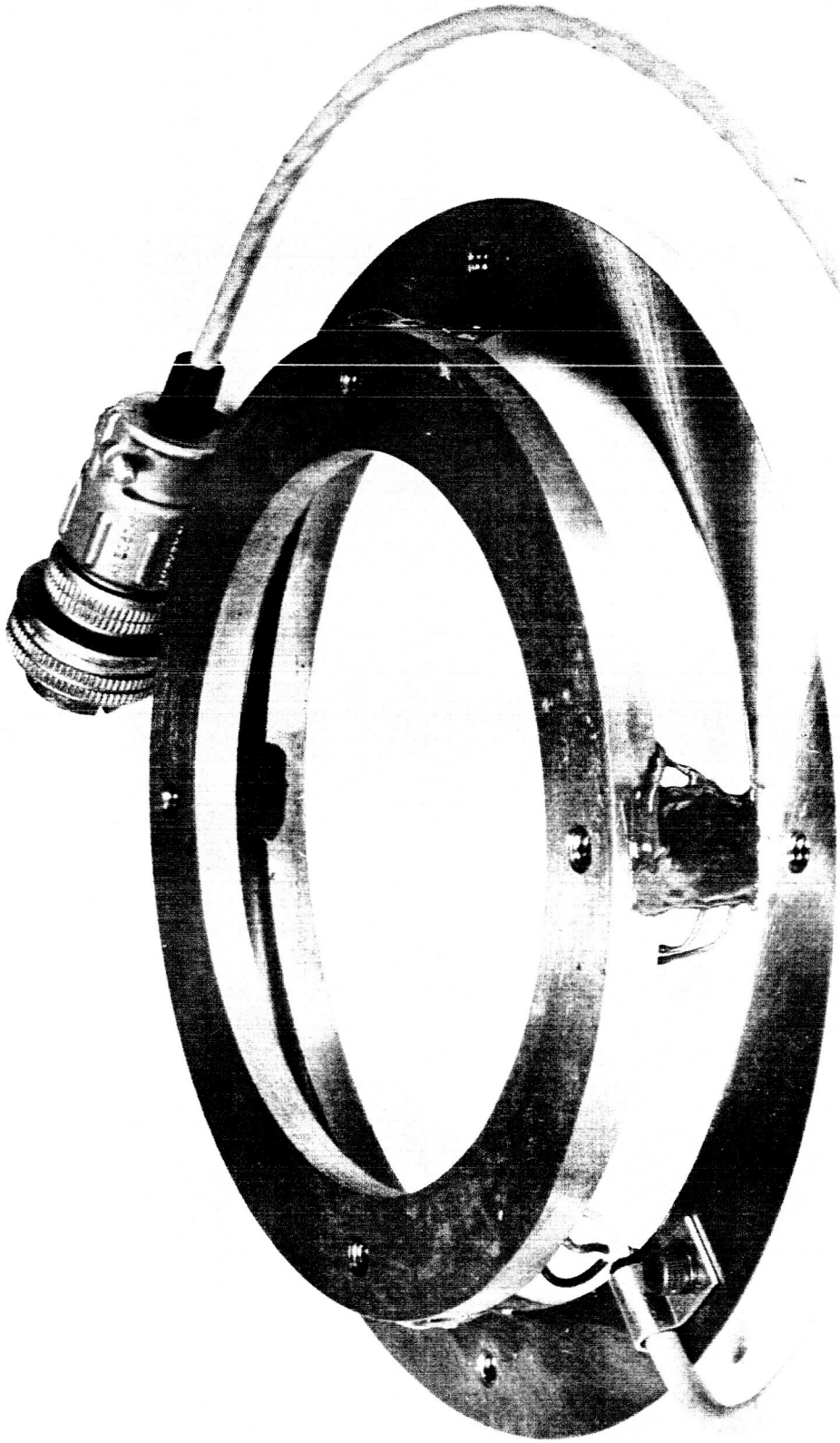

Vickers High Response Strain Bridge Load Cell

0 - 100# Thrust

FIGURE 44

B

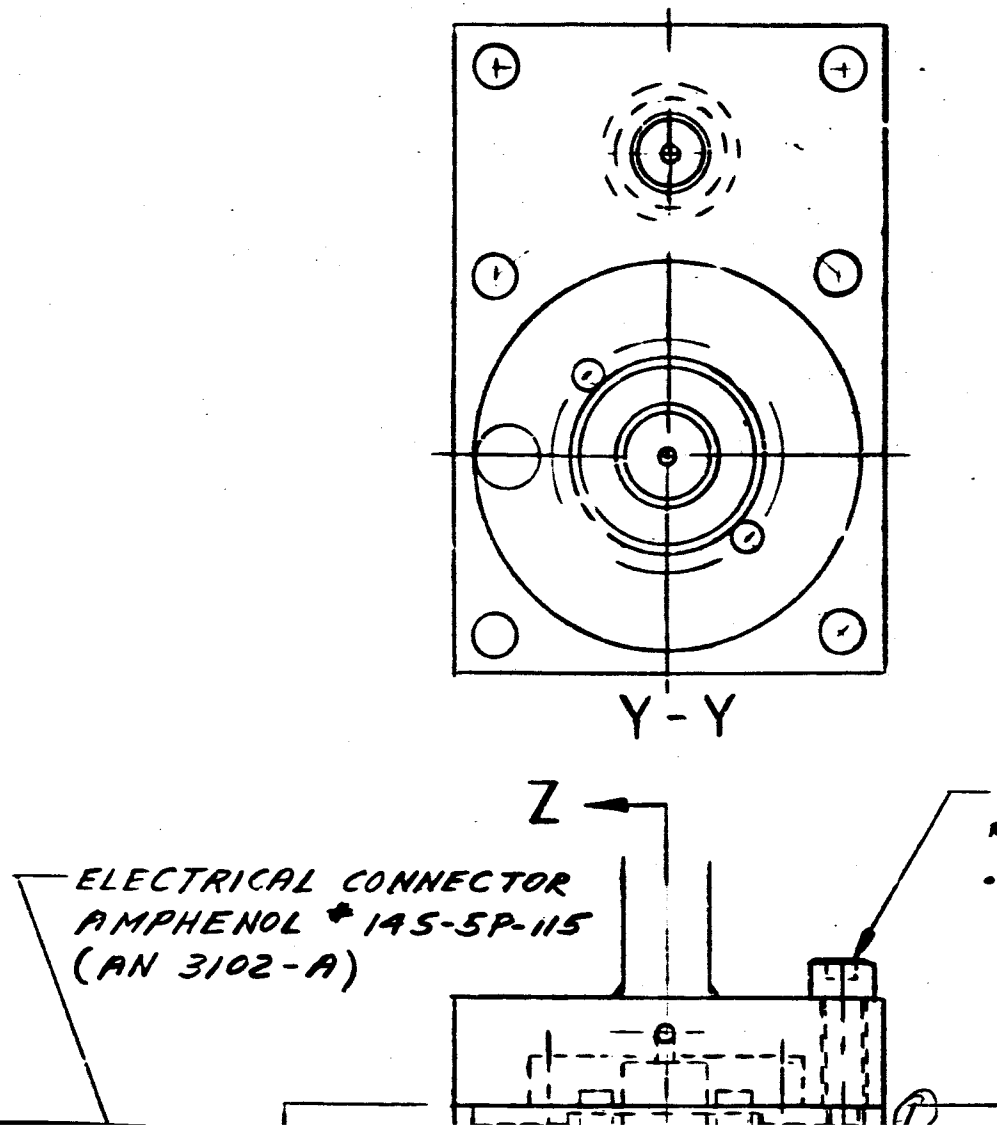

2 1

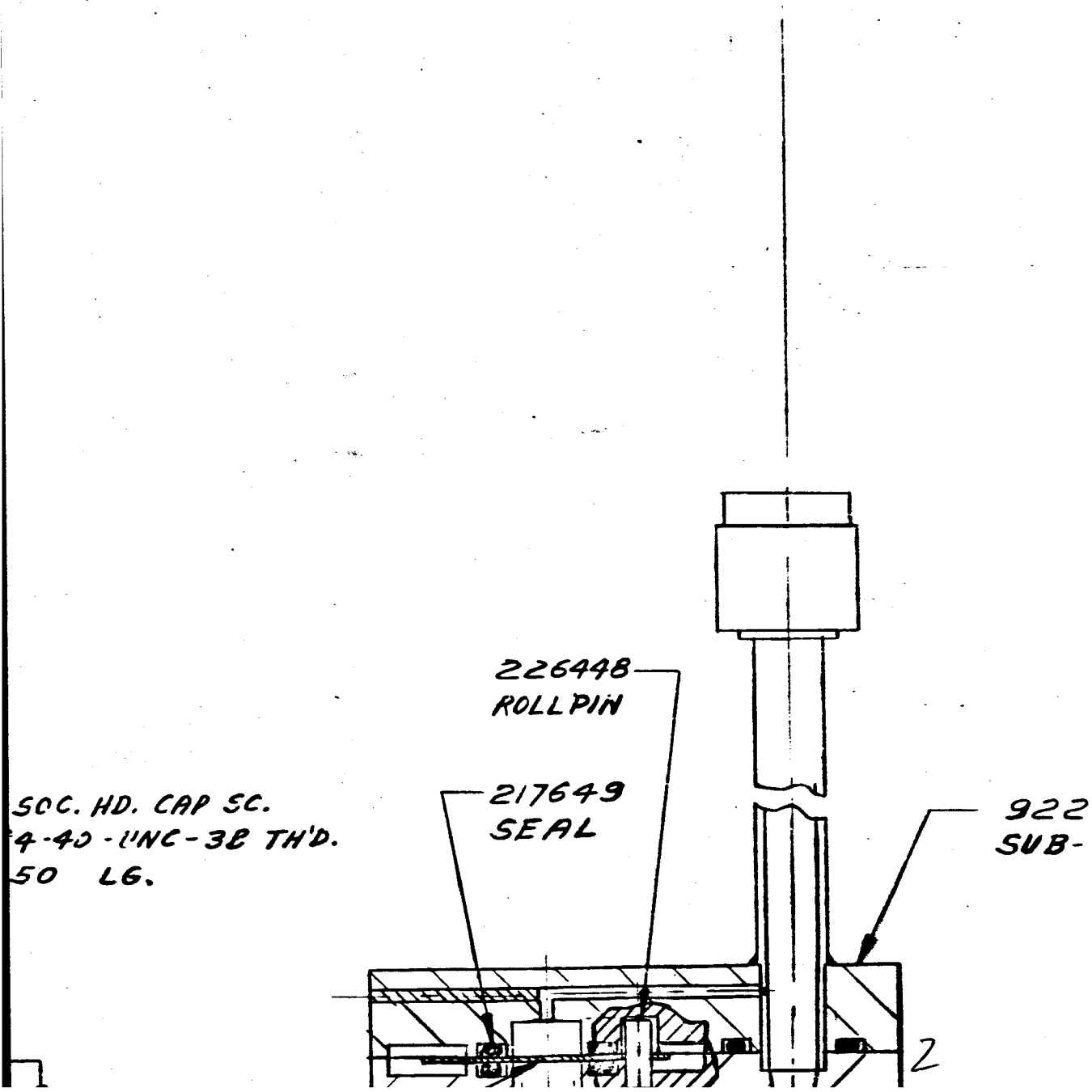
226448
ROLL PIN
217649
SEAL
SOC. HD. CAP SC.
4-40-UNC-3B TH'D.
50 LG.
922
SUB-
2

1

REVISIONS				
ZONE	SYM.	DESCRIPTION	DATE	APPROVAL

Figure 45

B

09-X
ASSY

3

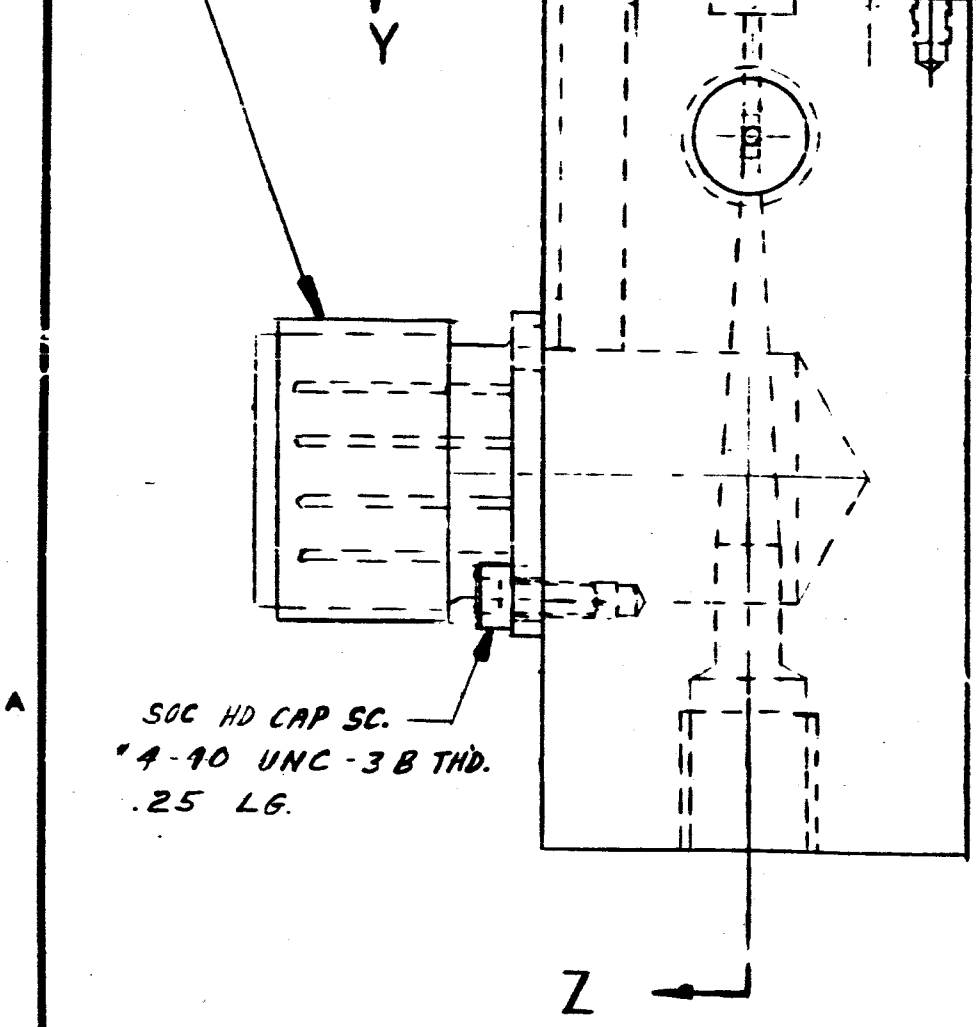

4

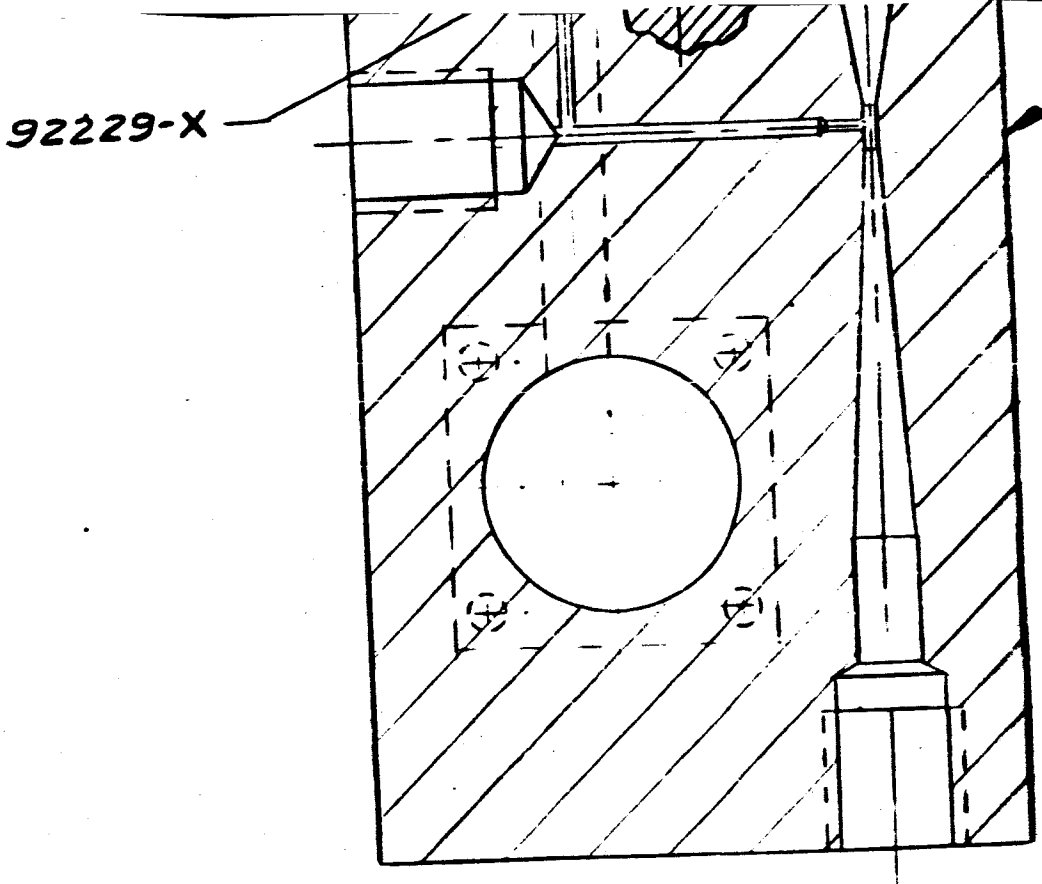

Z-Z

UNLESS OTHERWISE SPECIFIED	MODE
SURFACE FINISH 125	REF.
• 2 PLACE DECIMAL ± .06	DR.
• 3 PLACE DECIMAL ± .010	CHK.
*EXCEPT DRILLED HOLES	T. O.
ANGULAR DIMS. ± 2°	
MACHINE PER VS 1-3-3-1	
MATERIAL	PROT REL.
GOV'T. SPEC.	PROG REL.
HEAT TREATMENT	APP.
GOV'T. SPEC.	

92204-X	92204-X
NEXT ASSY.	USED ON
APPLICATION	

2207-X
DY

92204-X

A

UNLESS OTHERWISE SPECIFIED:

CONCENTRICITY OF MACHINED DIAMETERS ON SAME AXIS MUST BE WITHIN .010 TIR

REMOVE ALL BURRS & BREAK SHARP EDGES

VS 1-3-3-1

APPLICABLE SPECS.

MICROFILMED

92204-X		
PADTKE	DATE 11-7-62	
ZOYA	DATE 11-19-62	
EL ZOYA	DATE 11-23-62	
TYPE	DATE	
	DATE	
	DATE	

TITLE

FLOW PICK-UP ASSEMBLY (0.1 — 1.0 GPM)

6

SCALE 2/1 | WT. ACT. | CALC.

VICKERS

RED

VICKERS INCORPORATED

DIVISION OF SPERRY RAND CORPORATION

DETROIT, MICH. TORRANCE, CALIF.

DWG. SIZE C

92204-X

1

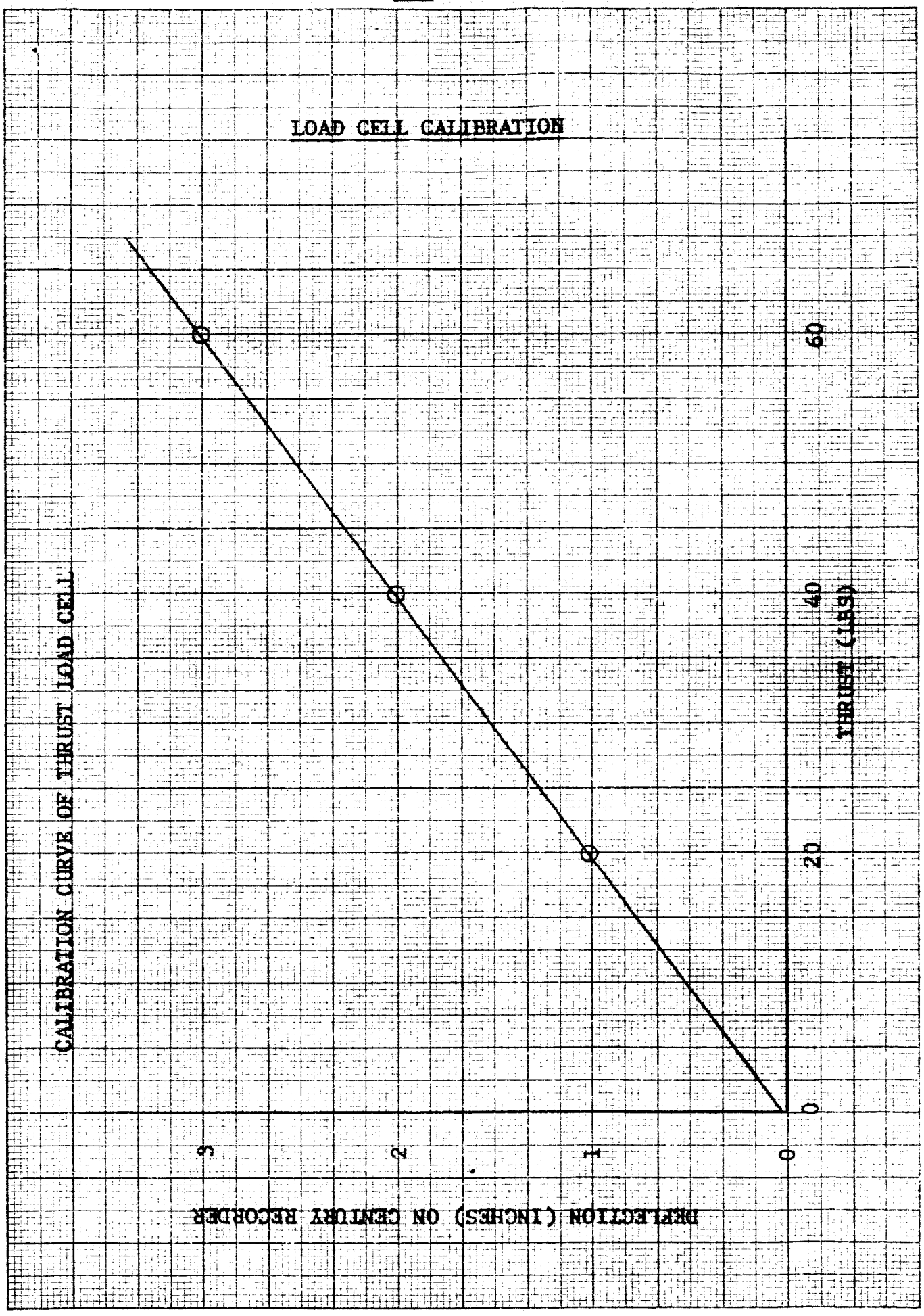
LOAD CELL CALIBRATION
CALIBRATION CURVE OF THRUST LOAD CELL
THRUST (LBS)
0
20
40
60
DEFLECTION (INCHES) ON CENTURY RECORDER
0
1
2
3

FIGURE 46

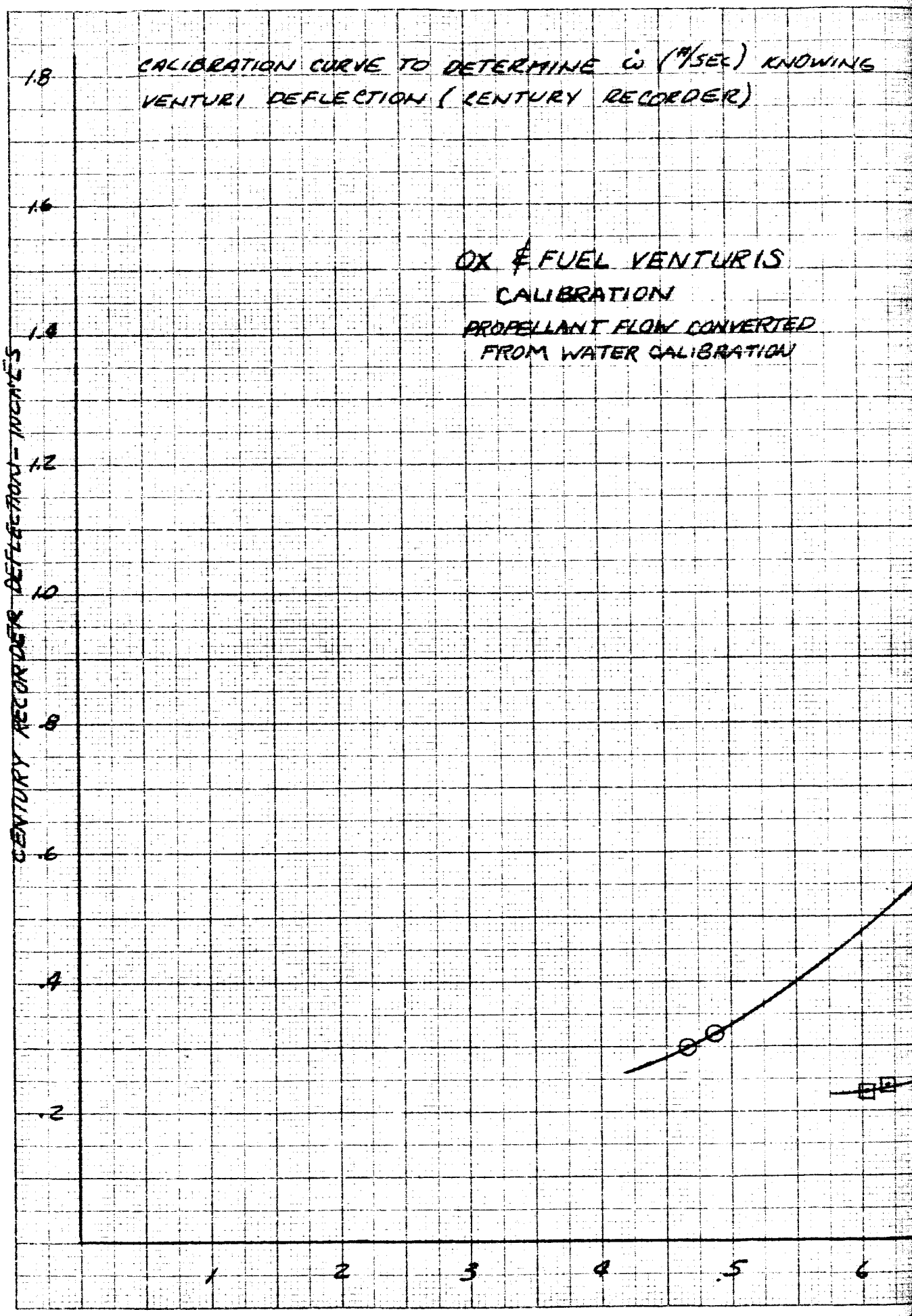
CALIBRATION CURVE TO DETERMINE ω (#/SEC) KNOWING VENTURI DEFLECTION (CENTURY RECORDER)
OX & FUEL VENTURIS
CALIBRATION
PROPELLANT FLOW CONVERTED FROM WATER CALIBRATION
CENTURY RECORDER DEFLECTION - INCHES
1.8
1.6
1.4
1.2
1.0
.8
.6
.4
.2
1
2
3
4
.5
6
ω(

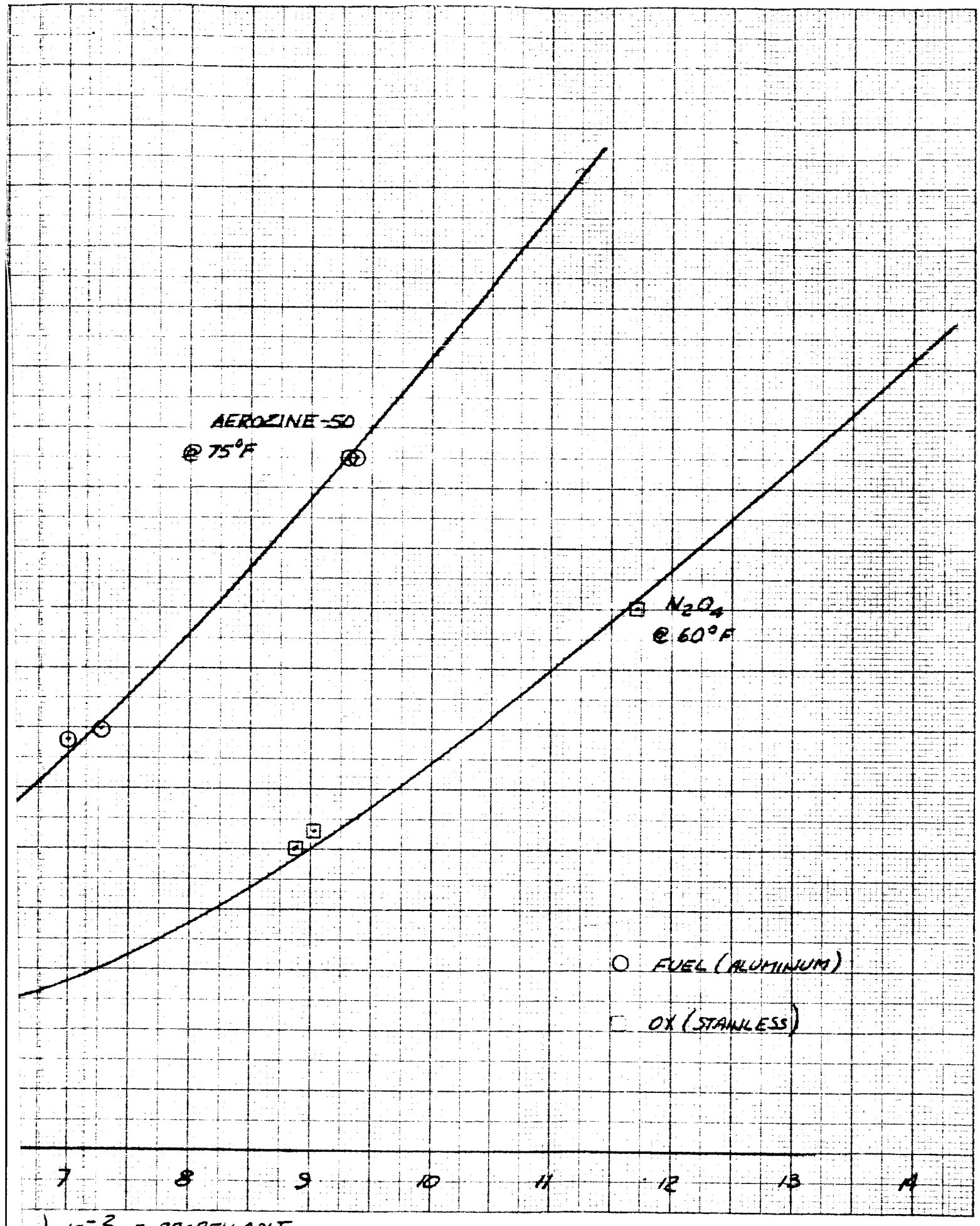
AEROZINE-50
@ 75°F
N_2O_4
@ 60°F
FUEL (ALUMINUM)
OX (STAINLESS)
7
8
9
10
11
12
13
14
τ) ×10⁻² OF PROPELLANT

FIGURE 47

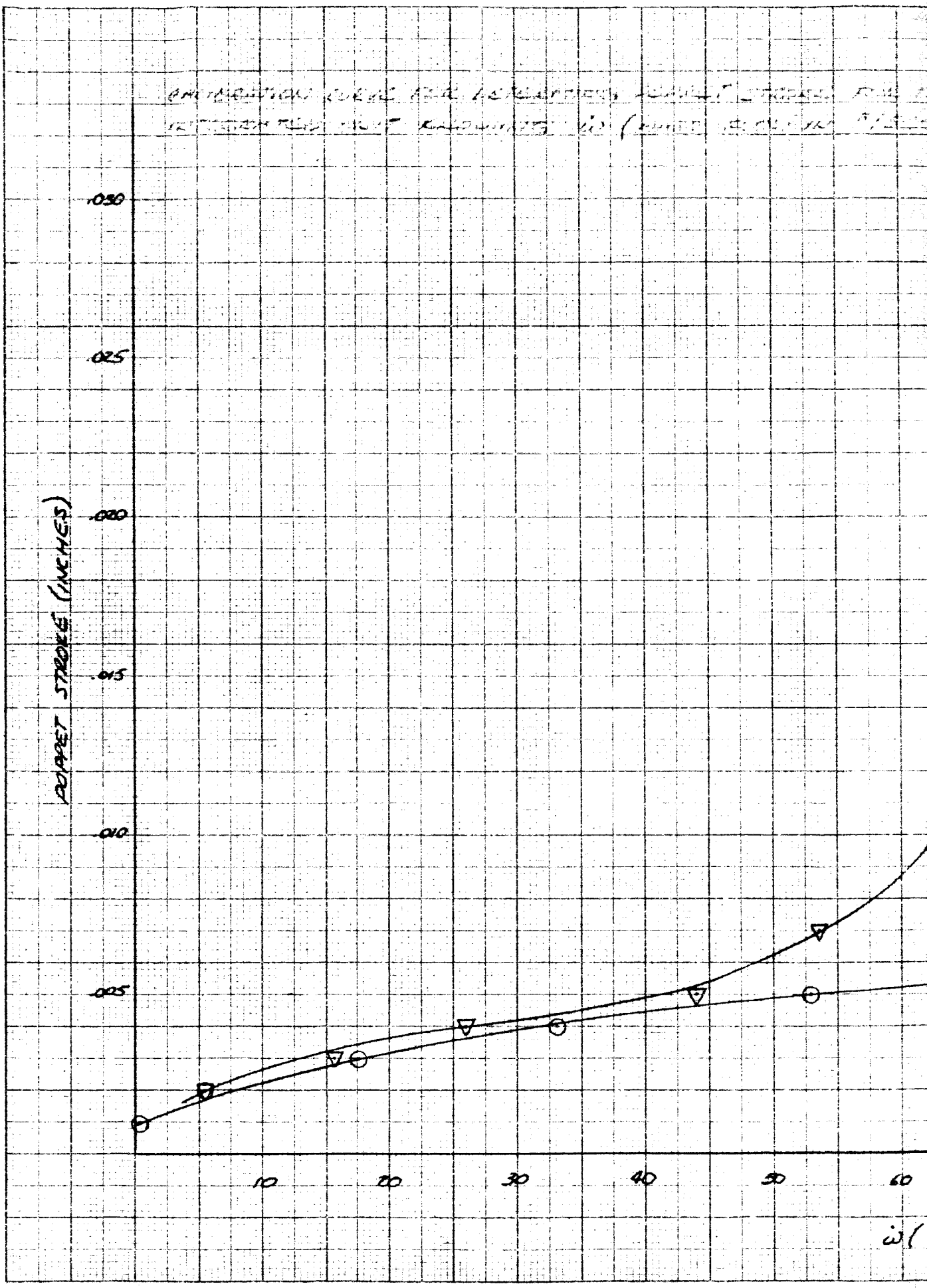
.030
.025
.020
.015
.010
.005
PISTON STROKE (INCHES)
10
20
30
40
50
60

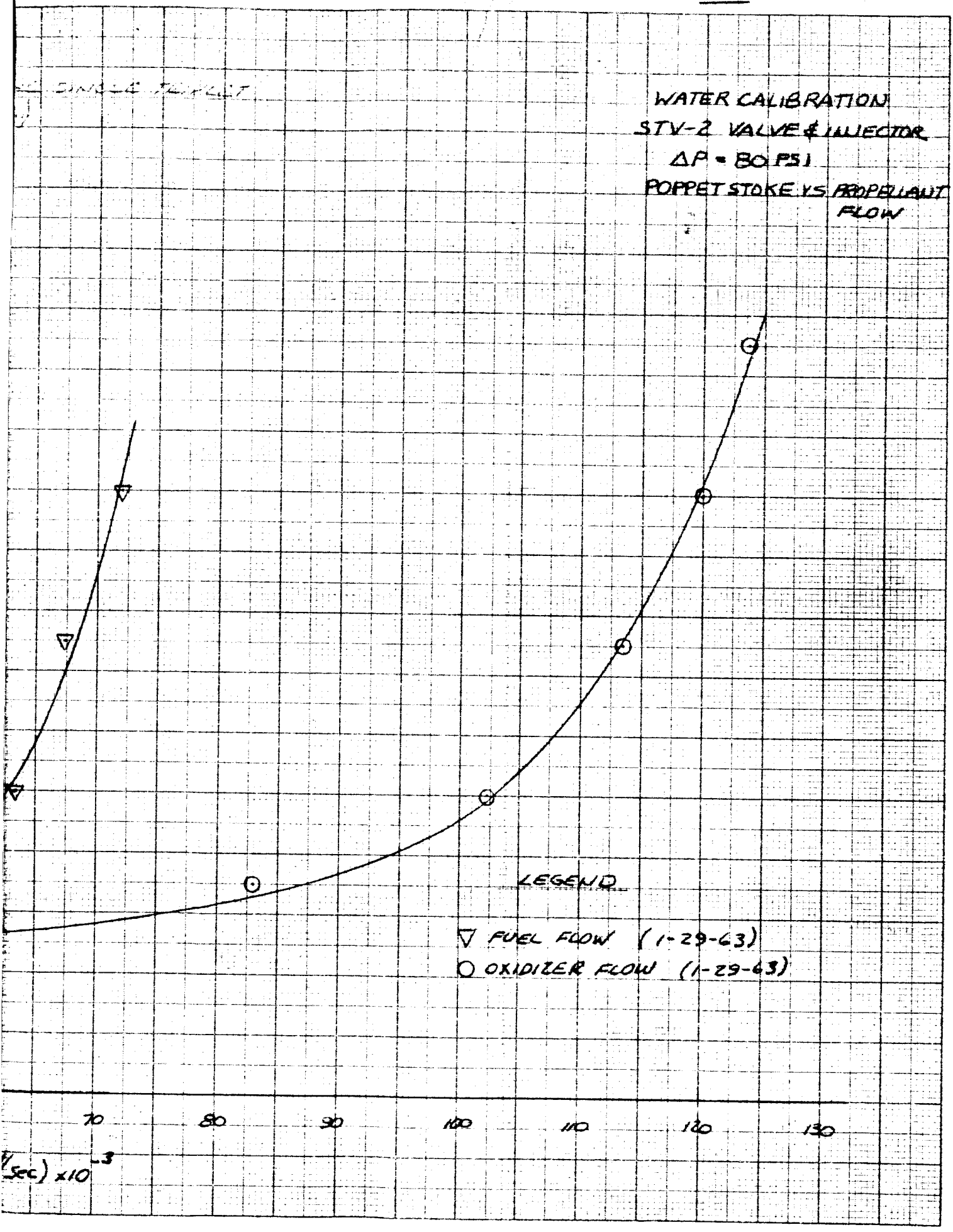
WATER CALIBRATION
STV-2 VALVE & INJECTOR
ΔP = 80 PSI
POPPET STOKE VS PROPELLANT FLOW
LEGEND
FUEL FLOW (1-29-63)
OXIDIZER FLOW (1-29-63)
70
80
90
100
110
120
130
(/sec) x10^-3

FIGURE 48

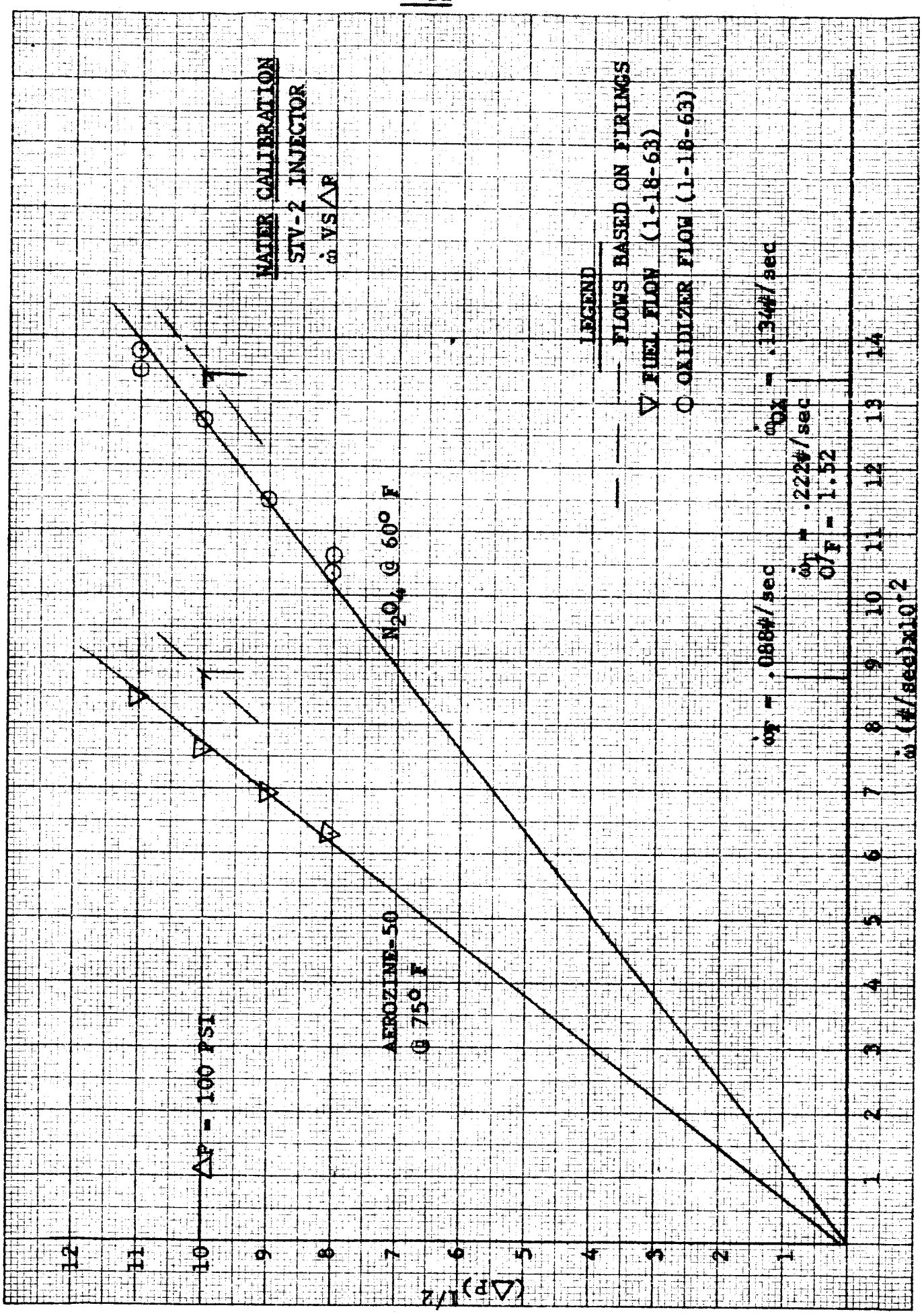
WATER CALIBRATION
STV-2 INJECTOR
ṁ VS ΔP
LEGEND
FLOWS BASED ON FIRINGS
FUEL FLOW (1-18-63)
OXIDIZER FLOW (1-18-63)
N2O4 @ 60° F
AEROZINE-50
@ 75° F
ΔP = 100 PSI
ṁF = .088#/sec
ṁOX = .222#/sec
O/F = 1.52
ṁOX = .134#/sec
ṁ (#/sec)x10-2
(ΔP)1/2
1
2
3
4
5
6
7
8
9
10
11
12
13
14

FIGURE 49

APPENDIX A

GAS TO LIQUID LEAKAGE CONVERSION

APPENDIX A

GAS TO LIQUID LEAKAGE CONVERSION
(Nitrogen Gas To Propellant Liquid)

The bipropellant system developed under this contract is classified as "hypergolic" or self igniting . The propellant liquids used are 50/50 mixture of hydrazine and UDMH as the fuel, the nitrogen tetroxide as the oxidizer.

The maximum leakage allowance of the bipropellant valve called out in the performance specifications is 0.1 cc/hr. To measure the leakages in this order of magnitude, and considering the characteristics of the propellant liquids, it was decided to use a substitute test fluid. Because of the very low flow range to be measured, the use of water was impractical from the standpoint of test time.

Therefore, dry nitrogen was selected as the test medium to determine the sealing characteristics of the various poppet and seat designs tested during the development program. Using nitrogen gas as the test fluid medium posed another problem however. With the bipropellant system using liquid propellants, conversion curves were necessary to properly evaluate the leakage tests.

An equivalent gas leakage thru an orifice was obtained in terms of water. For this purpose, the test rig shown in Figure 50 was used

WATER TO GAS FLOW TEST CIRCUIT

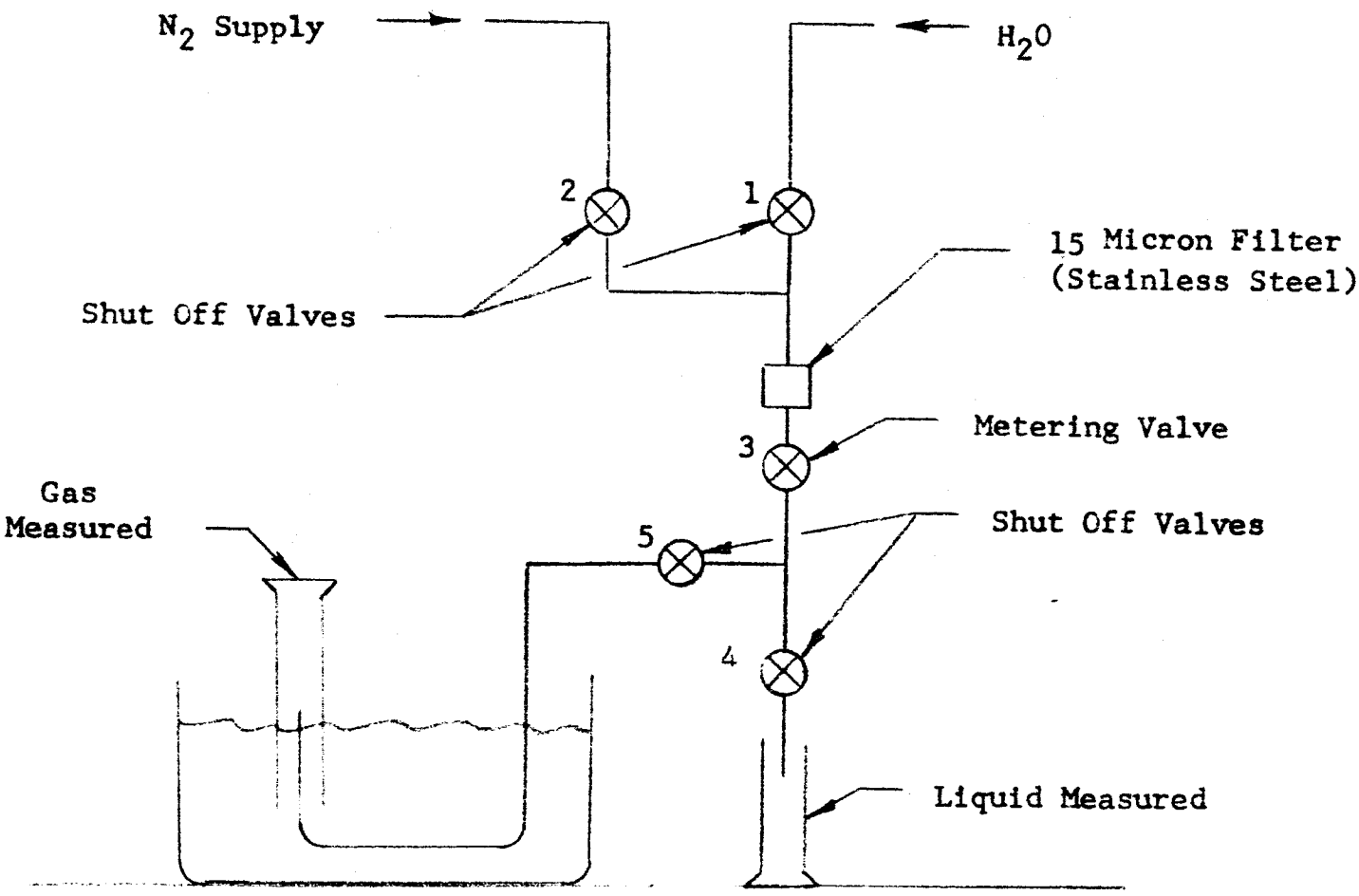

Figure 50

with the following operational sequence. An ambient temperature of 72°F was observed.

Liquid Flow Measurements

1. With valve 2 and 5 closed, distilled water is introduced through the open valves 1, 3 and 4 by gravity. The water is allowed to flow until free of any bubbles.
2. With the water still flowing, valves 1 and 3 are closed trapping a slug of water between these valves.

   Note: Since our flow values were very small, the volume of the slug was sufficient to obtain a data point for any given pressure or flow level.
3. N_2 supply valve 2 is opened and pressure set.
4. Metering valve 3 is cracked open to obtain the desired flow thru valve 4 which has been left open.
5. Flow rate was measured in a graduate.

N_2 Gas Flow Measurements

6. With the previous valving sequence undisturbed (metering valve 3 especially), the balance of the water is blown thru valve 4 until lines are dry.
7. Valve 4 is closed and valve 5 opened wide to divert the N_2 flow to the gas measuring device.
8. The nitrogen gas flow was measured by the displacement method in a water filled graduate.

The final results are shown in Figure 51 for the various pressure levels, where the volume of gas leakage per minute is compared with the leakage flow of water per minute.

During the actual development of the valve, the leakage past the poppet and seat in all cases was observed in terms of bubbles and no precise measurements were taken. To obtain a feel of the actual volumes contained in a bubble of gas in the size observed during development, an additional test was run employing 1/8 and 1/4 inch OD tubing. An actual count of bubbles were made in terms of displaced volume of water and two bubble sizes measured with .037 cc with the 1/8 diameter tube and .11 cc with the 1/4 dia. tube as shown in Figure 52. The size of these bubbles appeared to be close to the sizes of the bubbles observed during the valve development tests.

The leakage for nitrogen tetroxide which is the extreme case, can be obtained by assuming the leakage is inversely proportional to viscosity, Figure 51. This assumption is conservative.

Using the large bubble size realized from the 1/4 inch tubing of the vacuum test circuit at 260 psig, an estimate of the leakage past the valve was obtained. This leakage can be further resolved by extracting the following values from the curves shown in Figures 51 & 52.

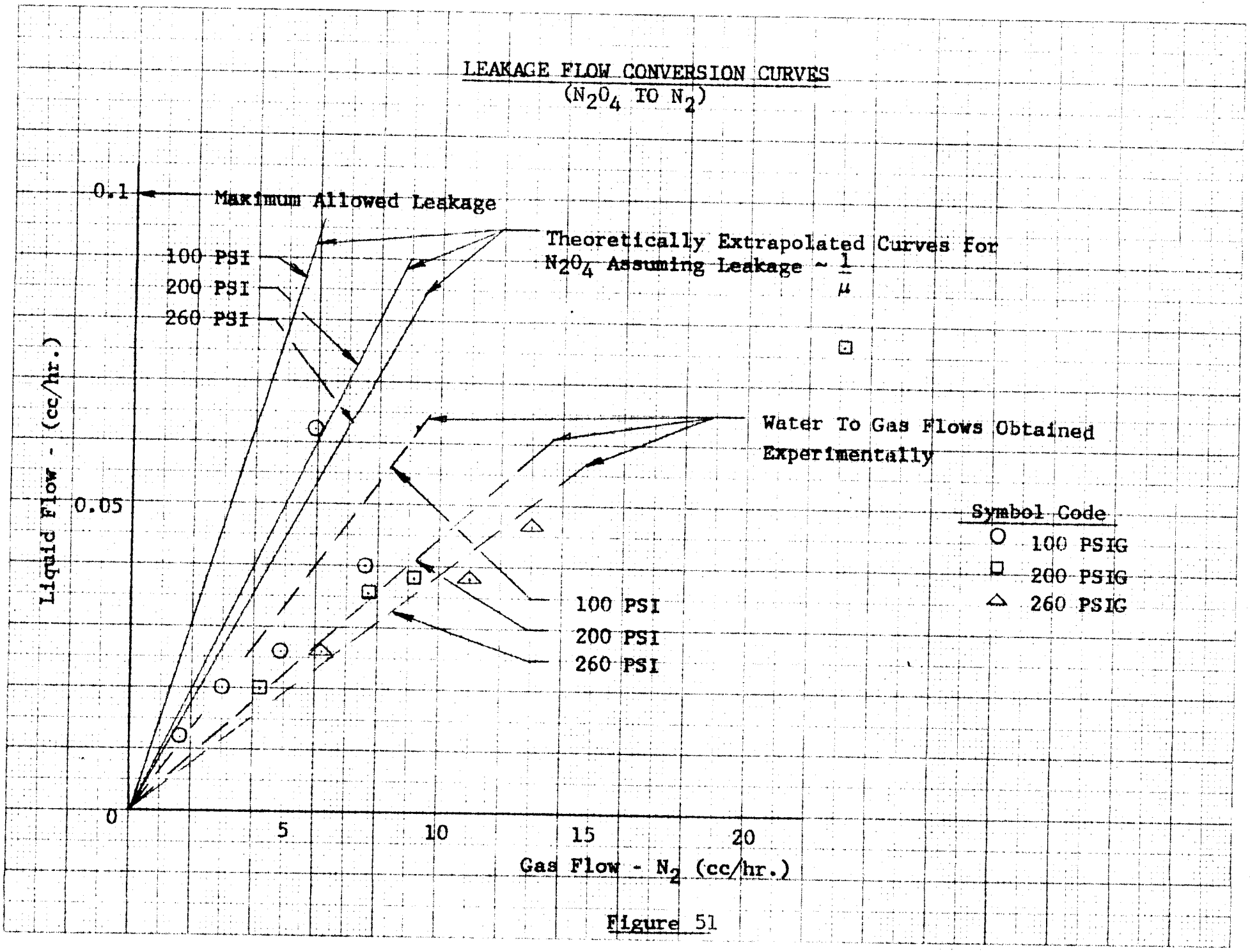
LEAKAGE FLOW CONVERSION CURVES
(N_2O_4 TO N_2)
0.1
0.05
0
Maximum Allowed Leakage
100 PSI
200 PSI
260 PSI
Theoretically Extrapolated Curves for N_2O_4 Assuming Leakage ~ $\frac{1}{\mu}$
Water To Gas Flows Obtained Experimentally
100 PSI
200 PSI
260 PSI
Symbol Code
100 PSIG
200 PSIG
260 PSIG
Liquid Flow - (cc/hr.)
5
10
15
20
Gas Flow - N_2 (cc/hr.)

Figure 51

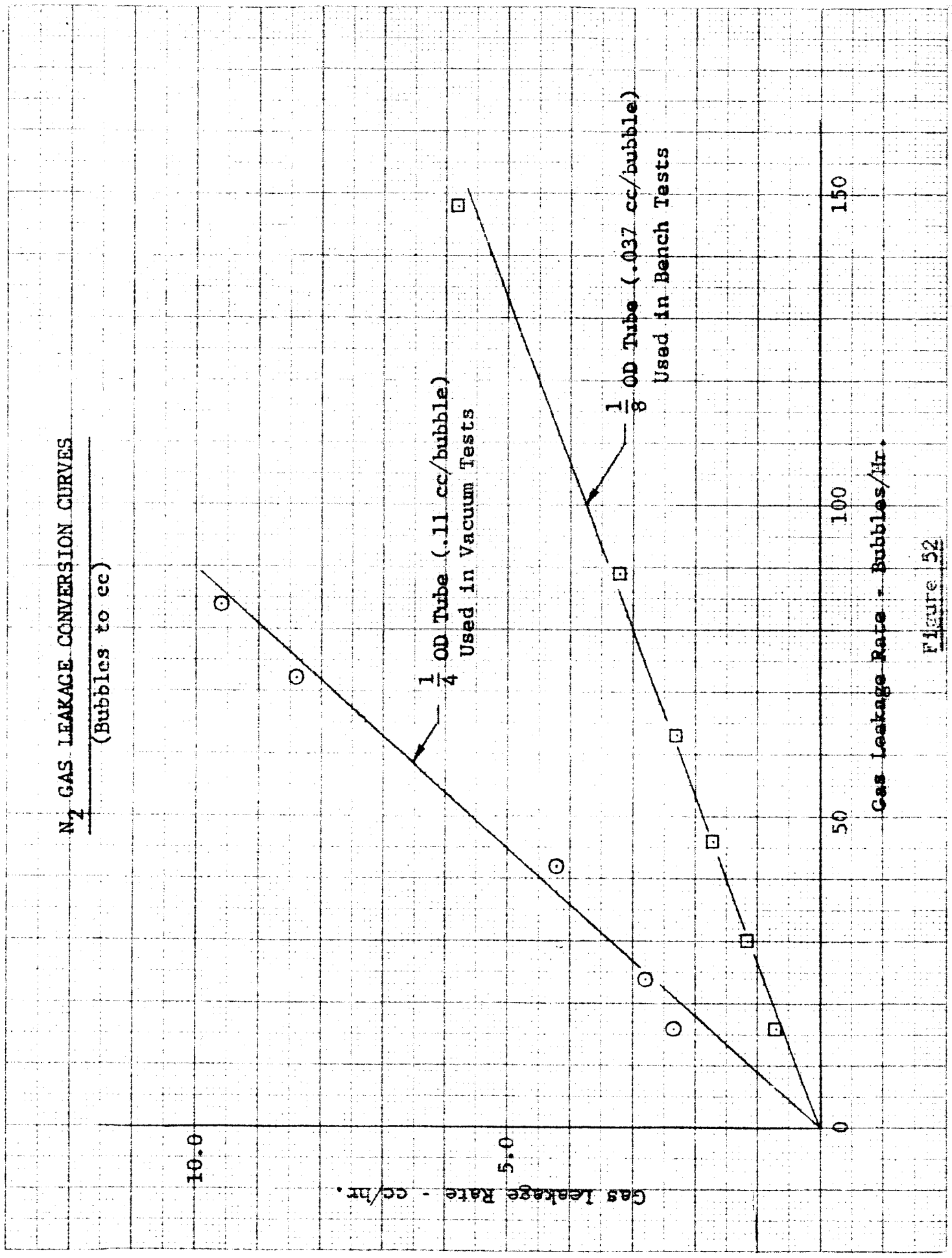
N_2 GAS LEAKAGE CONVERSION CURVES
(Bubbles to cc)
$\frac{1}{4}$ OD Tube (.11 cc/bubble)
Used in Vacuum Tests
$\frac{1}{8}$ OD Tube (.037 cc/bubble)
Used in Bench Tests
Gas Leakage Rate - cc/hr.
10.0
5.0
0
50
100
150
Gas Leakage Rate - Bubbles/Hr.

Figure 52

The maximum allowed leakage of 0.1 cc/hr. of nitrogen tetroxide (N_2O_4) is equivalent to 11 cc of N_2 gas per hr.

The 11 cc of gas is equivalent to approximately 100 bubbles per hr.

This can be reduced further by stating that a valve leakage of 0.1 cc/hr. of N_2O_4 is equivalent to 100 bubbles of N_2 gas/hr.

APPENDIX B

VACUUM EQUIPMENT

APPENDIX B

VACUUM EQUIPMENT

This section presents a description of the physical makeup and the capabilities of the vacuum coater and the ultra-high vacuum chamber manufactured by the National Research Company, Equipment Division.

Vacuum Coater Model 3166

The vacuum coater is a complete system for depositing one or more thin films by vacuum evaporating (resistance heating materials in a vacuum). The unit includes a high performance vacuum pumping system rated to attain pressures in the low 10^{-6} range ≈ to 125 miles of space flight, a stainless steel base plate with both electrical and mechanical motion seal feed-throughs, a pyrex bell jar vacuum chamber 18" in diameter by 30" high, vacuum gauging, and a built-in heater capable of temperatures up to 650°F. This unit can also be adapted to other non-coating vacuum applications; for example, space environmental testing, crystal growing or zone refining, vacuum leak testing, degassing of materials, and low temperature drying.

Ultra High Vacuum Chamber

The second unit is an ultra high vacuum test unit which includes a bell jar type stainless steel chamber, two stage valveless diffusion

pumping system and suitable vacuum instrumentation. The unit is capable of reaching pressures of 1×10^{-9} torr (mm of Hg) ≈ to 500 miles space flight.

The chamber is in the form of a vertical cylinder 14 inches outside diameter and is divided into a fixed lower section and a removable upper bell. The two sections offer a straight cylindrical stainless steel shell length of approximately 30 inches. The bell jar straight section is about 18 inches, terminating in a dished head closure. The bell jar contains three sight ports for viewing the work area from various angles. The bottom section carries four feed-through ports. Each external plate is sealed to a flanged port by means of a copper crush ring seal. The feed-through plates contain the following configurations used for various test work: multiple stainless steel tubulations, a bellows sealed rod to provide linear motion transfer of 1/8", 14 electrical pin connections rated at 25 amps 900 volts, and a 27 electrical pin connection plate rated at 7.5 amps 900 volts.

At the present time the only heat applied is used to bake out the chamber and elbow of the system. The temperature used is 400°F, but this heat is only applied for a short period of the long cycle test time causing this heat to be, only slightly if at all, effective in accelerating the evaporation of various materials.

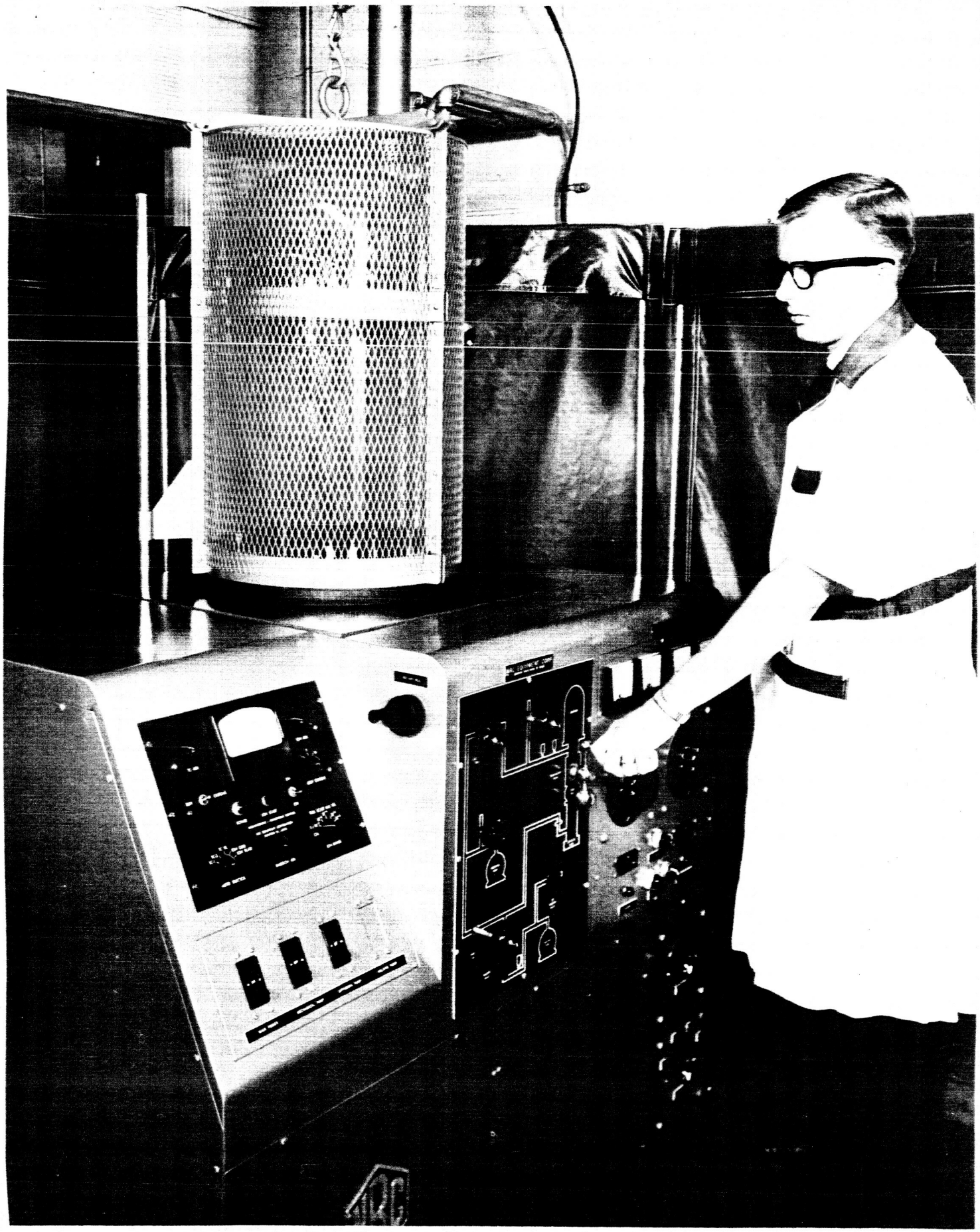

Fig. 53 - Vacuum Coater - Model 3166

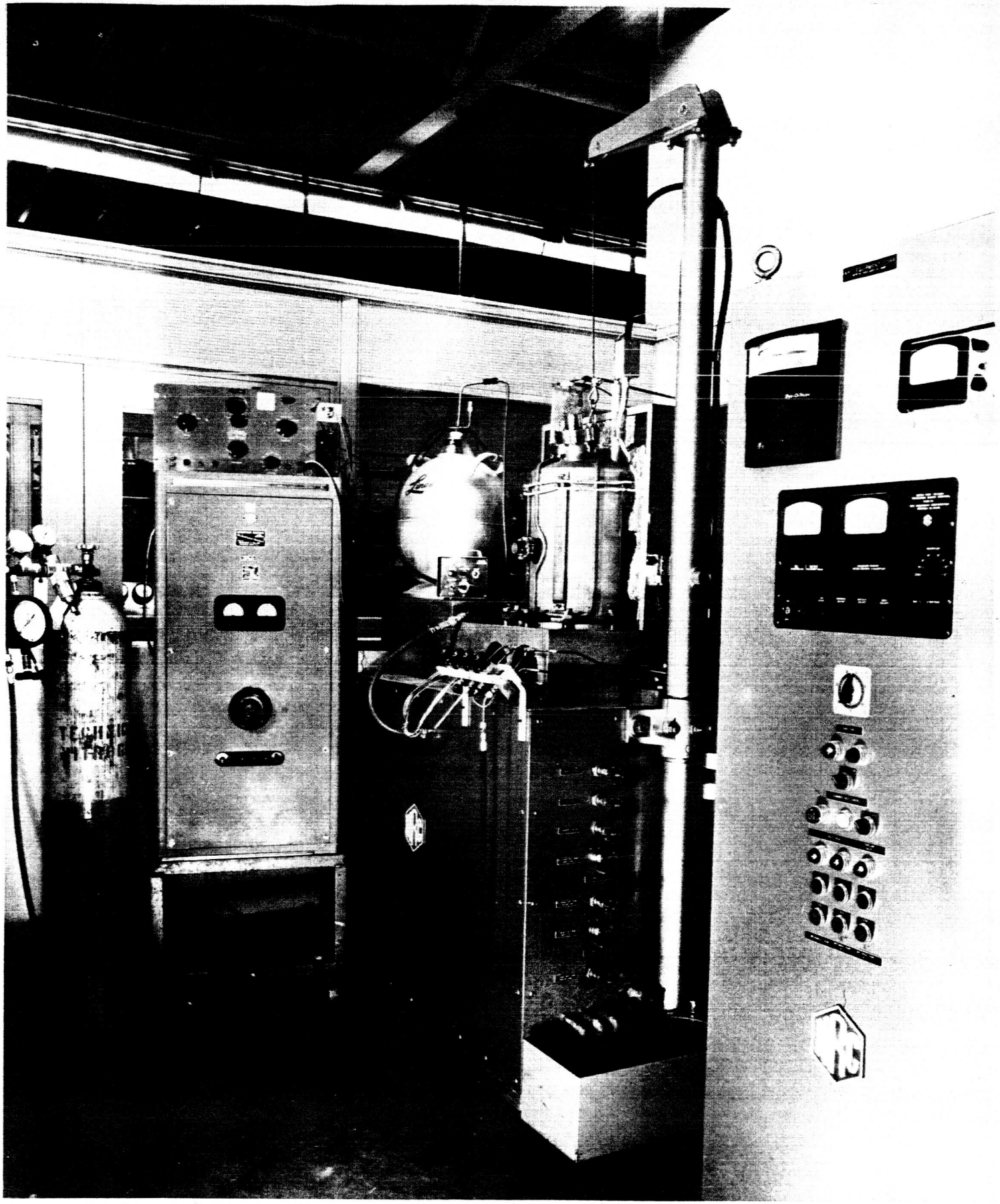

Ultra High Vacuum Chamber

FIGURE 54

APPENDIX C

LINKAGE AND SOLENOID PARAMETERS

SCHEMATIC OF ELECTRICAL LOAD CIRCUIT FOR 28 VOLT COILS

BASIC MAGNETIC EQUATIONS

APPENDIX C

LINKAGE AND SOLENOID PARAMETERS
SCHEMATIC OF ELECTRICAL LOAD CIRCUIT FOR 28 VOLT COILS
BASIC MAGNETIC EQUATIONS

The information in this section with the exception of the electrical load schematic was requested by NASA personnel. Presented are all the physical parameters and basic magnetic equations necessary for deriving solenoid and valve dynamics.

Although a complete dynamic analysis was not required under the contract (and is not presented in this report), Vickers undertook the task with in-house funding towards the end of the program. The reason this task was undertaken at the time was because of NASA's re-emphasis of the importance of minimum impulse bit near the end of the program.

It was felt that impulse bits even smaller than the 0.6#-sec contract target would be desirable. This brought out the need for an absolute maximum "off" response. In addition, fast "on" response was stressed. To achieve an "optimum" response system, Vickers endeavored experimentally, to match "on" and "off" response times on a best effort basis within the confines of the contract. The need for a comprehensive dynamic analysis was thus established to accurately define and optimize parameters affecting response.

The analysis was completed and was being set up on an analog computer at the time of this writing. All equations were generalized to

permit computer prediction of future designs allowing for gross changes to solenoid linkage, or valving.

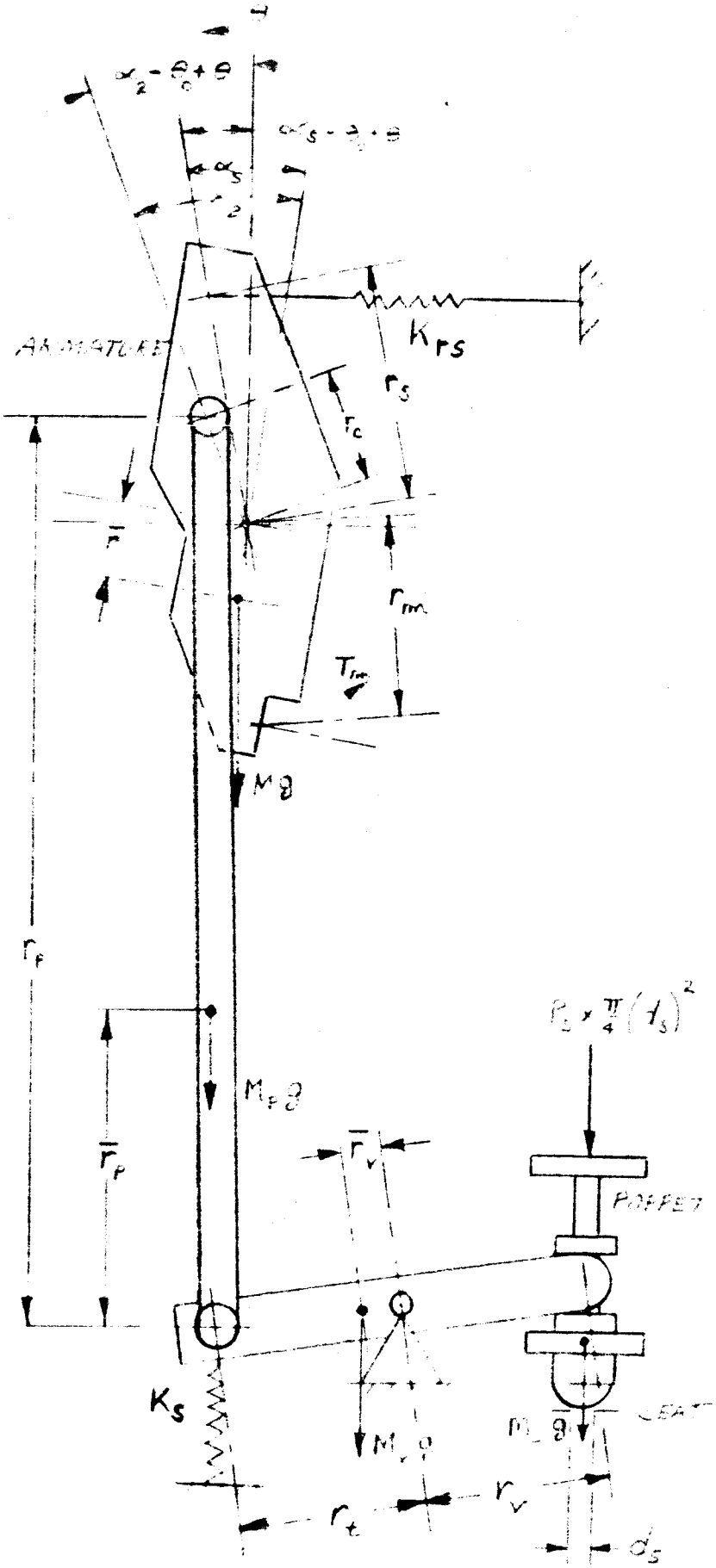

ARMATURE TO POPPET LINKAGE

REFERENCE ASSEMBLY 91575 X

VALUES OF PARAMETERS

For Dynamic Analysis of Electrical and Mechanical Systems of Assembly 91575-X

θ_o = -7° 40' nominal

θ = armature rotation angle

α_s = 17° 40' nominal

K_{rs} = 40#/in (.030" engagement)

r_s = .722

r_c = .397

r_m = .843

$\bar{r}$ = .135

r_p = 2.225

$\bar{r}_p$ = 1.1356

r_t = .440

r_v = .440

$\bar{r}_v$ = .022

d_s = .160 (assumed sealing seat diameter)

M = 1.9951×10^{-4} #sec^2/in.

M_p = 7.2222×10^{-5} #sec^2/in.

M_v = 2.3324×10^{-5} #sec^2/in.

M_s = 1.1425×10^{-5} #sec^2/in.

K_s = 7.7 #/in (1# pre-load)

P_s = supply pressure = 235 psig

P_c = chamber pressure = 150 psia (poppets open) = ambient (poppet closed)

Coil turns = 576

Coil wire size = # 30 awg copper

External Resistance = 8.25 ohms (+4.0 ohms/parallel leg)
See schematic, next page

Solenoid magnetic materials (See standard catalogs for magnetic characteristics)

Laminations: Transformer C - Alleghany Ludlum
Solid Plates: Relay #2 - Alleghany Ludlum

Circuit Supply Voltage: 28 volts (See circuit schematic next page)

Flux Path Areas: Refer to detail prints of Assembly 91575-X

The following parameters are functions of armature motion. Expression for these are derived from the given parameters applied to basic magnetic equations.

Circuit inductance

Permeance of back gap (.004" air gap width per side)

Permeance of linear gap (.008" air gap width)

Permeance of inverse gap (.004 non-magnetic gap-stop)

SCHEMATIC-ELECTRICAL LOAD
60# PULSE MARKET SOLENOID
RELUCTANT COIL OPERATION
[illegible] 28 [illegible]
PART # [illegible]39-X

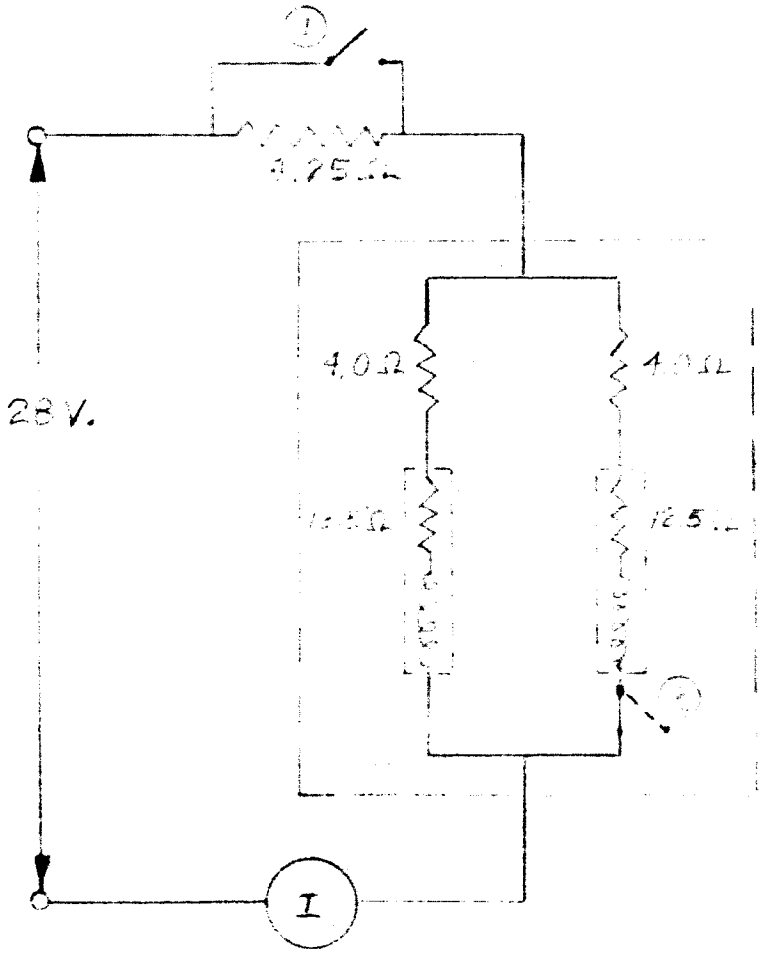

	PARALLEL COIL OPERATION	SINGLE COIL OPERATION
SWITCH 1	OPEN	CLOSED
SWITCH 2	CLOSED	OPEN
I	1.7 AMPS	.7 AMP

J.B. 4-2[illegible]

Basic Magnetic Equations for Derivation of the Torque Motor Developed Torque

The actual torque motor and the equivalent magnetic and electrical circuits are shown in the figures below:

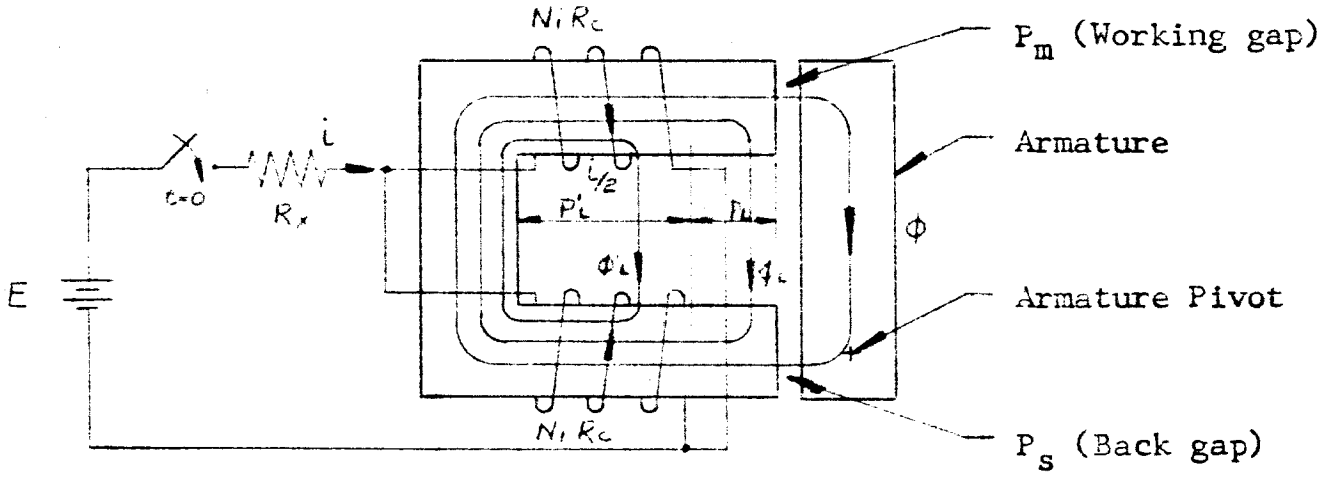

Actual Circuit

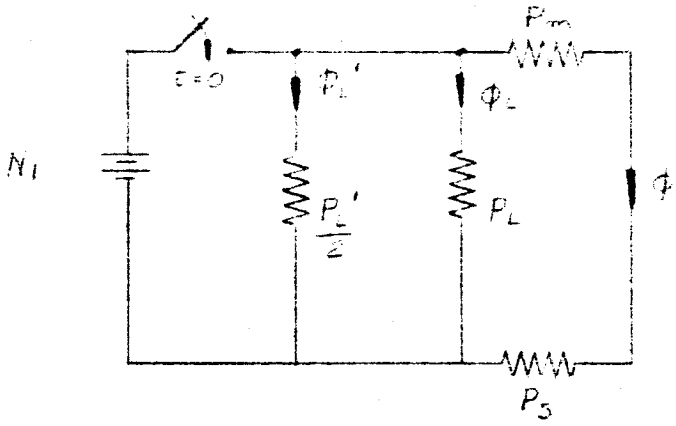

P_L and P_L' are the permeances of the leakage paths.

Equivalent Magnetic Circuit

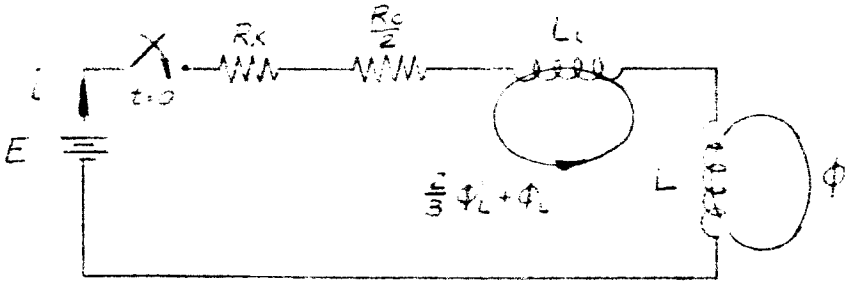

Equivalent Electric Circuit

The developed torque is given by

$$T = 4.43\ F_m^2 \frac{dP_m}{d\theta} \qquad \#\text{-in} \qquad (1)$$

where T = developed torque (#-in)

F_m = ampere-turns across the working gap (ampere-turns)

$\frac{dP_m}{d\theta}$ = the rate of change in working gap permeance (webers/ampere-turn-rad)

From the magnetic circuit,

$$Ni = \left(\frac{1}{P_m} + \frac{1}{P_s}\right) \varphi \qquad (2)$$

where N = turns per coil

i = input current (amperes)

P_m = permeance of working gap (webers/amp-turn)

P_s = permeance of back gap (webers/amp-turn)

φ = armature flux (webers)

Solve equation (2) for φ:

$$\varphi = \frac{P_m}{1 + \frac{P_m}{P_s}} \quad Ni \qquad \text{(webers)}$$

$$\text{or} \quad F_m = \frac{\varphi}{P_m} = \frac{Ni}{1 + \frac{P_m}{P_s}} \quad \text{(ampere-turns)} \tag{3}$$

Substitute equation (3) into (1):

$$T = \frac{4.43\ N^2\ i^2}{\left(1 + \frac{P_m}{P_s}\right)^2} \quad \frac{dP_m}{d\theta} \quad \#(\text{-in}) \tag{4}$$

From the electrical circuit:

$$E = (R_x + R_c/2)i + (L_e + L)\ \frac{di}{dt} \quad \text{(volts)} \tag{5}$$

$$\text{or} \quad i = \frac{E}{R}\ (1 - e^{-\frac{t}{\tau}}) \quad \text{(amperes)} \tag{6}$$

$$\text{where} \quad R = R_x + R_c/2 \quad \text{(ohms)} \tag{7}$$

$$\tau = \frac{L_e + L}{R_x + R_c/2} \quad \text{(seconds)} \tag{8}$$

and E = applied voltage

R_x = external resistance (ohms)

R_c = resistance of each coil (ohms)

L_e = leakage inductance (henries)

L = equivalent inductance of the working and back gaps (henries)

i = input current (amperes)

R = equivalent circuit resistance (ohms)

τ = circuit time constant (seconds)

Substitute equation (6) into (4):

$$T = \frac{4.43}{\left(1 + \frac{P_m}{P_s}\right)^2} \left(\frac{NE}{R}\right)^2 \left(1 - e^{-\frac{t}{\tau}}\right)^2 \frac{dP_m}{d\vartheta} \qquad (9)$$

We see that the developed torque is a function of both time, t, ϑ, since P_m is a function of ϑ.